CONDUCTED UNDER
NASA RESEARCH GRANT
NGR-17-002-043

WIND TUNNEL INVESTIGATIONS OF VORTEX BREAKDOWN ON SLENDER SHARP-EDGED WINGS

CRES

THE UNIVERSITY OF KANSAS • CENTER FOR RESEARCH INC
ENGINEERING SCIENCE DIVISION • LAWRENCE, KANSAS

Final Report

NASA Research Grant NGR-17-002-043

WIND TUNNEL INVESTIGATIONS OF VORTEX BREAKDOWN ON SLENDER SHARP-EDGED WINGS

by

William H. Wentz, Jr.
and
David L. Kohlman

University of Kansas Center for Research, Inc.
Engineering Sciences Division
Report FRL 68-013

November 27, 1968

ACKNOWLEDGEMENTS

The authors wish to express their appreciation to those who assisted in making this work possible: to the National Science Foundation and the National Aeronautics and Space Administration for their financial support; especially to Mr. Mark Kelly, NASA Ames Research Center, and Mr. Edward C. Polhamus, NASA Langley Research Center who made available to the author results of recent research conducted at their respective offices; and to their able research assistant, Mr. Dennis Cannon, for his perseverance.

TABLE OF CONTENTS

LIST OF FIGURES

LIST OF SYMBOLS

A	aspect ratio, b^2/S
BD	vortex core breakdown
b	wingspan
c	wing local chord
$\bar{C}$	wing mean geometric chord, $\int c^2 dy/S$
C_o	wing reference chord (usually centerline)
C_L	wing lift coefficient, Lift/qS
C_D	wing drag coefficient, Drag/qS
C_{D_i}	induced drag coefficient
C_{D_o}	drag coefficient at zero lift
C_M	wing pitching moment coefficient about 1/4 mean aerodynamic chord, Moment/qS$\bar{C}$
C_S	leading-edge suction coefficient, Suction Force/qS
K_p, K_v	constants in Polhamus' lift equation
q	dynamic pressure
S	wing planform area
TE	trailing edge
α	angle of attack
Λ	leading edge sweep angle

SUMMARY

Systematic wind tunnel investigations of vortex breakdown have been conducted on sharp-edged delta and modified delta wings with sweep angles from 45° to 85° at Reynolds numbers of about 1×10^6, utilizing a schlieren system for flow visualization. Vortex breakdown positions are presented as a function of angle of attack and sweep. Results agree well with the limited amount of previously published data. For the very slender wings (75° to 85° sweep), initial breakdown was nearly independent of sweep, a result not anticipated by extrapolation of previous data.

Lift measurements show that Pohlhamus' leading-edge suction analogy provides an excellent means for predicting lift for wings with sweep angles between 65° and 80°, at angles of attack below vortex breakdown. For very low sweep (< 65°) and very high sweep (> 80°) less than theoretical lift is achieved. The reasons for these discrepancies are discussed in some detail in the paper.

Drag due to lift is predicted quite satisfactorily as the streamwise component of a normal force for all models tested. Although no satisfactory method for predicting pitching moments is available, experimental effects of vortex breakdown on pitching characteristics are presented.

Results of tests of the modified delta wings show that vortex breakdown is influenced much more strongly by planform changes near the apex than changes near the trailing edge. Cropping the wing tips or changing trailing-edge sweep had practically negligible effects on vortex breakdown. The addition of strakes (double-delta and ogee wings) may greatly delay initial breakdown. It is shown that vortex breakdown and force measurements from the present tests of an ogee wing agree quite favorably with NASA flight test results at a twenty times larger Reynolds number.

CHAPTER I

INTRODUCTION

Vortex flow has long been recognized as a phenomenon associated with wing tips. For the high aspect ratio wings which have been popular since the origin of aviation because of their high efficiency at low speeds, this tip flow does not play a predominant role in determining overall wing lift. For this reason, the edge vortex effect was neglected in traditional aerodynamic theory as developed by Prandtl (lifting line theory); and it has also been neglected in the attached flow lifting surface theories more applicable to low aspect ratio wings, e.g., Multhopp (1). These attached flow theories are quite adequate even for slender wings at small angles of attack, but are not adequate for predicting the forces developed at higher angles of attack required for landing and takeoff.

At the higher angles, leading edge separation occurs, resulting in vortex sheets which roll up along the upper surface of the wing to form strong line vortices streaming aft along each edge. The low pressure fields induced by these vortices act to provide additional lift, referred to as "vortex lift." The proportion of vortex lift to total lift increases with angle of attack and sweep angle. For example,

vortex lift amounts to 50% of total lift for a 75° delta wing at a total lift coefficient of 1.0.

Various authors have undertaken theoretical analyses to predict vortex lift. An inherent shortcoming of all the theoretical methods, however, is that they do not account for the "breakdown" or "bursting" of the leading edge vortex cores which occurs at high angles of attack. Thus, knowledge of the limitations of vortex flow (i.e., vortex breakdown) is of great practical importance to the designer who uses the slender sharp-edged lifting surfaces which are required to obtain high performance at supersonic speeds.

Analyses of the instabilities of a simple fluid vortex which lead to breakdown have been undertaken by various investigators (for example, References 2 and 3) using fluid dynamic theory. Such theoretical considerations have not yet reached a state of sophistication which would permit their application to the general case of predicting breakdown of wing leading edge vortices. For the present it seems that one must rely on experimental measurements for determining the onset of breakdown on wings.

Several investigators have provided vortex breakdown information for particular wings, using dye in water or smoke in air to mark the vortex cores and, hence, to indicate the breakdown. Such investigations have provided a great deal of insight into the effects of leading edge sweep, pressure gradients, etc., on the breakdown.

Systematic investigations on a family of delta wings were conducted by Earnshaw and Lawford (4) for wings with leading-edge sweep angles ranging from 55° to 76°. In these tests vortex breakdown observations were conducted utilizing a small tuft on a probe. Tests reported by Werle (5, 6) show that a blockage in the flow field may influence vortex breakdown. Thus, there was some question as to whether the probe influenced the breakdown measurements of Earnshaw and Lawford.

Poisson-Quinton and his associates at ONERA (7) have correlated vortex breakdown observations from hydrodynamic flow visualization studies with measured vortex lift from wind tunnel tests. The published correlations are limited to a few configurations. In addition, they are based upon tests at differing Reynolds numbers with different models, different mounting systems, etc.

The purpose of the present research was to provide a rather complete parametric investigation of vortex breakdown for sharp-edged delta wings, and to obtain force measurements from these same models in the same test facility in order to correlate force and flow field characteristics in the most direct manner possible.

CHAPTER II

VORTEX BREAKDOWN

Prior Experimental Observations

The phenomenon of vortex core "breakdown," vortex "bursting" or "explosion," has been observed by numerous investigators, and is indeed visible to the casual observer in certain instances. Vortex breakdown is an abrupt increase in the effective diameter of the rotational core associated with the vortex. The high velocities and corresponding low pressures associated with the core of a real fluid vortex, prior to breakdown, frequently make it visible to the naked eye. In air this may occur under conditions of high relative humidity, leading to condensation of the water vapor within the vortex core. These condensation vortices are occasionally visible on delta wing aircraft. When this occurs, the breakdown of the wing vortices appears as a flaring of the core into a trumpet-like shape at which point the vortex seems to disappear, due to turbulent mixing of the water vapor.

Delta wing vortices may also become visible as cavitation regions in water at moderate pressures. Breakdown is discernible as the termination of a cavitation filament in this case. This technique is simple and, to the author's knowledge,

has not been used extensively for investigations of vortex breakdown.

Investigators at ONERA in France (Poisson-Quinton, et al.) have developed a water tank facility to a high degree using colored dyes as tracers for vortex breakdown studies. (See for example, Reference 7). Their investigations utilize models of small proportions (Reynolds numbers $\approx 10^4$). However, the results of these flow visualizations have been correlated with wind tunnel force tests conducted at higher Reynolds numbers with impressive results (Reference 8).

Earnshaw (9) reported in 1964 on the use of a schlieren system in a subsonic wind tunnel to observe vortex breakdown. This work consisted of testing of 65° and 70° delta wings and some modified delta wings, and correlations of vortex breakdown results obtained from water tank tests. He presented data showing the progressive forward movement of the breakdown with angle of attack, and discussed the importance of using trip strips to stabilize the secondary separation at low Reynolds numbers.

Theoretical Considerations

Various investigators have attacked the problem of vortex breakdown from a theoretical standpoint, utilizing viscous flow theory. These analyses have been restricted to the problem of a simple isolated line vortex of constant strength, and have not included the effects of a wing or a variable strength vortex (Such as is associated with a wing

leading edge).

Kwan L. So (10) has shown experimentally that as many as five different vortex flow regimes are possible in a simple conical diffuser, indicating the complexity of the vortex breakdown problem. Bossel and others (2) have shown theoretically that the maximum helix angle for stability of a vortex with an axial velocity is about 50°. Unfortunately, neither the core radius nor the vortex strength (circulation) is known in advance for wings. Thus, there is no method at present for applying this theoretical vortex stability criterion to a wing.

CHAPTER III

SLENDER WING THEORY AND VORTEX LIFT

Lift

Slender wing theory was developed in 1946 by R. T. Jones (11), who adopted Munk's slender body theory to the problem. For very slender wings (A << 1) and small angles of attack, Jones' theory predicts:

$$C_L = \frac{\pi}{2} A \alpha .$$

More sophisticated attached flow lifting theories have been developed by Multhopp (1) and have been modified by others, such as Lamar (12). These theories are applicable to a wide range of aspect ratios and, in fact, may be used to bridge the gap from very low to high aspect ratio wings (between Jones' slender wing theory and Prandtl's lifting line theory). These theories do not include the effects of leading-edge vortices, however.

In 1955 Brown and Michael (13) developed a mathematical model for predicting lift of slender delta wings, which includes the effect of upper surface vortices. Unfortunately, their model predicts significantly more lift than is achieved

experimentally. Bartlett and Vidal (14) used a simple cross-flow theory to provide more accurate values of vortex lift. Their method relies, however, on experimentally determined coefficients.

Mangler and Smith (15) attempted to predict the shape of the coiled vortex sheet for a limited number of cases, in order to obtain a better estimate of lift. Their results predict less lift than Brown and Michael, but still more than experimentally obtained. More recent work by Smith (16) shows considerable refinement in the calculation technique, and corresponding improvements in agreement between theoretical and experimental pressure distributions are illustrated. The results are still restricted to conical flows, however.

Others (for example, Gersten (17)) have attempted to calculate the non-linear lift by assuming that the trailing vortex system is inclined to the wing planform. Although this technique relies on an arbitrary assumption concerning the inclination of the trailing vorticity, it has proven fairly successful for predicting lift for a variety of planforms.

Sacks, Lundberg, and Hanson (18) have developed a digital computer technique for predicting the trajectories of a family of discrete leading-edge vortex filaments, and utilizing the resultant vorticity distributions to obtain lift. Such a technique, while very tedious, is adaptable to wings of rather arbitrary planform, including those with

discontinuous leading edge sweep, i.e., double deltas, etc.

More recently, Polhamus (19) published a method for calculating vortex lift for slender deltas based upon a "leading-edge suction analogy." Polhamus first corrected the attached flow lift (usually referred to as "linear lift") for non-linear effects due to large angles of attack, and for leading edge separation. The resulting term is called "potential flow lift." Vortex lift is then calculated, based upon the assumption that the effect of a sharp leading edge is to rotate the leading-edge suction force vector 90°, from the chordwise direction to a normal force direction. In his report, Polhamus shows comparisons of his theoretical method with experimental data for delta wings having leading-edge sweep ranging from 63.4° to 83°, with good agreement. The result of Polhamus' analysis is an equation for lift of the form:

$$C_L = K_p \, \mathrm{Sin}\alpha \, \mathrm{Cos}^2\alpha + K_v \, \mathrm{Cos}\alpha \, \mathrm{Sin}^2\alpha \ .$$

Polhamus also shows that the K_p and K_v factors may be obtained from conventional lifting surface theories. K_p is $\left(\frac{\partial C_L}{\partial \alpha}\right)_{\alpha = 0}$ the familiar small angle lift-curve slope; and K_v is related in a simple way to K_p and $\frac{\partial C_{D_i}}{\partial C_L{}^2}$, the induced drag factor. The first term in the C_L equation represents the potential flow lift (corrected for leading-edge separation) and the second term represents the vortex lift.

Because of the success of the Polhamus method in predicting vortex lift and induced drag for simple deltas, it has been used as a basis for predicting lift and drag for the models of the present investigation. Some of the limitations of the method are discussed in more detail in later sections of this dissertation.

Pitching Moment

It should be noted that the Polhamus method, in its present form, yields no information as to the distribution of lift, i.e., pitching moments, associated with the vortex flow.

Wagner (20) has developed a potential flow linear lifting surface theory which yields information as to the distribution of leading-edge suction. It is possible that this technique, or some similar method, may be combined with the Polhamus theory to permit theoretical calculation of pitching moment information for configurations with vortex lift. For the present, however, no really satisfactory theoretical technique is available for predicting pitching moments for cases involving vortex lift.

Drag

For thin wings with sharp leading edges, the drag due to lift should be given by $C_D - C_{D_o} = C_L \tan \alpha$, the familiar relation for wings developing a pure normal force. Thus, the induced drag is determined entirely by the C_L vs. α relationship. A recent publication by Polhamus (21) utilizes

this technique in conjunction with the leading-edge suction analogy to theoretically predict induced drag for a number of configurations. Since the leading-edge suction analogy provides a much better estimate of C_L than previous techniques, the induced drag is also predicted with much better accuracy.

CHAPTER IV

THE EXPERIMENTAL INVESTIGATION

Test Facility

All tests were conducted in the University of Kansas low-speed wind tunnel, a closed-return tunnel with a three- by four-foot test section. The facility is equipped with large (three- by four-foot) plexiglas windows in the test section sidewalls, which give a wide field of view for flow visualization. The test section operates at atmospheric pressure. The tunnel is equipped with a six-component pyramidal balance for force measurements.

Test Conditions

Most of the testing was conducted at a dynamic pressure of 30 psf, which corresponds to a Reynolds number of 1.0×10^6 per foot. Early in the program, measurements of vortex breakdown were conducted at dynamic pressures ranging from 15 to 45 psf in order to investigate possible effects of Reynolds number changes. These tests showed that vortex breakdown was insensitive to the changes in Reynolds number, confirming the observations established by previous investigators.

Model Geometry - Delta Wings

In order to investigate rather completely the effects of geometry variations on vortex breakdown, a family of thirteen delta wing models was fabricated, with leading edge sweep angles from 45° to 85°. These models were constructed from 0.10-inch aluminum sheets with leading edges milled to a 15° wedge-shape with a 0.010-inch blunt edge. The very slight blunt edge was retained to insure straight leading edges (Figure 2.1). Since vortex core breakdown is associated with angles of attack greater than 10°, it was felt that planform geometry was of primary importance. For this reason, only uncambered, untwisted wings were tested. Since slender wing theory predicts that lift depends only on span and is independent of area, model span was held constant at a value of ten inches for the models having sweep angles from 45° to 72.5°.

For the higher sweep angles, the length of the maximum chord increases rapidly with increasing sweep. For example, an 85° sweep wing with a ten-inch span would have a maximum chord length of 57.3 inches. Since the test section height was only 36 inches, and the models were to be tested up to 60° angle of attack, a maximum centerline chord dimension of eighteen inches was established. The models with sweep angles from 75° to 85° fall into this category.

Models were mounted on a two-point strut system, with a pivot point near the trailing edge and a pitch strut located forward (Figure 3.1). This mounting system was selected over

a sting mount because the forward pitch strut provided a simple means for controlling model deflections without the necessity for adding a sting, which would cover a large portion of the more slender models.

During the course of the testing, some questions arose concerning the possibility of adverse effects of the wind tunnel boundaries on the very long (eighteen-inch chord) models. In order to examine this possibility, a series of nine-inch chord models was fabricated with sweep angles of 75°, 80°, and 85°. The nine-inch chord 75° and 80° models were constructed by shearing 0.030-inch aluminum sheet stock to the desired planform. The nine-inch chord 85° model was made from .125-inch steel for increased stiffness. These three models had square unbeveled edges.

During testing of the very slender (82.5 and 85°) eighteen-inch chord models, it became apparent that large model deflections were taking place near the apex. The wedge-shaped leading-edge design had resulted in a very thin cross section near the apex. As the load carried by this section increased, large bending moments were applied to this thin section. Consequently, the wings took on a "negative camber" which sometimes resulted in premature vortex breakdown, since the apex section was then at three or four degrees greater angle of attack than the main wing. Testing at reduced dynamic pressure (15 psf) reduced these deflections to acceptable levels.

On the large 85° delta model, a very low frequency "flutter" of sorts occurred. As the angle of attack for complete vortex breakdown to the apex was approached, the apex would deflect as described above, and breakdown would move forward to the apex. Then the loading was reduced, the deflection decreased, and the vortices reappeared. In such instances, the breakdown position could oscillate more than 50% of the chord at a fixed angle of attack. The frequency of these oscillations was of the order of one cycle per second. Testing at reduced dynamic pressure as noted above eliminated this effect. Thus, although the testing was intended to be concerned with rigid models, aeroelastic effects were occasionally present.

The nine-inch chord models with square leading edges did not suffer from this acute loss of stiffness near the apex, and consequently were not susceptible to the aeroelastic effects described above. In order to establish more clearly that a square-edged model was equivalent to a sharp-edged model for purposes of investigating vortex breakdown (except for elastic effects), a square-edged 60° delta model was constructed for direct comparison with a sharp-edged 60° delta of the same size. Although the results of vortex breakdown measurements indicate a shift of about 2° in initial breakdown angle, the progression trends are quite similar (Figure 4.2). Lift, drag, and pitching moment also compare favorably (Figures 5.20.1 and 5.20.2). It was felt that these results were sufficiently comparable to justify

the testing of square-edged models, and the modified deltas described in the next section were constructed with square edges.

Model Geometry - Modified Delta Wings

In order to ascertain more fully the effects of planform variations on vortex breakdown, a series of modified delta models was designed. From tests of simple deltas, an apparent relationship between breakdown angle and sweep angle has been established. However, as Earnshaw (4) has pointed out, if local sweep angle and angle of attack were the sole parameters involved, i.e., conical flow, simultaneous breakdown from trailing edge to apex would occur. This is, of course, in contradiction to experimental observations. Since the upper surface suction must go to zero at the trailing edge, a positive pressure gradient exists along the axis of the vortex. If breakdown is related to this pressure gradient, perhaps trailing edge geometry is of great importance. To test this hypothesis, several modifications were made to delta wings. A cropped 60° delta was designed to test the effects of wing tip geometry variations near the trailing edge. A diamond and an arrow wing were designed with a common 70° leading edge sweep and aspect ratios of 1.0 and 2.0 respectively. These values were selected to "bracket" the basic 70° delta, which has an aspect ratio of 1.46.

Because of the interest in recent years in double-delta planforms for supersonic and hypersonic airplane designs,

two double-delta models were designed. These models have forward panel leading-edge sweep angles of 75° and 80° respectively, and a common aft panel sweep of 65°. These models were designed to have the same aspect ratio (1.60) in order to investigate whether aspect ratio is more important than sweep in determining vortex breakdown.

The forward panel sweep angles of these models were selected to evaluate a step, or kink, which had appeared in the C_L versus α relationship of some similar models tested previously by the author (22). In the earlier tests, it appeared that an 80°/62° double-delta sweep combination resulted in an abrupt breakdown of the aft panel vortex, whereas a 75°/62° sweep combination resulted in a progressive continuous breakdown.

Because of the recent interest in ogee planforms, such as the Anglo-French Concorde supersonic transport, an ogee model was tested. The planform for this model was selected to match the outboard panel of a modified F5D tested by the NASA Ames Research Center (Reference 23). This planform has also been the subject of extensive flow visualization studies (References 7, 24). It was hoped that force and flow visualization data from this model could be correlated with data from other sources.

A complete table of model geometry is given in Figure 1. Model drawings are given in Figures 2.1 through 2.7.

Flow Visualization Technique

The flow visualization technique selected for these tests was a conventional schlieren system utilizing eight-inch diameter parabolic mirrors of seventy-two-inch focal length. A 375 watt incandescent lamp fitted with a knife-edge was used as a light source, and photos were obtained using the back of a 35 mm single-lens reflex camera with focal plane shutter system. Use of a focal plane shutter camera permitted mounting the lens system on a simple open optical bench, without the necessity of constructing a lengthy light-tight box between lens and camera. Since the image area to be photographed was relatively small, the 375 watt lamp provided sufficient illumination for use with black and white ASA 1200 film.

The system was arranged to pass the collimated beam horizontally through the test section windows which are one-inch thick plexiglas, three- x four-foot. The beam was angled vertically a few degrees to distinguish right and left panel vortices, following the method suggested by Earnshaw (9). Provisions were made for moving the schlieren system fore and aft, as well as vertically, in order to cover the required field of view from several inches aft of the trailing edge up to the apex.

Visualizing vortices in a low speed flow turned out to be much easier than the author had anticipated. Vortices were seen on the very first test run, and although the tunnel windows contained numerous flaws and scratches, vortex

breakdown is rather distinct as seen in the photographs (Figure 3). Furthermore, extremely high airspeeds were not required to make the vortices visible. For example, using a 75° wing, the vortices produced sufficient density gradients to remain visible at tunnel speeds as low as forty miles per hour.

The schlieren technique proved so satisfactory during initial trials that it was quickly adopted as the primary flow visualization method, because of its obvious advantages over methods which require placing instruments into the flow field.

Force Measurements

Force measurements were made using the wind tunnel main balance, a pyramidal strain gage balance system with manual readout. Since yawed configurations were not tested, only lift, drag and pitching moment data were recorded.

Corrections

The question of wind tunnel boundary corrections is always problematical, since accurate prediction of the corrections requires a prior knowledge of chordwise and spanwise loading distributions. It is always desirable to test the largest possible models from the standpoint of measurement ease and obtaining the highest possible Reynolds number. On the other hand, boundary corrections are minimized by utilizing the smallest possible models. In the present tests, it

was felt vital to make the models rather small, since neither the load distributions nor the possible viscous wall effects on the wing vortices were known in advance.

The force data obtained were corrected for wing induced downwash and blockage effects using the theoretical methods given by Pope (25). These corrections were relatively small, amounting to 0.7° maximum downwash correction to the angle of attack and 0.7% maximum blockage correction to velocity. The blockage correction was primarily due to wake blockage, a result of the high drag characteristics of the wings tested.

In addition, the results were corrected for mounting support interference effects based upon image runs. These corrections were uncomfortably large, amounting to a maximum ΔC_L of 0.05 to 0.06, with corresponding drag and pitching moment corrections. Detailed build-up runs established that the principal interference effects were due to the mounting lugs which attached the wing to the support struts. Furthermore, because of the symmetry of the models tested, inverted runs could be utilized to check the image corrections. These correlations confirmed the ΔC_L corrections within $\pm.005$. Apparently the forward mounting lug created a wake which significantly reduced the lower surface lift. As might be expected, these corrections were largest for the most slender models.

Since all wings tested were symmetrical, zero C_L and C_M should correspond to zero angle of attack. Therefore, to account for tunnel upwash, all data have been corrected to

zero angle of attack at zero lift. This correction did not result in zero C_M for all models at zero angle of attack, however. A residual C_M implies a curvature in the tunnel flow field at zero angle of attack. Furthermore, the C_M data at low angles contained anomalous non-linearities which were apparently induced by a slight leakage around the support strut windshield.

Since the primary interest of these investigations was in characteristics near the angles for vortex breakdown, the questionable C_M data at low angles of attack have been discarded, and only data corresponding to angles of attack greater than 10° are presented.

CHAPTER V

RESULTS OF THE EXPERIMENTAL INVESTIGATIONS

Vortex Breakdown at the Trailing Edge for Delta Wings

During the initial testing period, an attempt was made to determine the importance of upper surface boundary layer trip strips in stabilizing the secondary separation as suggested by Earnshaw (9) and, hence, possibly stabilizing the vortex breakdown position. To investigate this effect, the 72.5° sweep model was tested without roughness, and with medium, and then coarse grit sandpaper glued to the upper surface. The roughness did not effect the initial breakdown at the trailing edge, but it did seem to stabilize somewhat the breakdown position on the wing upper surface. Since both grades of sandpaper provided the stabilizing effect, the finer grade was selected (120 grit). All subsequent testing was conducted with wings fitted with sandpaper of this grit. The sandpaper covered the entire upper surface, except for a 0.15-inch margin allowed at all edges to insure that the clean edge geometry would not be disturbed.

Even though the angle of attack for initial breakdown did not change, comparisons of schlieren photos from the 72.5° delta wing with and without the fine grade roughness reveal a distinct difference in flow characteristics

(Figure 3.2). The vortex core patterns without roughness show definite evidence of longitudinal waves prior to breakdown, and as shown, the actual breakdown process appears to be a rapid coiling of the vortex filament. Initial breakdown on the run with roughness, on the other hand, is not preceded by the appearance of the waves. Furthermore, the breakdown patterns appear as completely turbulent wakes, without evidence of the helical coiling described above. During subsequent testing, more than 500 photos were recorded of vortices on wings with roughness, and not a single one of these photos showed the coiling pattern.

The terms "breakdown at the trailing edge" or "initial breakdown" require rather careful definition, since the breakdown point was never stable at the trailing edge. Rather, the terms refer to the lowest angle of attack at which breakdown crosses the trailing edge. The initial breakdown data obtained in the present tests for delta wings with sweep angles less than 75° are generally in agreement with the results given by Poisson-Quinton and Ehrlich (8). It is noted that for sweep angles greater than 75°, breakdown angle is nearly constant, a fact not evident in earlier data. Since these results indicated a change in the trend from previously published data, some additional tests were conducted to establish the results more firmly. First, a question arose as to whether the forward support strut mounting lug used on the models might trigger breakdown prematurely. To check this possibility a second dummy

mounting lug was attached just forward of the standard lug, and hence closer to the leading edge. Runs with and without the dummy lug showed no change in initial breakdown angle of attack.

Second, the possibility of wind tunnel wall interactions on vortex breakdown was examined. The three nine-inch chord delta models described earlier in this thesis were designed for this purpose. The results of tests with the small models show excellent agreement with the larger scale results (Figure 6).

This correlation demonstrates that the results obtained were not influenced significantly by the wind tunnel boundaries. Furthermore, the small 85° delta wing was sting mounted. Therefore, agreement between the data obtained from this model and the larger 85° delta wing is further indication that the vortex breakdown results were not influenced adversely by model mounting struts.

Lowson (26) published a very interesting paper in 1964 in which the mechanism of breakdown on an 80° delta is lucidly discussed. He found that the breakdown on this wing was subject to a hysteresis effect in the range of 35° to 40° angle of attack. In the present investigations, numerous attempts were made to produce such a hysteresis in vortex breakdown on various models, with entirely negative results. It should be noted again, at this point, that the models of the present investigation were fitted with roughness on the upper surfaces, while Lowson's model was apparently smooth.

Unfortunately, the hysteresis checks of the present tests were not carried out using a smooth model in order to clarify the origin of this discrepancy. At least the range of angles for initial breakdown from Lowson's tests (36° to 41°) is in agreement with the present results for an 80° wing (38° to 38.5°). Extrapolation of the data given by Poisson-Quinton and Erlich (8) would lead one to predict an initial breakdown angle of at least 45° for the 80° sweep wing, a significantly higher value.

The abrupt change in trend of vortex breakdown versus sweep for sweep angles greater than 75° suggests the existence of a different limiting mechanism for breakdown of these very slender wings. It was observed that vortex breakdown on these wings was quite sensitive to yaw. There was a definite tendency for the vortex from one wing panel to become displaced vertically above the other, and subsequently for vortex breakdown to take place on the displaced vortex at an angle of attack as much as 10° below the angle of attack for breakdown on the second side. When this occurred, a small yaw adjustment of the model was made to restore the symmetry of the vortices. Often a yaw adjustment of 0.1° or 0.2° was sufficient to restore the symmetry, and, subsequently, the right-and left-hand panel vortices experienced breakdown at angles of attack differing by 2° or less. In these cases, the average of the two angles of attack has been designated as the initial breakdown angle for the particular wing being tested.

Chordwise Progression of Vortex Breakdown - Delta Wings

During initial testing, specific attempts were made to establish vortex breakdown points aft of the trailing edge as a function of angle of attack. These attempts were entirely unsuccessful. As mentioned previously, when breakdown first appeared, it moved rapidly from a position aft of the field of view (20% to 30% of C_o behind the trailing edge) to a position approximately 20% forward of the trailing edge. This is reflected in the flat portion of the curves (Figure 4.1). As the angle of attack was further increased, the perturbations of the breakdown point at a given angle of attack became much smaller. For example, at the angle of the attack for initial breakdown at the trailing edge, perturbations in breakdown position were as much as 20% to 50% C_o, while the perturbations in breakdown position near the apex were of the order of only 1% C_o. For wings having lower sweep angles, the perturbations were much less than with the highly swept configurations.

The character of progression indicated above may be implied from considerations of the relationship between pressure gradient along the axis of the vortex core and the stability of an isolated vortex. That is, a pressure increasing in the direction of flow along the axis is destabilizing and conversely, a pressure decreasing along the axis is stabilizing (See Bossel (2) or Werle (5, 6)).

Since the adverse pressure gradient, dp/dx, is maximum near the trailing edge of the wing, the vortices first become

unstable here. At more forward positions dp/dx is reduced in magnitude, resulting in more stable vortices. Furthermore, the very slow movement of breakdown position near the apex is a result of the presence of a nearly conical flow field in this region (dp/dx approaching zero).

For the wings of lower sweep (45°, 50°, 55°), vortices at the trailing edges were not observed. These vortices apparently produced such low density gradients at the angles for breakdown, that they were not clearly visible with the schlieren system. At higher angles, however, the vortices became visible on the 50° and 55° wings, and the breakdown positions could be identified. Vortices were never observed on the 45° delta wing, even though the tunnel dynamic pressure was doubled for one run in an attempt to increase the density gradients to a level which would make the vortices, if present, more easily visible. The vortex lift produced by the 45°, 50°, and 55° wings is so small that knowledge of initial breakdown is probably not of great practical importance.

Comparisons of vortex breakdown positions from the present tests with the results of other investigations generally show quite similar trends as to the forward progression of vortex breakdown (Figures 4.1.2 and 4.1.3). There are, however, distinct shifts in the angles for initial breakdown. It should be noted that some of the results from other sources were obtained using models which were beveled on only one surface. Such models are not quite symmetric,

having a slight camber which influences the angle for zero lift. The discrepancies in angle for initial breakdown are about 2° or 3° at most, which is the order of magnitude of such camber effects on angles of zero lift.

Chordwise Progression of Vortex Breakdown - Modified Delta Wings

A special remark needs to be made concerning the definition of vortex breakdown at the "trailing edge" for wings with swept trailing edges (diamond, arrow, and ogee wing). For these wings, the trailing edge is defined herein as most aft portion of the wing. Since measurements of spanwise position of the vortex cores were not made, it is not possible to state unequivocally when a given breakdown point is at the local trailing edge. Examination of the breakdown position plots (Figures 4.4 and 4.7) shows that upon initial breakdown, the breakdown point moves to a position approximately 20% C_o forward of the trailing edge (the flat region of the curves from 0 to 20% C_o as discussed previously for delta wings). Therefore, the breakdown point crosses even the swept trailing edges at approximately the angle of attack for initial breakdown.

Cropped Delta Wing

The 12.4% tip cropping of a 60° delta wing has a nearly negligible effect on vortex breakdown (Figure 4.3). In fact, the effect of cropping was less than the effect of changing

the edge shape from beveled to square.

Diamond and Arrow Wings

Variations in trailing edge geometry have a surprisingly small effect on initial breakdown (Figure 4.4). Since vortex breakdown is related to pressure gradient, one might expect that a parameter such as aspect ratio would be appropriate for correlating breakdown behavior. The data below, however, convincingly illustrates the fact that leading edge sweep is much more important than trailing edge sweep or aspect ratio in the determination of initial breakdown.

EFFECT OF ASPECT RATIO ON VORTEX BREAKDOWN

Wing	Aspect Ratio	Initial Breakdown Angle of Attack	Equivalent Delta Sweep	Breakdown Angle for Equivalent Delta
70° Diamond	1.0	27.0°	(76°)	37.5°
70° Delta	1.46	29.0°	--	--
70° Arrow	2.0	28.0°	(63.4°)	16.5°

Double-Delta Wings

Breakdown characteristics for the double-delta wings are quite different than for simple deltas (Figures 4.5 and 4.6). The schlieren photos for these configurations are particularly interesting since they show the interaction between two distinct vortex cores. The aft panel vortex

core, having less strength, coils in a helical fashion about the apex panel vortex (Figure 3.3). Similar wind tunnel observations have been made with the water vapor condensation vortices reported by Sacks, Lundberg and Hanson (18). At higher angles of attack the aft panel vortex disappears, apparently as a result of breakdown. The forward panel vortex remains visible, without breakdown, for another 4° to 6°.

Previous investigations by the author (22) which consisted of velocity measurements in the vortex fields of double-delta wings did not reveal the coiling of the aft panel vortex core which is shown by the water vapor and schlieren photographs. Certainly the strength of the aft panel vortex is much less than that of the strake vortex. Therefore the velocities induced by the aft panel vortex would be much smaller and thus more difficult to measure. On the other hand, the probe utilized in the prior investigations was sensitive enough to detect even the small secondary counter-rotating vortices located near the leading edge. A more plausible explanation is that the position of the coiled aft panel vortex core was affected by the presence of the velocity probe.

As noted above, initial breakdown for both double-delta wings is delayed considerably by the addition of the strake, as shown below:

EFFECT OF STRAKES ON BREAKDOWN

Wing	Angle of Attack for Initial Breakdown	
	Aft Panel Vortex	Strake Vortex
65° Delta	19.3°	--
75°/65° Double-Delta	29.5°	35.1°
80°/65° Double-Delta	31.5°	35.5°

Thus, the strake vortex has a definite stabilizing influence on the aft panel vortex. This observation concurs with the conclusion reached by Earnshaw (9) that apex sweep is more important than sweep near the trailing edge in influencing breakdown.

Ogee Wing

With this planform a single continuously curved vortex is formed on each side. The vortex breakdown position results as a function of angle of attack for the ogee wing show a number of interesting characteristics associated with the ogee planform (Figure 4.7). First, the initial breakdown occurs at 18°, a much higher angle of attack than would be anticipated for the aft panel alone. The basic aft panel has a leading-edge sweep of 55°, which would result in an initial breakdown angle of attack of 10° based upon the delta wing results (Figure 6).

Second, the forward progression of vortex breakdown is at a much lower rate than for delta wings. While the delta wings required an angle of attack change of 18° to 20° for vortex breakdown to move from trailing edge to apex, the ogee wing requires 33°. This is not surprising when one realizes that the ogee wing sweep increases as the apex is approached. Thus, the vortices become much more stable near the apex. The angle of attack of 51° for breakdown at the apex corresponds roughly to an apex breakdown angle of 58° for a delta wing having the same apex sweep (77° sweep).

The breakdown curve also shows a definite tendency for the breakdown point to remain at the 81% chord position. This kink apparently is associated with the inflection in the leading edge.

Discussion of Force Characteristics

Lift and Pitching Characteristics - Delta Wings

Using the Polhamus leading-edge suction analogy discussed earlier, theoretical potential lift and total lift relationships for each delta wing have been calculated for comparison with the experimental results. For the 45° and 50° delta wings (Figures 5.1.1 and 5.2.1), very little vortex lift is produced. The 55° to 67.5° wings show that an increasing percentage of theoretical vortex lift is produced (Figures 5.3.1 to 5.6.1). Mr. Polhamus has pointed out to the author that the leading-edge suction analogy is apt to over-predict vortex lift for wings of moderate sweep, since the vortices

produced by such wings do not stream perpendicular to the trailing edge and cannot, therefore, produce full suction lift. If the wing planform trailing edge were perpendicular to the vortex core, the full vortex lift could be effective. As illustrated in the sketch below, for highly swept deltas, the additional area required becomes vanishingly small.

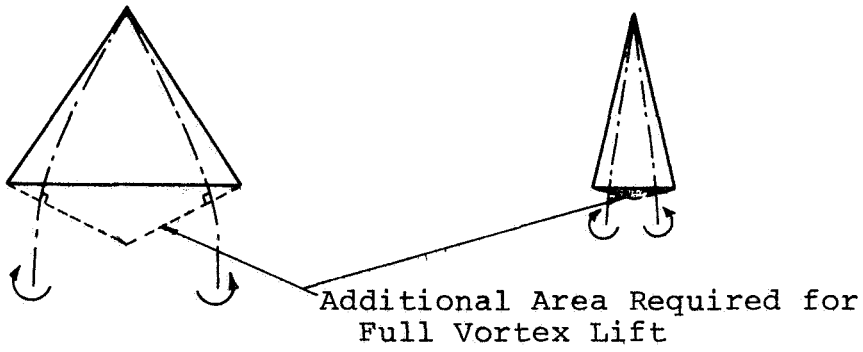

Low Sweep High Sweep

Limitations of Vortex Lift Theory

Thus the theory should be more accurate for the more highly swept wings.

In the range of sweep angles from 70° to 77.5°, the experimental results show excellent agreement with the Polhamus theory. Furthermore, the initial vortex breakdwon measurements, as indicated on the graphs, mark clearly the onset of deviation from the theory. Thus the vortex breakdown measurements, in conjunction with the Polhamus theory, provide an excellent means for predicting lift for these configurations.

For wings with sweep angles from 80° to 85°, a progressive deviation of experimental results from theory is noted

prior to initial breakdown (Figures 5.11.1 to 5.13.1). This range of leading-edge sweep angles corresponds approximately to the range of sweep angles for which vortex breakdown is independent of sweep, as discussed in the earlier section concerning vortex breakdown.

Maltby and Peckham (27) have shown that for very slender wings a condition can be reached wherein the vortex sheets from the two sides meet at the centerline, eliminating the region of reattached streamwise flow usually found in the center region of the wing upper surface. This effect is indicated in the sketches of cross-flow vortex sheets below:

Moderate Sweep
(No Contact)

Very High Sweep
(Vortex Sheets in Contact)

Limitations of Vortex Lift Theory

At angles of attack above initial contact, the vortex sheets elongate vertically and the vortex cores are forced to move upward. Such displacement would be accompanied by a reduction in vortex lift.

In extreme cases (very slender wings) the vortex sheets may "tear" and form multiple rolled up cores from each side. The tearing mechanism is not usually symmetric and often

results in one vortex core becoming vertically displaced above another. From a practical standpoint, the onset of vortex sheet tearing probably limits the usable angle of attack range for such wings because of the rolling moments associated with the unsymmetrical flow fields.

The lift loss resulting from parallel vortex displacement would presumably not be abrupt, but rather a gradual reduction in the proportion of vortex lift actually achieved relative to the theoretical amount. Although measurements of vortex sheet trajectories were not conducted in the present investigation, it seems reasonable to assume that the deviations noted from the theoretical lift for very slender (> 80°) wings are due to this displacement phenomenon. When vortex breakdown occurs on these wings, it precipitates a rather abrupt loss in lift, as with the wings of somewhat lower sweep.

As previously discussed, no theory exists presently for adequately predicting pitching moment characteristics of wings with vortex lift. The experimental pitching moment characteristics associated with the 45° to 67.5° delta wings (Figures 5.1.1 to 5.6.1) show a pitch-down tendency at maximum C_L (which corresponds approximately to vortex breakdown at the apex). Initial vortex breakdown seems to have little effect on the force characteristics of these configurations.

For the wings with sweep angles from 70° to 85°, the maximum C_L corresponds approximately to vortex breakdown at

the trailing edge, and also to a marked pitch-up tendency (Figures 5.7.1 to 5.13.1). As the breakdown approaches the apex, the pitch-up tendency is reduced, and in some cases is replaced by a pitch-down. After complete breakdown to the apex, a level of stability is restored which is approximately equal to that which existed prior to initial breakdown. Thus initial breakdown is accompanied by a loss in lift over the aft portion of the wings, causing pitch-up. As the breakdown point moves forward, the loss of lift becomes distributed over the entire surface, and the pitch-up tendency vanishes.

Lift and Pitching Characteristics - Modified Delta Wings

Cropped Delta Wing - Theoretical lift, based upon the leading-edge suction analogy for this wing, has been calculated by two methods: first, using the K_p and K_v values for a delta wing of the same aspect ratio; and second, by utilizing Wagner's method (20) which is appropriate to the non-delta planform. The C_L values calculated by these methods are labeled "POLHAMUS-Delta" and "POLHAMUS-Cropped Delta," respectively, on the graph (Figure 5.14.1). It should be pointed out here that Polhamus (19) specifically warns against using the delta wing results for non-delta planforms. Nevertheless, the two theoretical curves are reasonably close. Comparison of the two theoretical curves reveals that the "exact" (Wagner) method predicts more potential lift and less vortex lift than the equivalent delta, as one might suppose. The experimental lift data

for this configuration show little difference from the basic 60° delta. The pitching moment data for the cropped delta show slightly less pitch-down tendency after maximum C_L than the basic delta, apparently as a result of removing the area near the trailing edge.

Diamond and Arrow Wings - The effects of adding and removing area near the trailing edge are illustrated by comparing the 70° delta results with those from the diamond and arrow wings (Figures 5.7.1, 5.15.1 and 5.16.1). For the diamond and arrow wings, theoretical values have been determined using the K_p and K_v values for the actual planforms (calculated using the methods of Reference 20), and also using K_p and K_v values for delta wings of the same respective aspect ratios. Although the two methods give quite different amounts of potential lift and vortex lift, the total theoretical lifts calculated are surprisingly close. The experimental data for the arrow wing show less lift than either theoretical curve, but in fact almost the same lift coefficients as the basic 70° delta, prior to initial breakdown. After initial breakdown, the arrow wing lift decreases much less rapidly than the delta.

The diamond wing theoretical curves illustrate that the potential lift is practically uneffected by the re-distribution of area, while the vortex lift is reduced significantly for the diamond. The experimental data for the diamond show even more lift than predicted for the equivalent delta. This

is attributed to additional vortex lift generated by the influence of the vortices acting on the area aft of the maximum span point. As discussed in an earlier section, the Polhamus theory does not account for gains or losses in vortex lift due to such area changes.

Comparisons of the pitching characteristics of the arrow, diamond, and delta wings illustrate the effects of area near the trailing edge. First, it is noted that all three wings exhibit a pitch-up tendency at a lift coefficient of about 0.8, prior to initial vortex breakdown. As area at the trailing edge is added (progressing from arrow to delta to diamond), the post-breakdown behavior is a progressive pitch-down tendency. Thus, the addition of area at the trailing edge is effective in controlling pitch-up; but the effectiveness of this area addition seems to be greatest <u>after</u> initial vortex breakdown.

<u>Double-Delta Wings</u> - At the time of this writing, the problem of obtaining satisfactory leading-edge suction values for double-delta wings has not been resolved. Therefore, "exact" values for K_p and K_v for use in Polhamus' equation cannot be calculated. In principle, it should be possible to obtain these values using the potential flow lifting surface method of Wagner, and the author understands that work on this problem is being conducted by researchers at NASA Langley Research Center. It is quite possible that within a few months this problem will be resolved. For the

present, however, it was necessary to use the approximate method for determining K_p and K_v based upon a simple "equivalent" delta wing of the same aspect ratio as the double-delta wings. Since the two double-delta wings tested were designed to have the same aspect ratio, the theoretical equivalent delta C_L values are equal for the two wings. In spite of its limitations, the theoretical equivalent delta C_L curve compares favorably with the experimental results (Figures 5.17.1 and 5.18.1).

Ogee Wing - Wind Tunnel Results - The theoretical K_p and K_v values for use in Polhamus' equation are based upon a delta wing of the same aspect ratio, for the same reasons as noted above. Again, the equivalent delta provides a fair theoretical approximation to the experimental results (Figure 5.19.1). In this case however, the experimental lift slightly exceeded the theory in the angle of attack range prior to initial breakdown.

At initial breakdown, both the lift and pitching moment curves show a slight kink. As the angle of attack is increased further, the lift curve shows a progressive loss in vortex lift as the breakdown point moves forward. The loss in lift for angles beyond maximum C_L is rather gradual compared to the delta wings.

The pitching moment curve shows a slight pitch-up kink at initial breakdown, but then recovers fully and even reflects a pitch-down beyond maximum C_L. It appears that

the ogee leading edge, with its slow progression of vortex breakdown, provides very desirable stability characteristics beyond initial breakdown.

Ogee Wing - Comparisons with Flight Test - A comparison between this model and flight test is afforded by the results obtained by NASA Ames Research Center with a modified F5D airplane as reported by Rolls, Koenig, and Drinkwater (23). The ogee wing of the present tests was designed to match the outboard panel of this aircraft. The lift and drag results from flight tests compare quite favorably with the present ogee wing results (Figure 5.21).

Based upon tuft observations and statements made in the reference concerning buffeting of the airplane, it appears that initial vortex breakdown occurred on the airplane at an angle of attack between 15° and 18°. This corresponds with the occurrence of a noticeable change in slope of the flight test C_L - α curves, another indication of the effects of breakdown. Furthermore, it is noted that no flight test data points were obtained in the range of angles of attack from 18° to 20°. Based upon the present wind tunnel results, initial vortex breakdown should be accompanied by a loss of stability which would be recovered at higher angles of attack. It would be very difficult, however, to obtain stabilized flight at the particular angle of attack for vortex breakdown. These observations add additional support to the conclusion that breakdown on the aircraft occurred between 15° and 18°.

The present wind tunnel results (Figure 4.7) show initial breakdown at about 17.5°.

The flight test results show a somewhat greater loss in lift after initial breakdown than the present results, indicating a more rapid movement forward of the vortex breakdown position.

It should be noted that the flight test drag data presented are total C_D, rather than $C_D - C_{D_o}$. It was not possible, of course, to determine C_{D_o} from the flight test results. In spite of this, the flight test drag results show that the shape of the polar corresponds quite closely with the present results, indicating good correlation of drag due to lift.

Since the ogee model of the present tests was not fitted with control surfaces, it was not possible to compare pitching moment results from the present tests with the trimmed flight test conditions. From the comparisons of lift and drag results, however, as well as breakdown observations, it is evident that rather good force correlations are possible between full scale flight tests (Reynolds number $\simeq 20 \times 10^6$) and rather small scale wind tunnel models (Reynolds number $\simeq 0.7 \times 10^6$).

Drag Due to Lift - Delta and Modified Delta Wings

The induced drag characteristics of all the thin sharp-edged wings tested in the present investigations are compared

with theoretical values based upon zero leading-edge suction given by the following expression:

$$C_D - C_{D_o} = C_L \tan \alpha \ .$$

The appropriate experimental C_L vs. α data have been used in this equation. These comparisons (Figures 5.1.2 to 5.20.2) show excellent agreement, indicating clearly the validity of the assumption of zero leading-edge suction.

The only significant discrepancies between measured and theoretical drag due to lift occur at lift coefficients beyond maximum C_L. In these cases, the measured drag is somewhat higher than predicted by normal force theory. This indicates an increase in parasite drag at these very high angles. Since even the thin wings used in the present tests had finite thickness, it is not unreasonable that such a change might occur. In any case, the theory is quite adequate for all but the extreme post-stall angles of attack.

One might argue that a theoretical C_L vs. α relationship should be used in the expression above to obtain a more "pure" theoretical result. Of course, one would use such a theoretical method in any preliminary design analysis. However, in the present instance such a method would not be helpful, since deviations between experimental and theoretical drag could not be attributed to an error in drag theory without first checking to see whether there was discrepancy between the theoretical and experimental <u>lift</u> relationship.

From the present results, it is clear that adequate lifting theories will lead to accurate drag prediction, as indicated by Polhamus' recent report on this subject (21).

An alternate approach to the analysis of slender, sharp-edged wings would be to analyze the forces in terms of normal and chordwise components. Since the chordwise forces are virtually zero, such an analysis method would be somewhat simpler. In fact, the only reason for the lift and drag component analysis used in the present thesis is the strong custom associated with the use of the C_L and C_D parameters.

CHAPTER VI

CONCLUDING REMARKS

The initial vortex breakdown boundary for delta wings published by Poisson-Quinton and Erlich has been closely verified. In addition, the boundary has been extended to sweep angles of 85°. For sweep angles greater than 75°, the present tests have established that breakdown is nearly independent of sweep.

Forward progression of breakdown for a given wing from trailing edge to apex proceeds rapidly at first, then more slowly near the apex. The total angle of attack change associated with breakdown movement from trailing edge to apex is about 18° to 20° for simple deltas.

Force measurements have verified that Polhamus' leading-edge suction analogy provides an excellent means for predicting C_L for wings of medium sweep, operating below the critical angle for initial vortex breakdown. For very slender wings, a merging of right-and left-wing panel vortex sheets seems to reduce vortex lift, resulting in significant deviations from Polhamus' theory prior to initial breakdown. The advent of vortex breakdown, of course, limits the vortex lift on all configurations.

While no adequate theory exists for predicting pitching moments generated by vortices, the observed pitching characteristics are compatible with the observed vortex breakdown patterns. Drag due to lift for all models tested was predicted adequately as the streamwise component of a pure normal force.

Tests of modified delta wings have verified that apex sweep is much more important than trailing edge geometry in determining initial breakdown. Initial breakdown appears independent of trailing edge sweep. Strakes, however, have a dominant influence on breakdown behavior.

Force results and vortex breakdown observations of an ogee wing compare quite favorably with NASA flight test results from a similar configuration, in spite of a factor of 20 change in Reynolds number, indicating the validity of small scale tests.

REFERENCES

1. Multhopp, H., "Methods for Calculating the Lift Distribution of Wings (Subsonic Lifting-Surface Theory)," A.R.C. R. & M., No. 2884, 1955.

2. Bossel, H. H., "Stagnation Criterion for Vortex Flows," AIAA Journal, Vol. 6, No. 6, June, 1968, p. 1192.

3. Ludwieg, H., "Erklarung des Wirbelaufplatzens mit Hilfe der Stabilitatstheorie fur Stromungen mit schraubenlinienformigen Stromlinen," Zeitschrift fur Flugwissenshaften, Vol. 13, No. 12, 1965, p. 437.

4. Earnshaw, P. B. and Lawford, J. A., "Low-Speed Wind Tunnel Experiments on a Series of Sharp-Edged Delta Wings," RAE TN Aero. 2780, 1961.

5. Werle, H., "Sur L'Eclatement des Tourbillons d'Apex d'une Aile Delta aux Faibles Vitesses," La Recherche Aeronautique, No. 74, Janvier-Fevrier, 1960. (Translated into English in Ref. 6).

6. Snyder, M. H., Jr., "On the Theory of the Delta Wing," Report AR 66-4, Wichita State University, 1966.

7. Poisson-Quinton, Ph. and Werle, H., "Water Tunnel Visualization of Vortex Flow," Astronautics and Aeronautics Mag., June 1967.

8. Poisson-Quinton, Ph. and Erlich, E., "Hyperlift and Balancing of Slender Wings," NASA TT-F-9523, August, 1965.

9. Earnshaw, P. B., "Measurements of Vortex-Breakdown Position at Low Speed on a Series of Sharp-Edged Symmetrical Models," RAE Tech. Rept. No. 64047, November, 1964.

10. So, Kwan L., "Vortex Phenomena in a Conical Diffuser," AIAA Journal, Vol. 5, No. 6, June, 1967, p. 1072.

11. Jones, R. T., "Properties of Low-Aspect-Ratio Pointed Wings at Speeds Below and Above the Speed of Sound," NACA Rept. 835, 1946.

12. Lamar, John E., "A Modified Multhopp Approach for Predicting Lifting Pressures and Camber Shape for Composite Planforms in Subsonic Flow," NASA TN D-4427, July, 1968.

13. Brown, C. E. and Michael, W. H. Jr., "On Slender Delta Wings with Leading-Edge Separation," NACA TN 3430, 1955.

14. Bartlett, G. E. and Vidal, R. J., "Experimental Investigation of Influence of Edge Shape on the Aerodynamic Characteristics of Low Aspect Ratio Wings at Low Speeds," Jour. Aero. Soc., Vol. 22, No. 8, August, 1955.

15. Mangler, K. W. and Smith, J. H. B., "A Theory of the Flow Past a Slender Delta Wing with Leading Edge Separation," Proc. Royal Soc. of London, Series A, Vol. 251, 1959, p. 200.

16. Smith, J. H. B., "Improved Calculations of Leading-Edge Separation From Slender, Thin, Delta Wings," Proc., Royal Society of London, Series A, Vol. 306, 1968, p. 67.

17. Gersten, K., "Calculation of Non-Linear Aerodynamic Stability Derivatives of Aeroplanes," Deutsche Forshungsanstalt fur Luftfahrt, Braunschweig Institut fur Aerodynanik DK 533.691.11, March, 1961.

18. Sacks, A. L., Lundberg, R. E., and Hanson, C. W., "A Theoretical Investigation of the Aerodynamics of Slender Wing-Body Combinations Exhibiting Leading-Edge Separation," NASA CR-719, 1967.

19. Polhamus, E. C., "A Concept of the Vortex Lift of Sharp-Edge Delta Wings Based on a Leading-Edge Suction Analogy," NASA TN D-3767, 1966.

20. Wagner, Siegfried, "Singularitatenverfahren der Tragflachentheorie bei inkompressibler Stromung," Ingenieur-Archiv, Vol. 36, 1968, p. 403. ↓ Beitrag zur

21. Polhamus, Edward C., "Application of the Leading-Edge Suction Analogy of Vortex Lift to the Drag Due to Lift of Sharp-Edge Delta Wings," NASA TN D-4739, August, 1968.

22. Wentz, W. H., Jr. and McMahon, M. C., "Further Experimental Investigations of Delta and Double-Delta Wing Flow Fields at Low Speeds," NASA CR-714, February, 1967.

23. Rolls, Stewart; Koenig, David G.; and Drinkwater, Fred J., III, "Flight Investigation of the Aerodynamic Properties of an Ogee Wing," NASA TN D-3071, December, 1965.

24. Rolls, Stewart, "Ogee Wing Improves Low-Speed Characteristics of Deltas," Space/Aeronautics, December, 1965.

25. Pope, Alan, Wind Tunnel Testing, John Wiley and Sons.

26. Lowson, M. V.: Some Experiments with Vortex Breakdown, Jour., Royal Aero. Soc., May, 1964.

27. Maltby, R. L., and Peckham, D. H., "Low Speed Flow Studies of the Vortex Patterns Above Inclined Slender Bodies Using a Smoke Technique," R.A.E., Addendum to Tech Note Aero 2482, March, 1957.

MODEL GEOMETRY

Model	Leading-Edge Sweep	Aspect Ratio	Area (in^2)	Span (in)	$\bar{C}$(in)	C_0(in)	Edges
45° Delta	45°	4.00	25.00	10.00	3.33	5.00	Chamfered
50° Delta	50°	3.36	29.80	10.00	3.97	5.96	Chamfered
55° Delta	55°	2.80	35.70	10.00	4.76	7.14	Chamfered
60° Delta	60°	2.31	43.30	10.00	5.77	8.66	Chamfered
65° Delta	65°	1.86	53.61	10.00	7.15	10.72	Chamfered
67.5° Delta	67.5°	1.66	60.36	10.00	8.05	12.07	Chamfered
70° Delta	70°	1.46	68.69	10.00	9.16	13.74	Chamfered
72.5° Delta	72.5°	1.26	79.29	10.00	10.57	15.86	Chamfered
75° Delta	75°	1.07	86.81	9.64	12.00	18.00	Chamfered
77.5° Delta	77.5°	.886	71.82	7.98	12.00	18.00	Chamfered
80° Delta	80°	.706	57.13	6.35	12.00	18.00	Chamfered
82.5° Delta	82.5°	.526	42.66	4.74	12.00	18.00	Chamfered
85° Delta	85°	.350	28.35	1.58	12.00	18.00	Chamfered
Small 75° Delta	75°	1.07	21.70	4.82	6.00	9.00	Square
Small 80° Delta	80°	.706	14.28	3.18	6.00	9.00	Square
Small 85° Delta	85°	.350	7.09	.788	6.00	9.00	Square
Square-Edged 60° Delta	60°	2.31	43.30	10.00	5.77	8.66	Square
Cropped 60° Delta	60°	1.80	42.63	8.76	5.85	8.66	Square
70° Arrow	70°	2.00	50.00	10.00	6.64	9.48	Square
70° Diamond	70°	1.00	100.00	10.00	13.32	19.96	Square
75°/65° Double-Delta	75°/65°	1.60	62.50	10.00	9.06	14.48	Square
80°/65° Double-Delta	80°/65°	1.60	62.50	10.00	9.38	16.32	Square
Ogee	Variable	1.70	58.82	10.00	6.89	10.83	Square

Figure 1. Tabulated Model Geometry

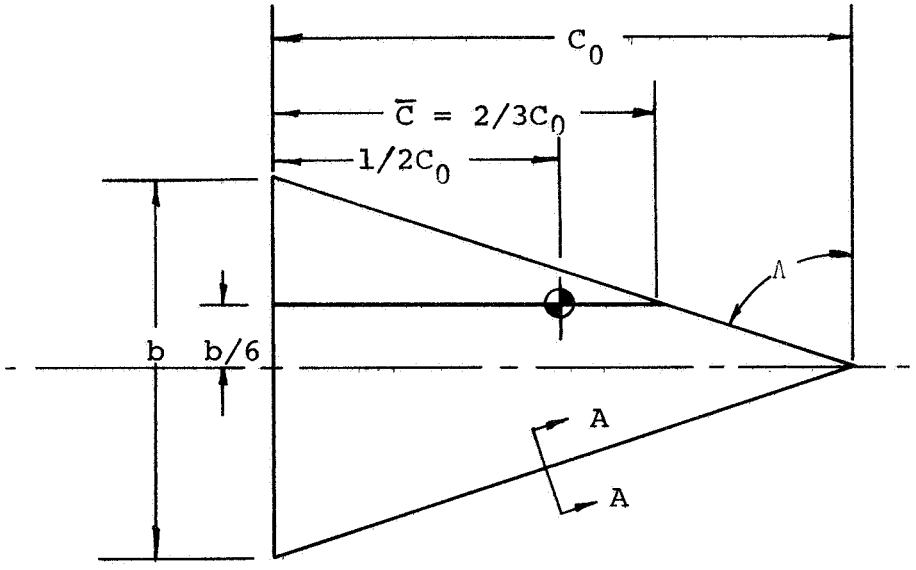

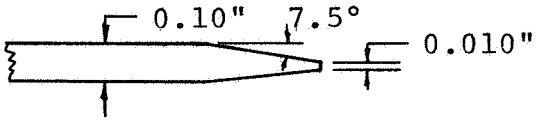

Section A-A (Enlarged)

Notes: 1) Section A-A is typical of all edges.

2) Area = $b^2 \tan\Lambda/4$.

3) Aspect Ratio = $4/\tan\Lambda$.

Figure 2.1 - Model Geometry - Delta Wings

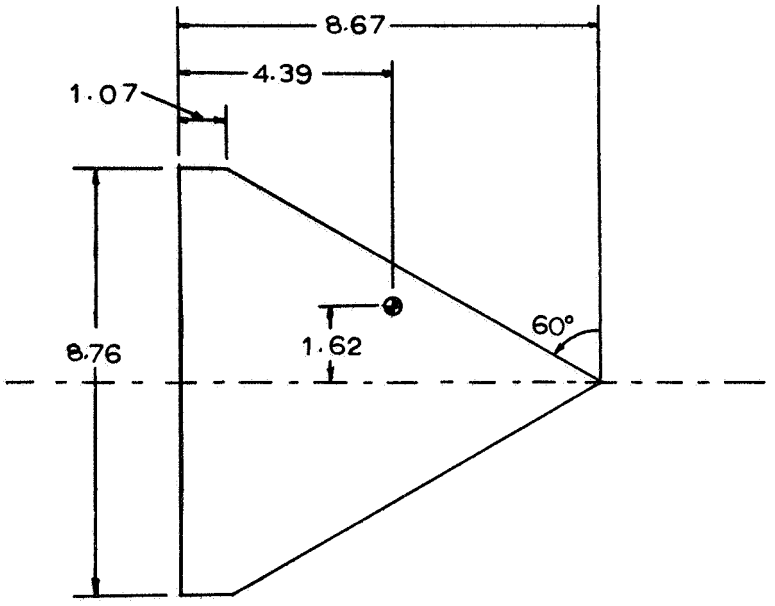

Figure 2.2 - Model Geometry - Cropped 60° Delta Wing

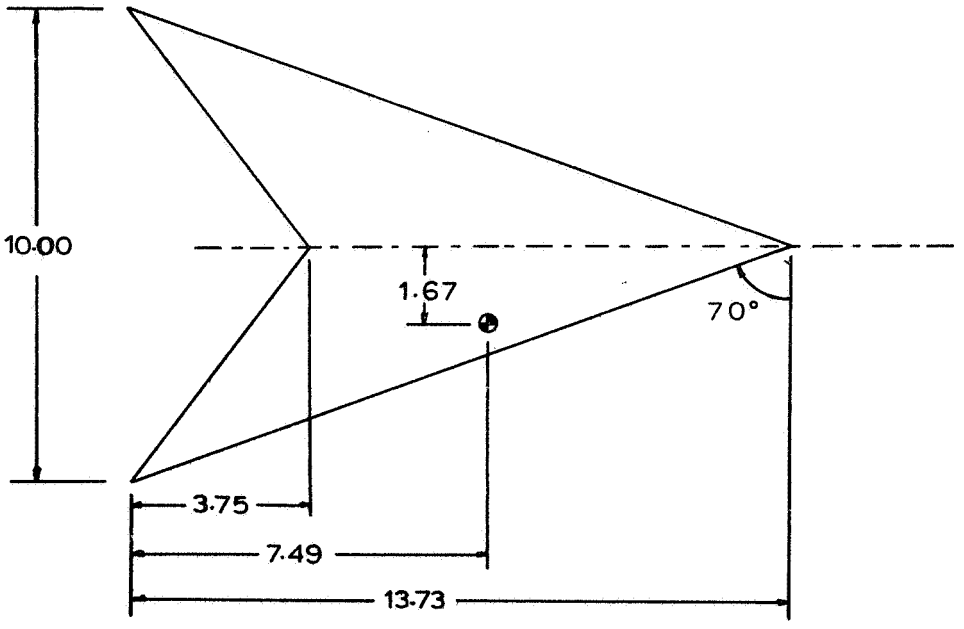

Figure 2.3 - Model Geometry - 70° Arrow Wing

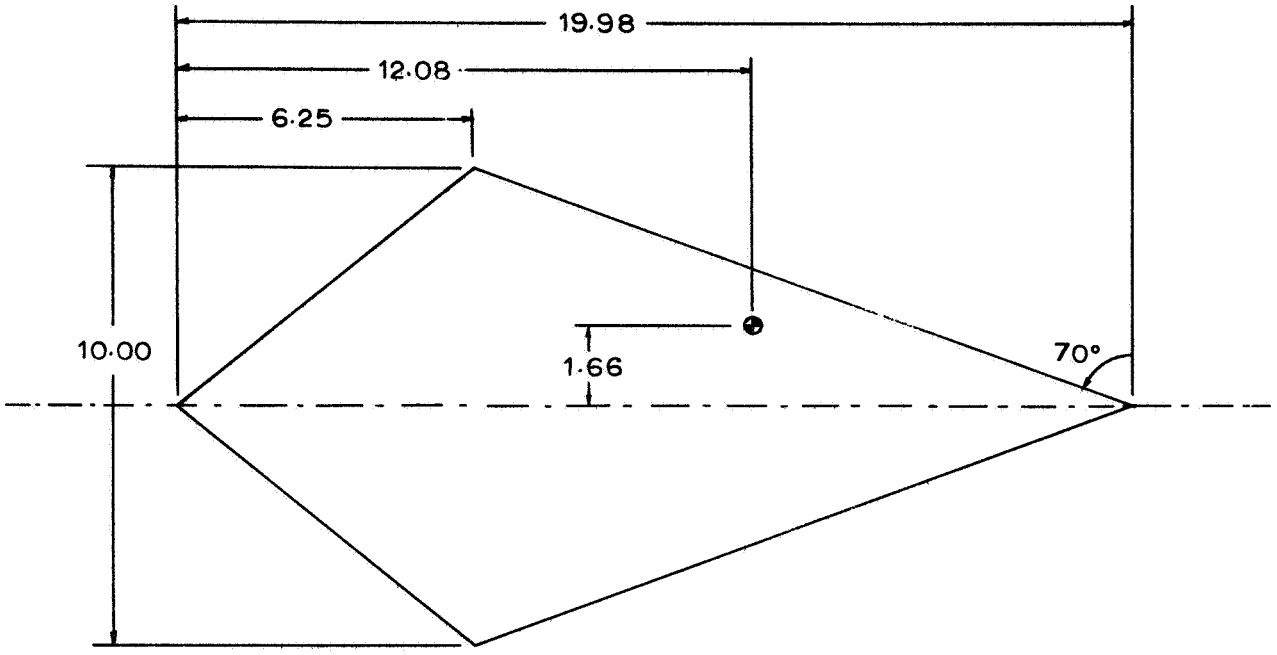

Figure 2.4 - Model Geometry - 70° Diamond Wing

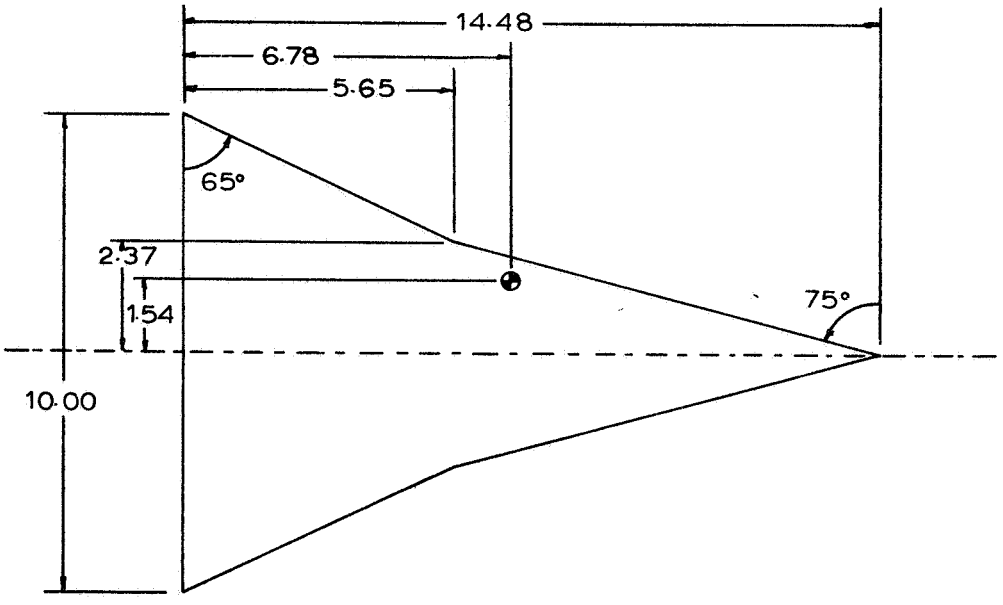

Figure 2.5 - Model Geometry - 75°/65° Double-Delta Wing

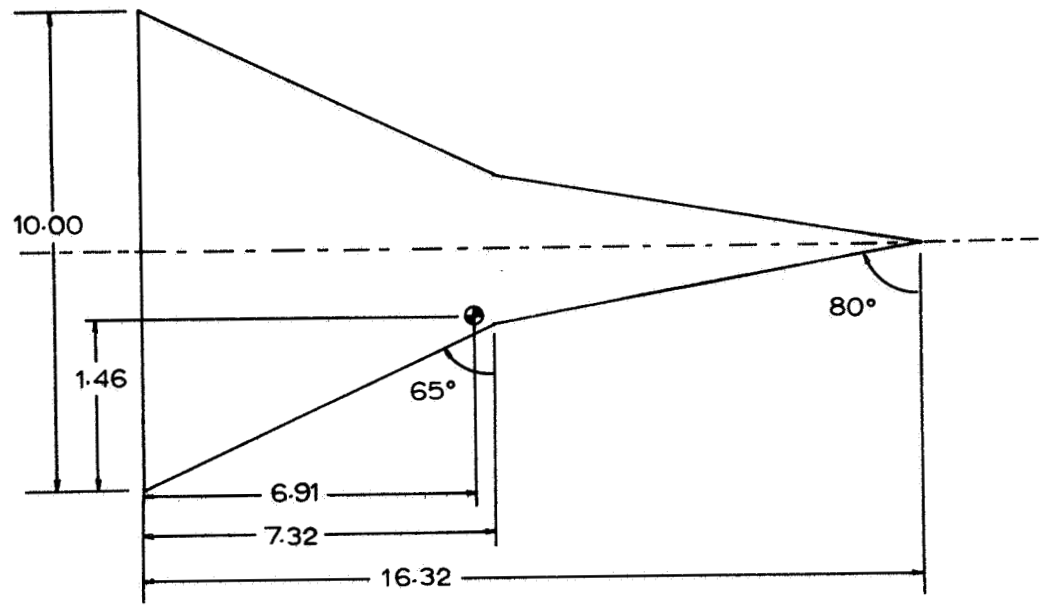

Figure 2.6 - Model Geometry - 80°/65° Double-Delta Wing

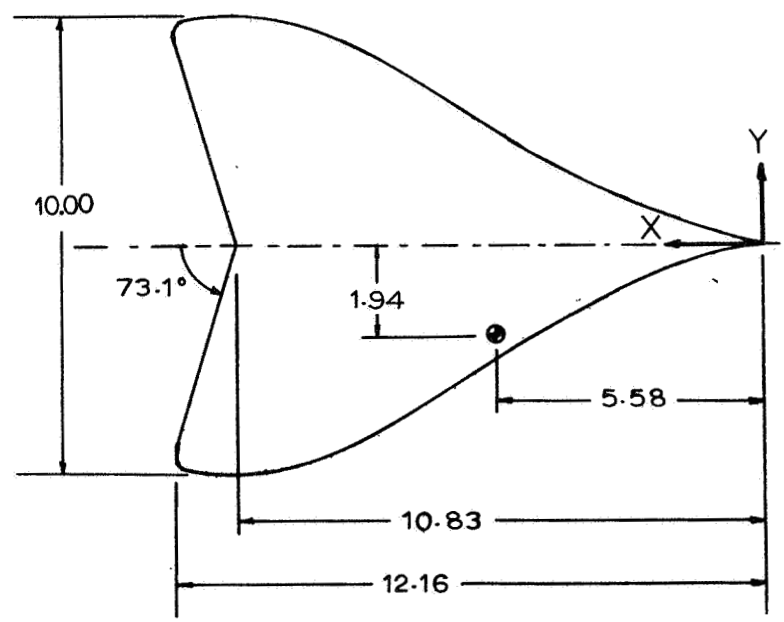

X	Y
0.500	0.118
1.000	0.249
2.000	0.562
3.000	0.955
4.000	1.438
5.000	2.015
6.000	2.664
7.000	3.341
8.000	3.968
9.000	4.465
10.000	4.791
11.000	4.951
12.000	4.740
12.160	4.400

Figure 2.7 - Model Geometry - Ogee Wing

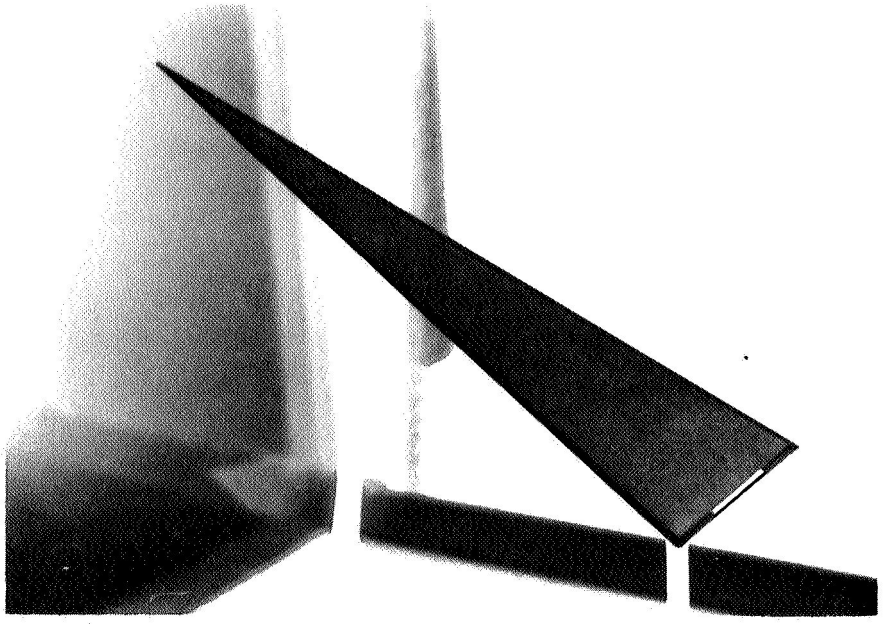

Top View (With Sandpaper)

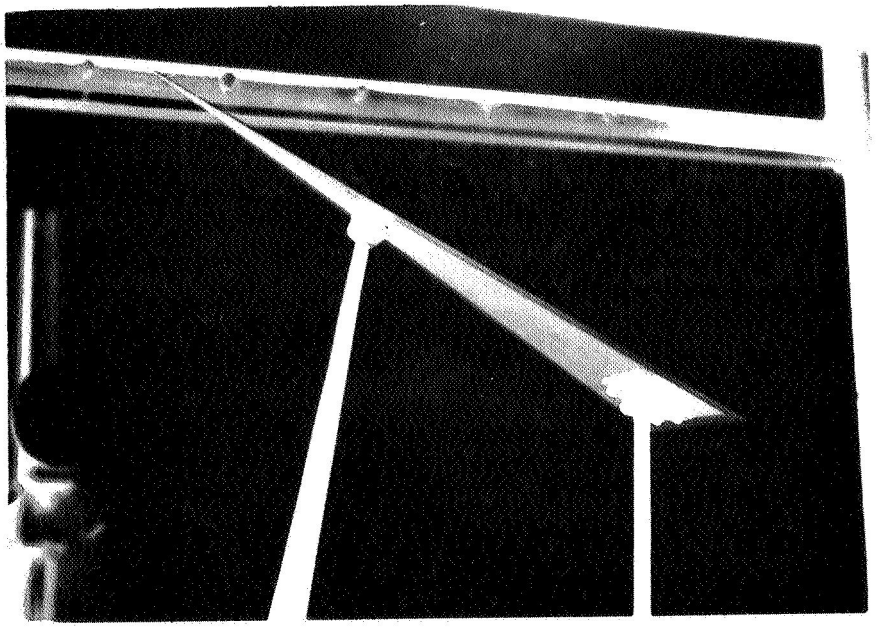

View Showing Mounting Struts

Figure 3.1 - Model Installation Photos

SMOOTH

α = 27.5° No Breakdown

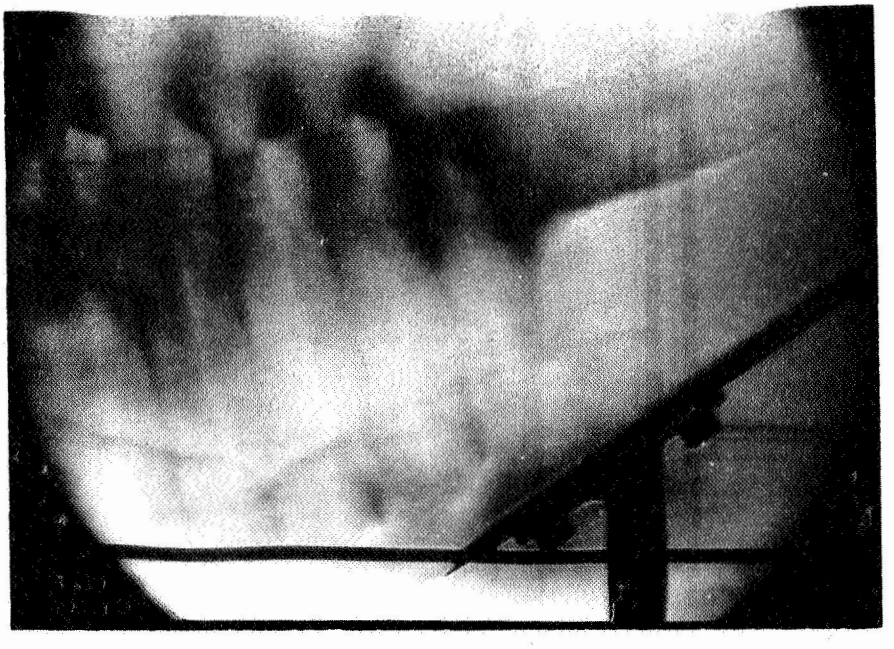

α = 32.5° Breakdown

Figure 3.2 - Effect of Roughness on Breakdown Characteristics (72.5° Delta Wing)

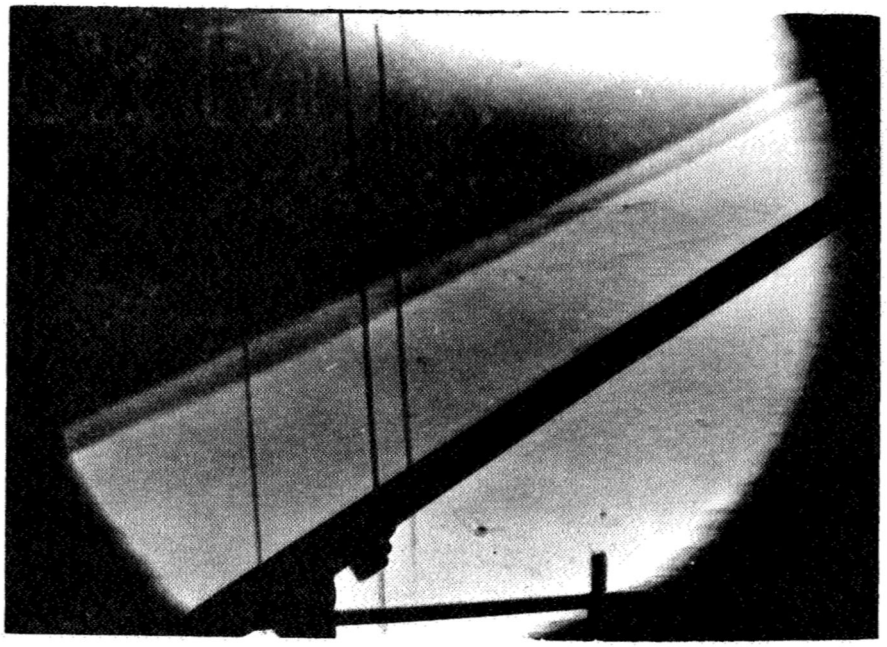

α = 30.0° No Breakdown

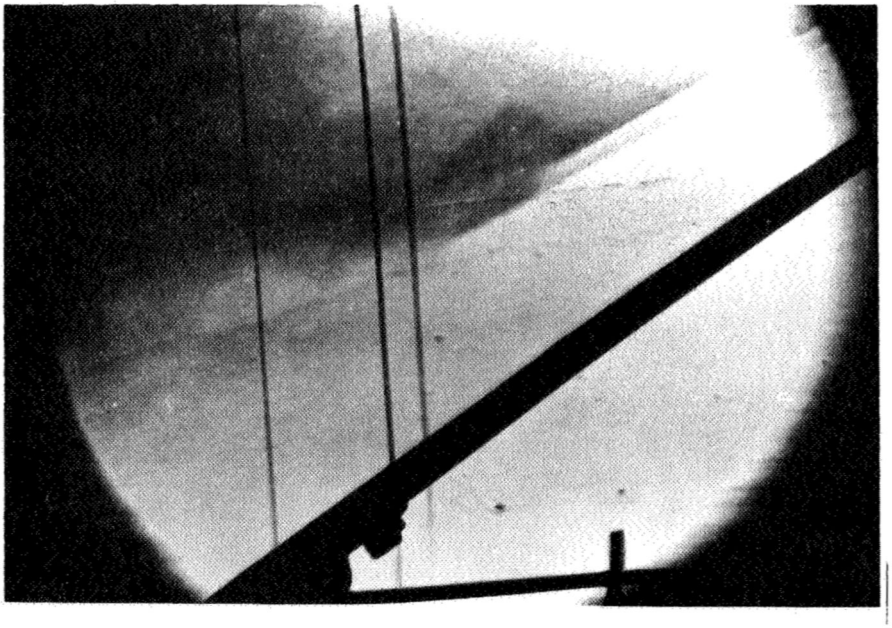

α = 32.0° Breakdown

Figure 3.2 - (Continued)

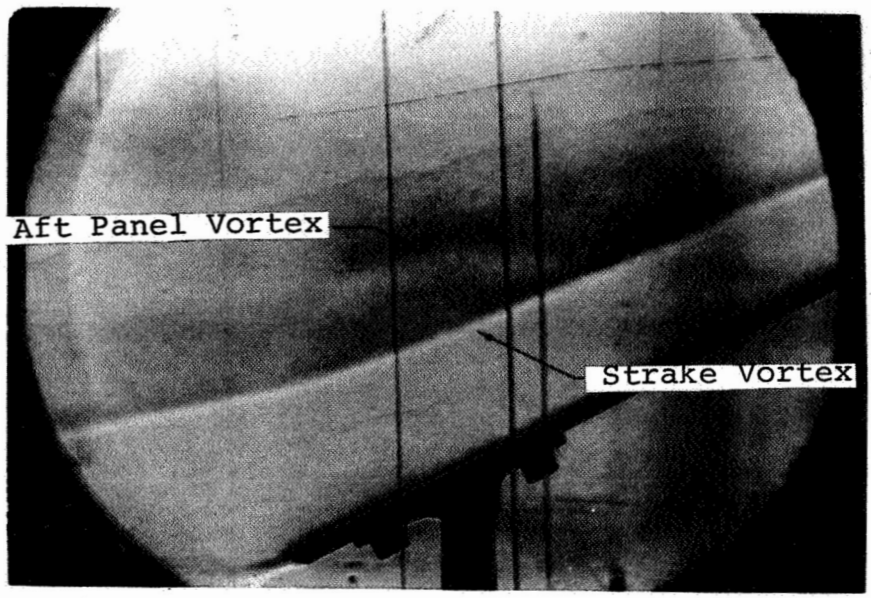

α = 24.4° No Breakdown

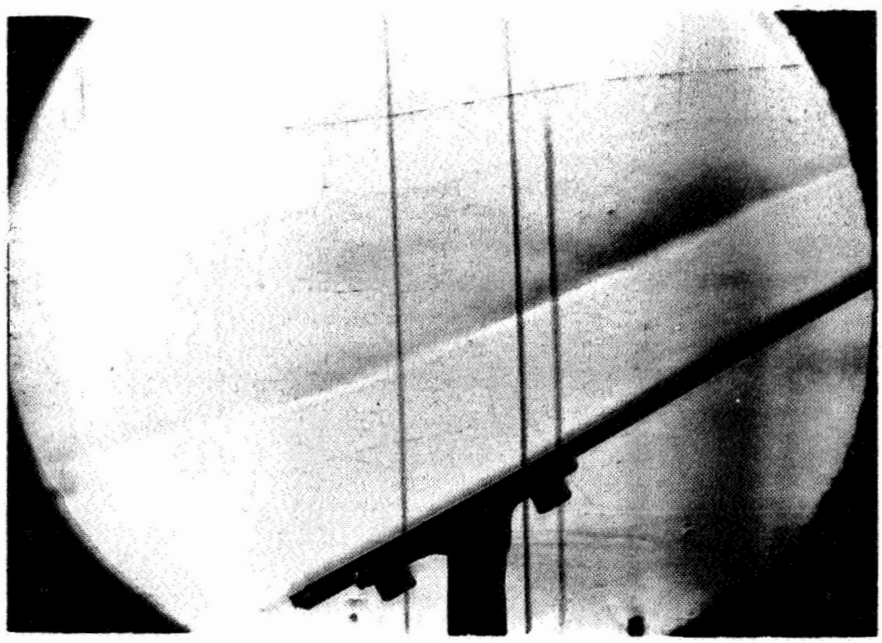

α = 28.7° Aft Panel Breakdown

Figure 3.3 - Vortex Breakdown Photos - 75°/65° Double-Delta Wing

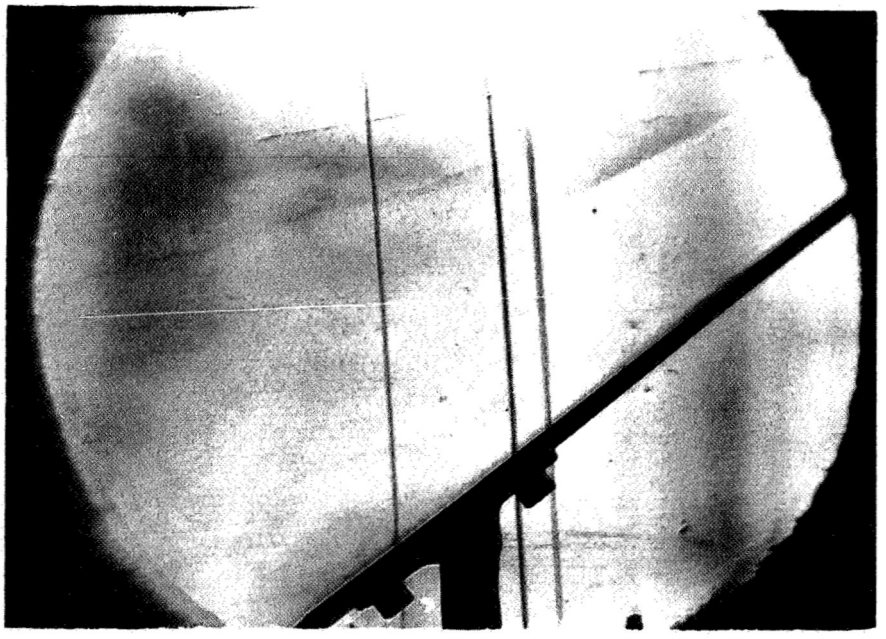

α = 35.6° Strake Vortex Breakdown

Figure 3.3 - (Continued)

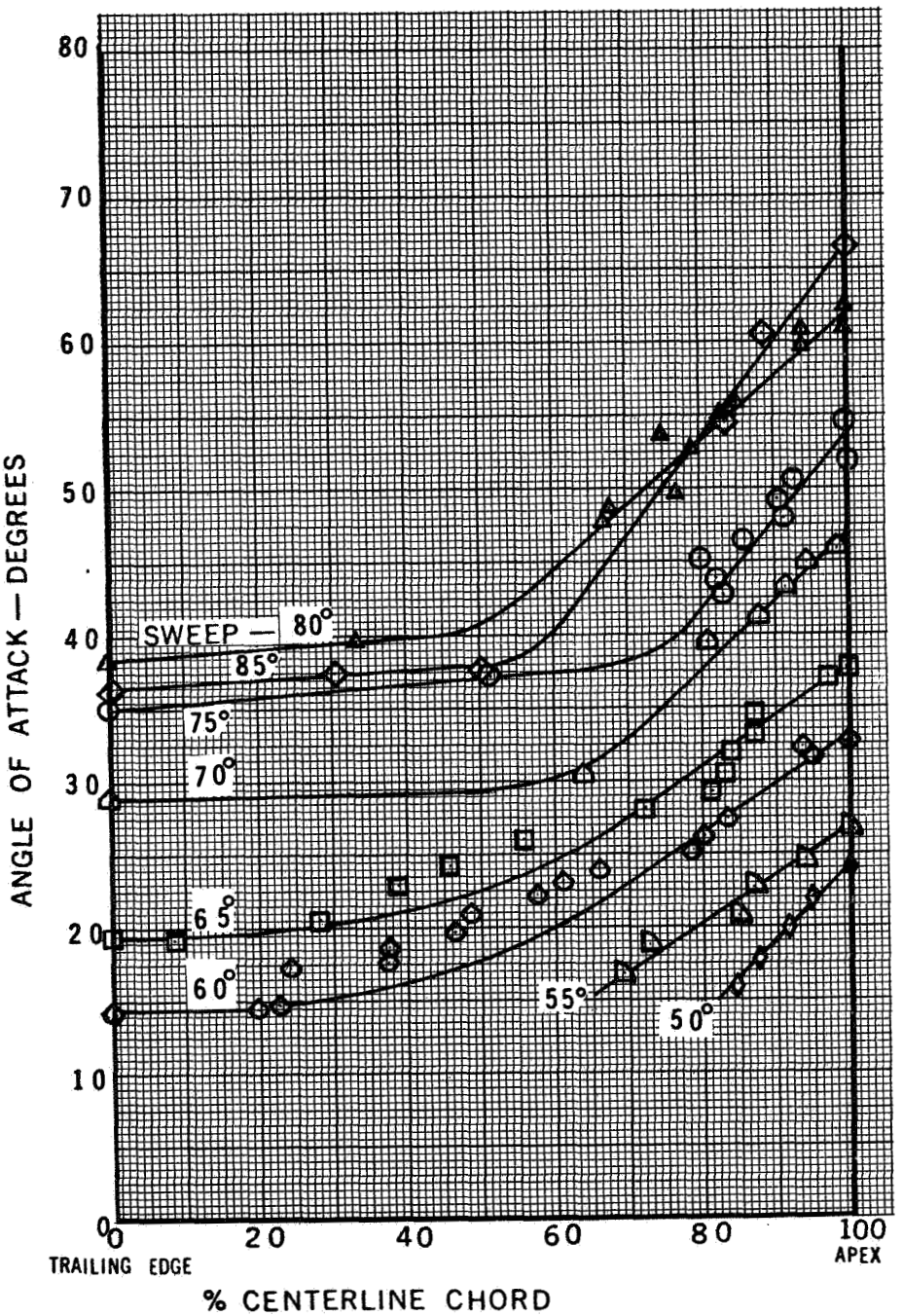

Figure 4.1.1 - Vortex Breakdown Position - Delta Wings

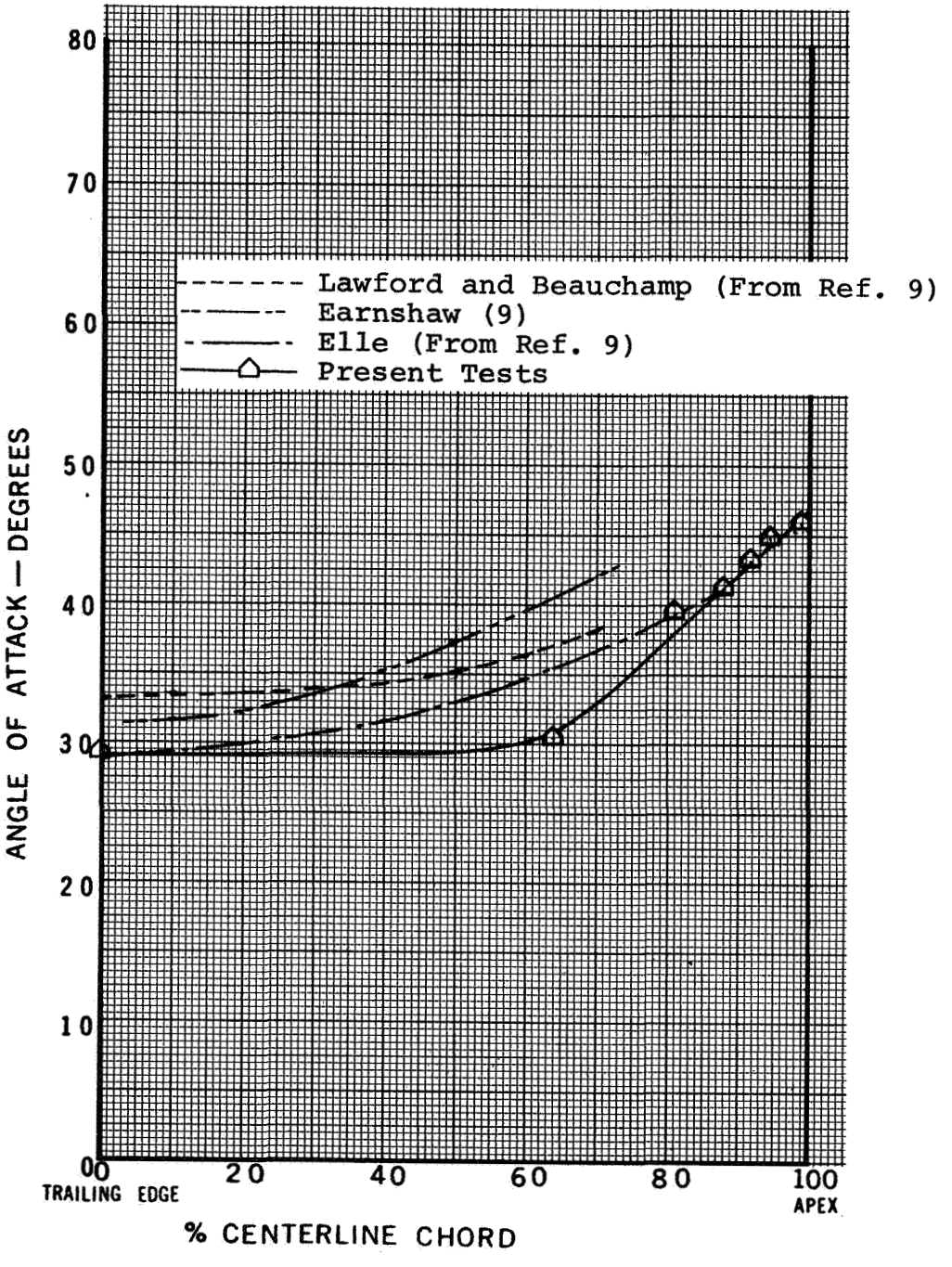

Figure 4.1.2 - Comparison of Vortex Breakdown Results with Previously Published Data - 70° Delta Wing

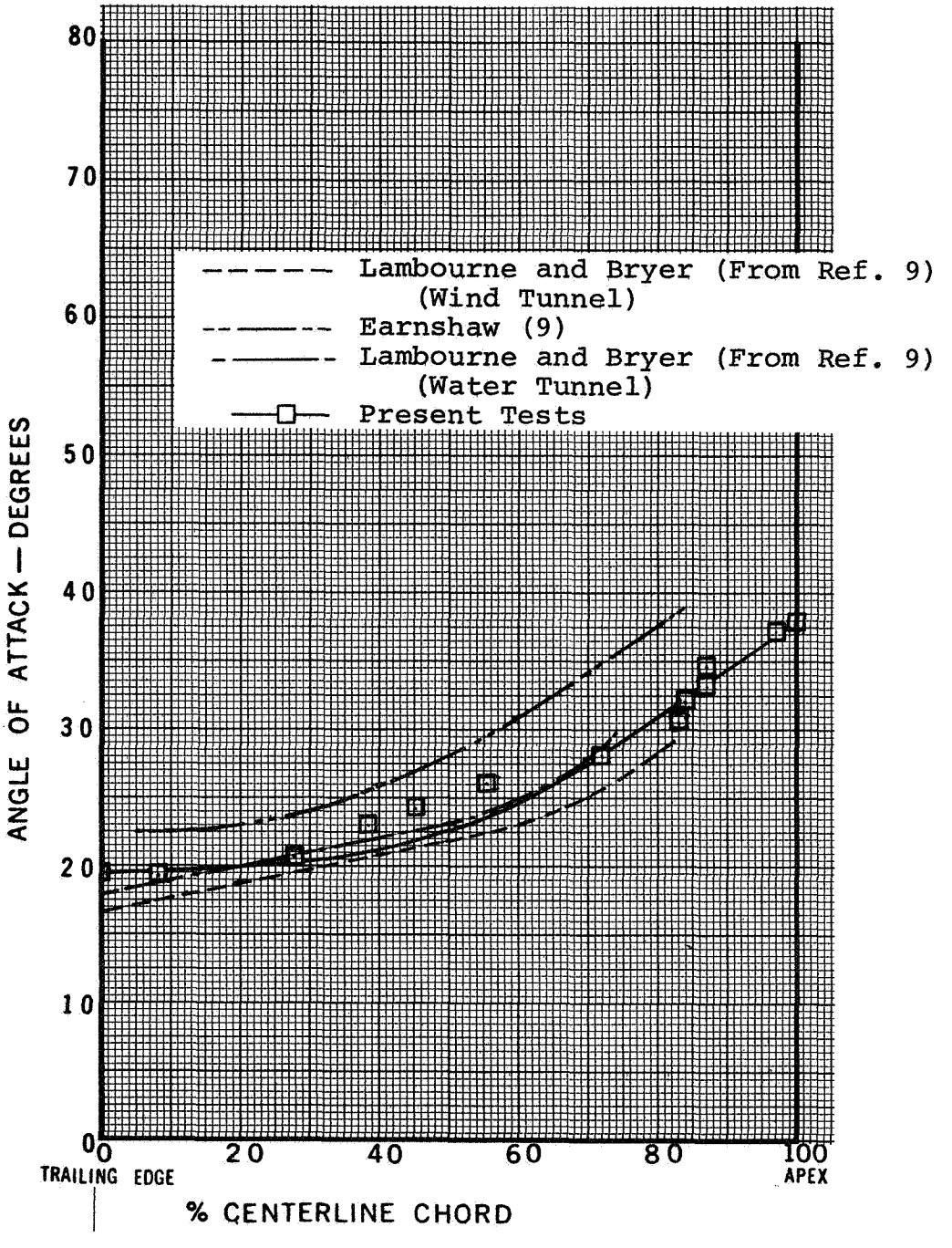

Figure 4.1.3 - Comparison of Vortex Breakdown Results with Previously Published Data - 65° Delta Wing

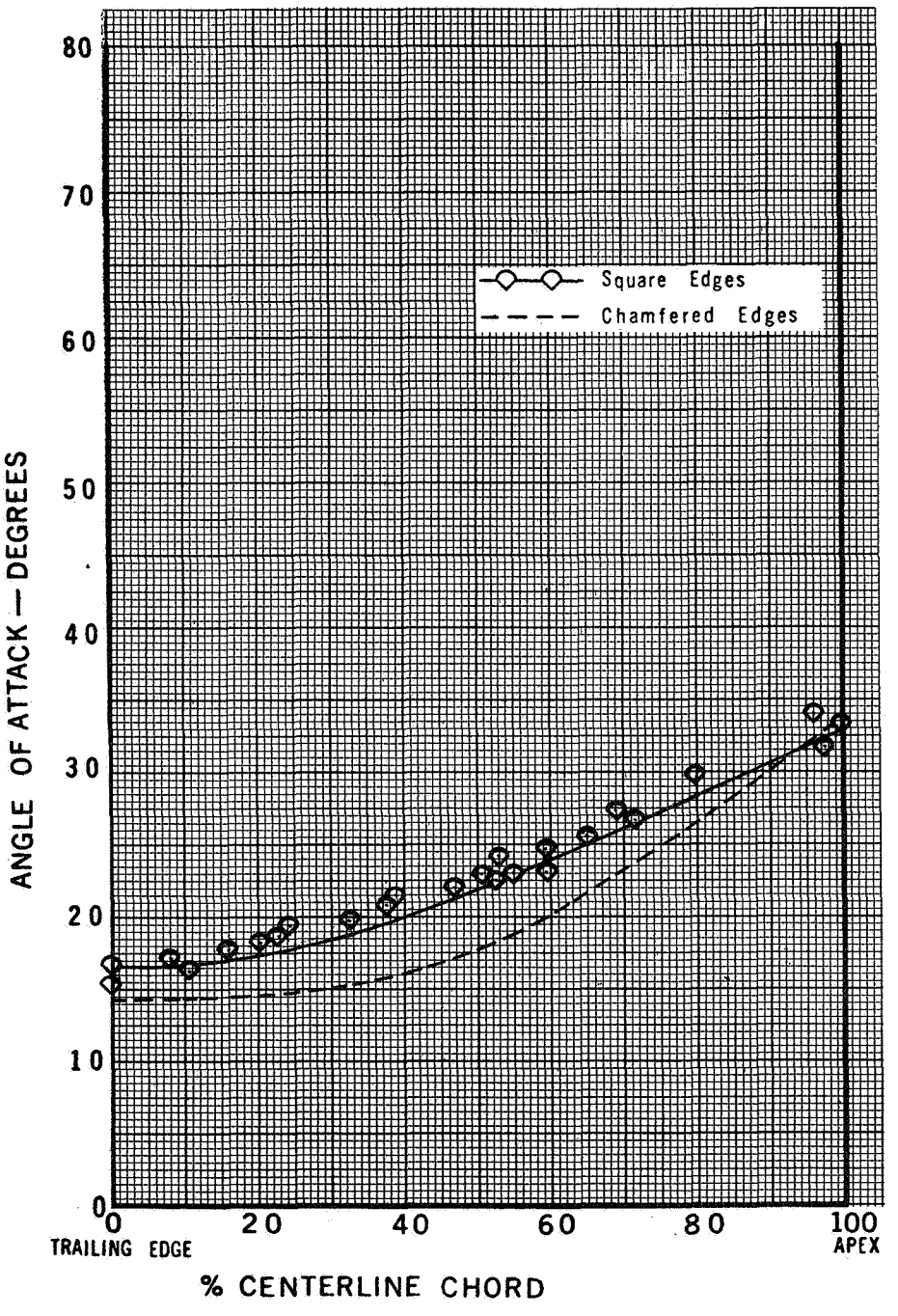

Figure 4.2 - Effect of Edge Shape on Vortex Breakdown - 60° Delta Wing

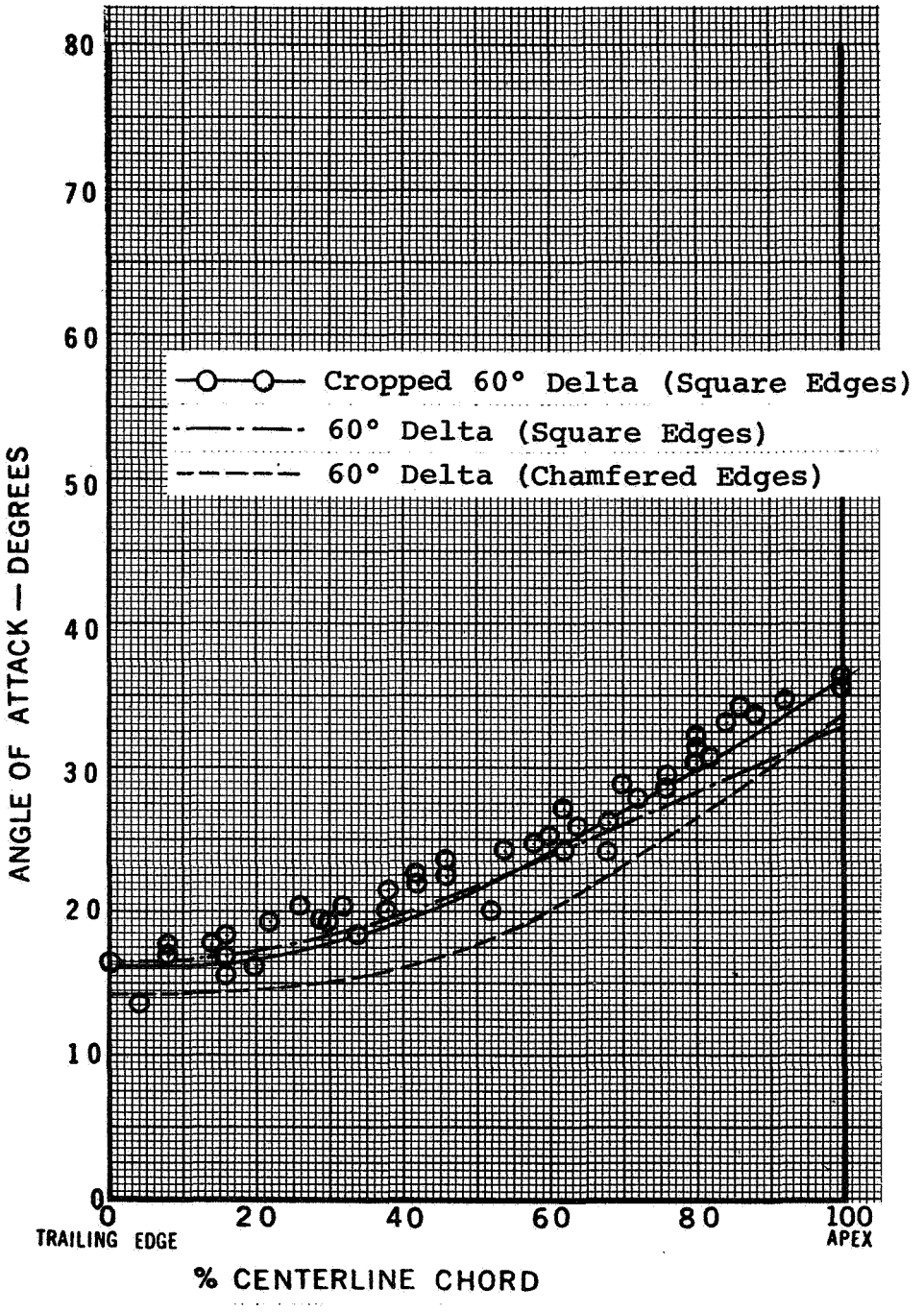

Figure 4.3 - Vortex Breakdown Position - Cropped 60° Delta Wing

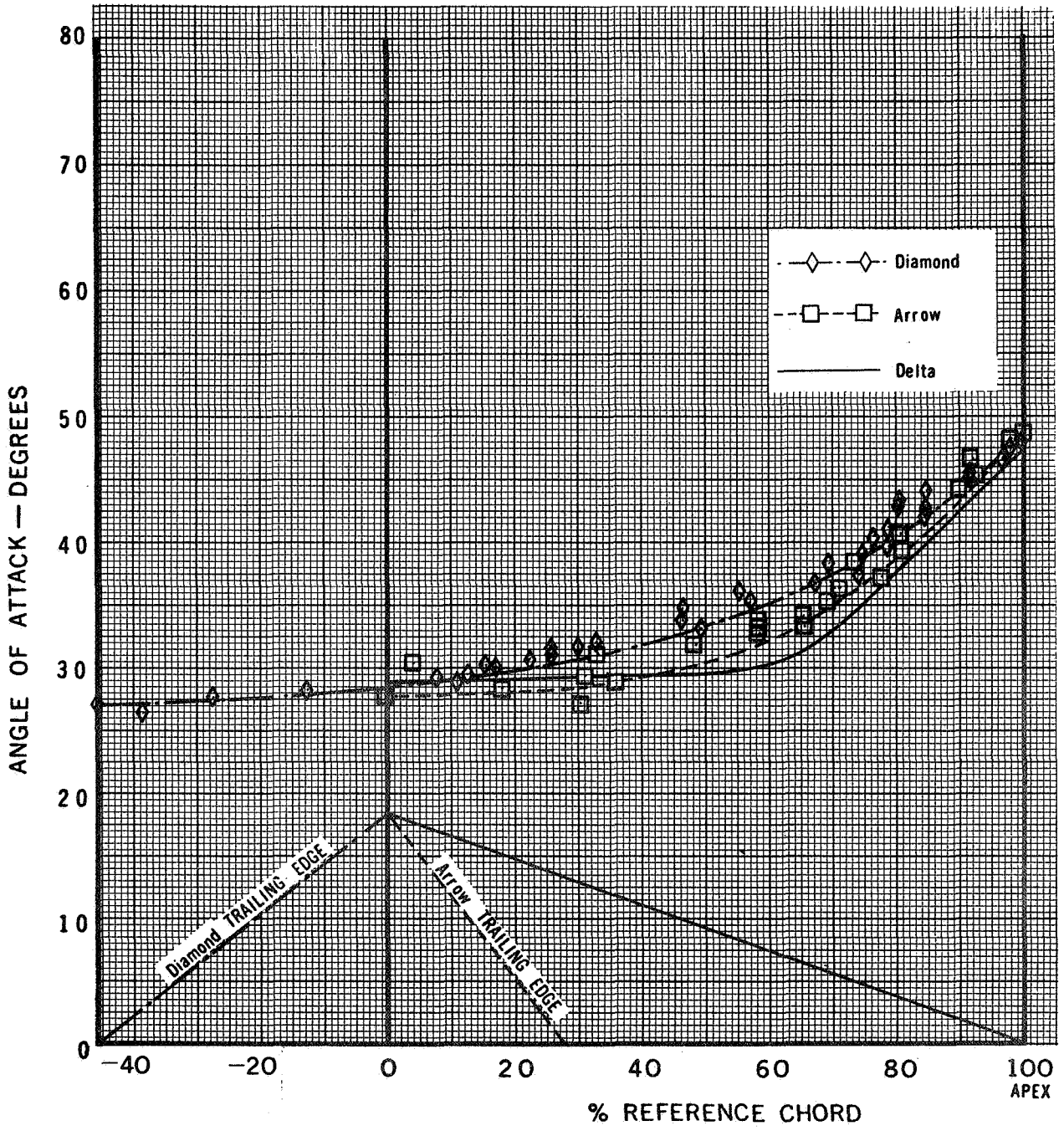

Figure 4.4 - Vortex Breakdown Position - 70° Arrow, Delta, and Diamond Wings

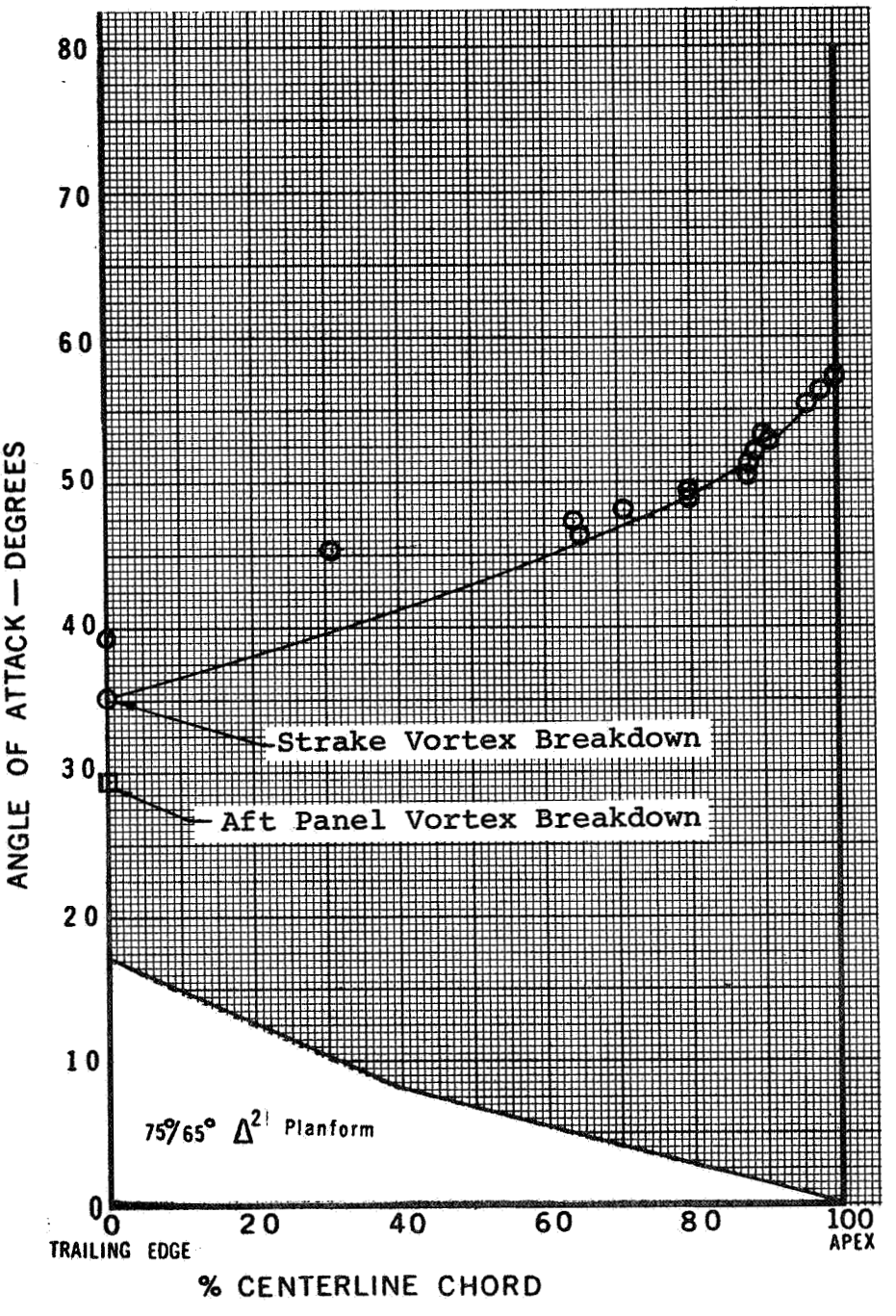

Figure 4.5 - Vortex Breakdown Position - 75°/65° Double-Delta Wing

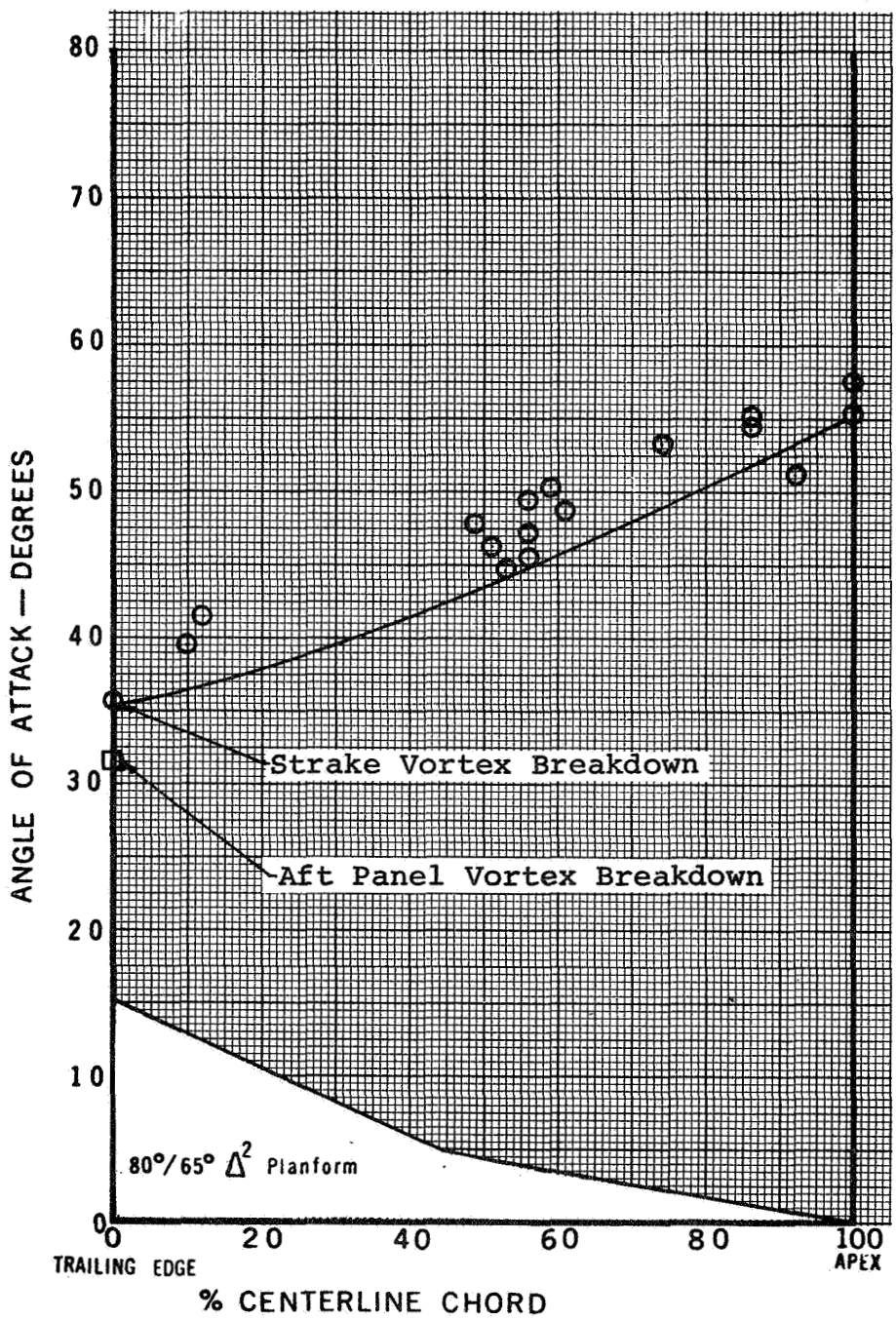

Figure 4.6 - Vortex Breakdown Position - 80°/65° Double-Delta Wing

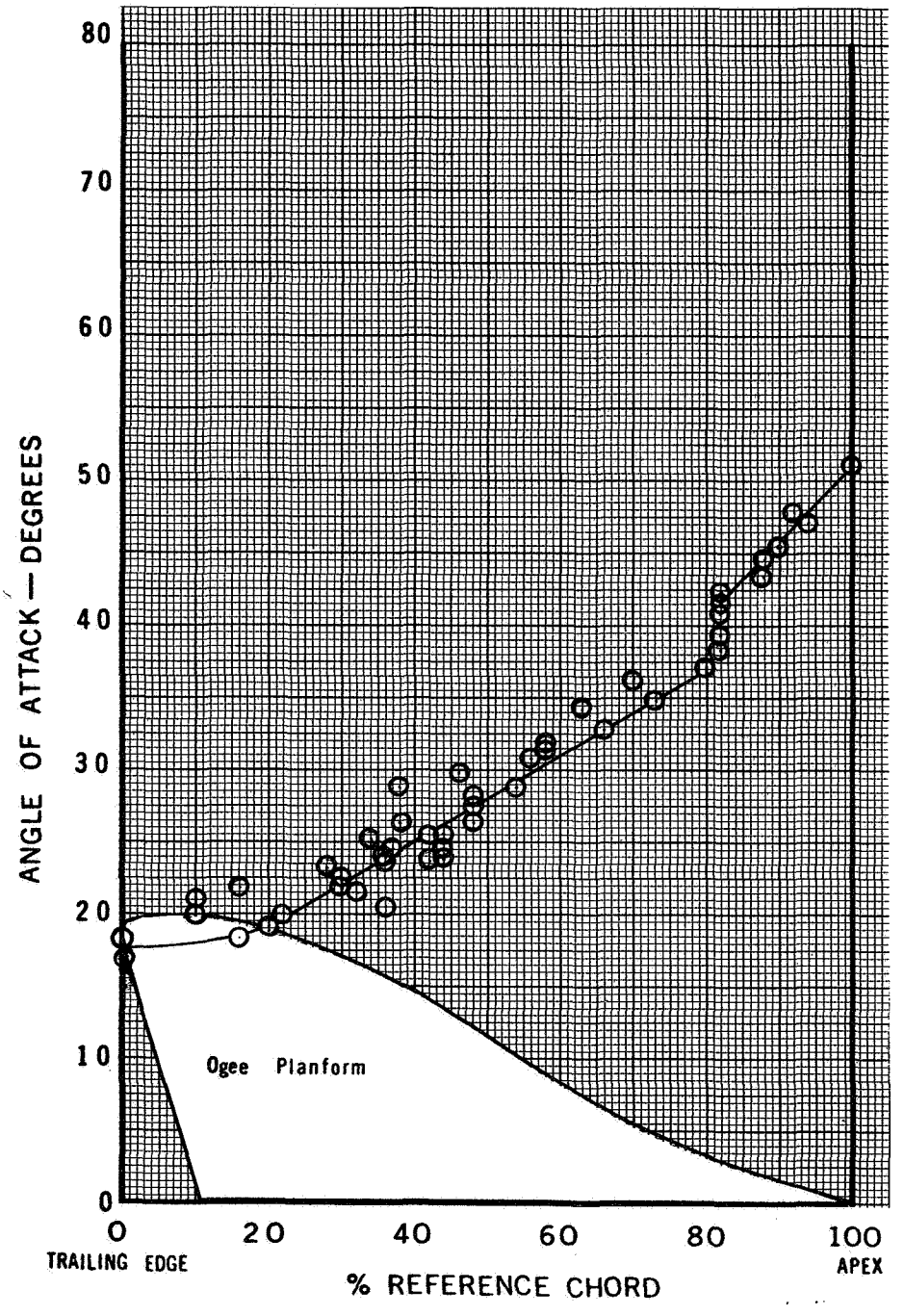

Figure 4.7 - Vortex Breakdown Position - Ogee Wing

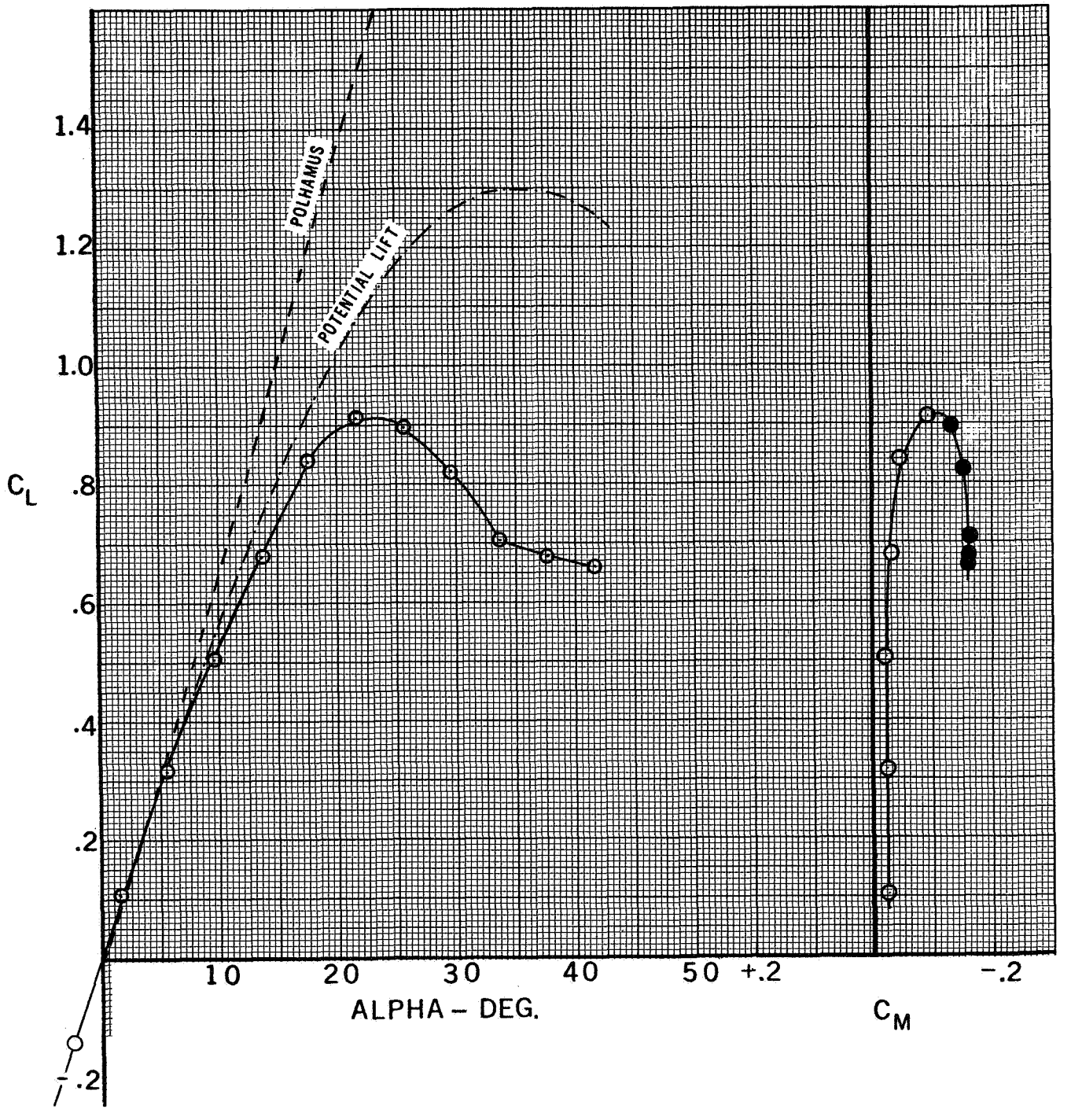

Figure 5.1.1-Lift and Pitching Characteristics - 45° Delta Wing

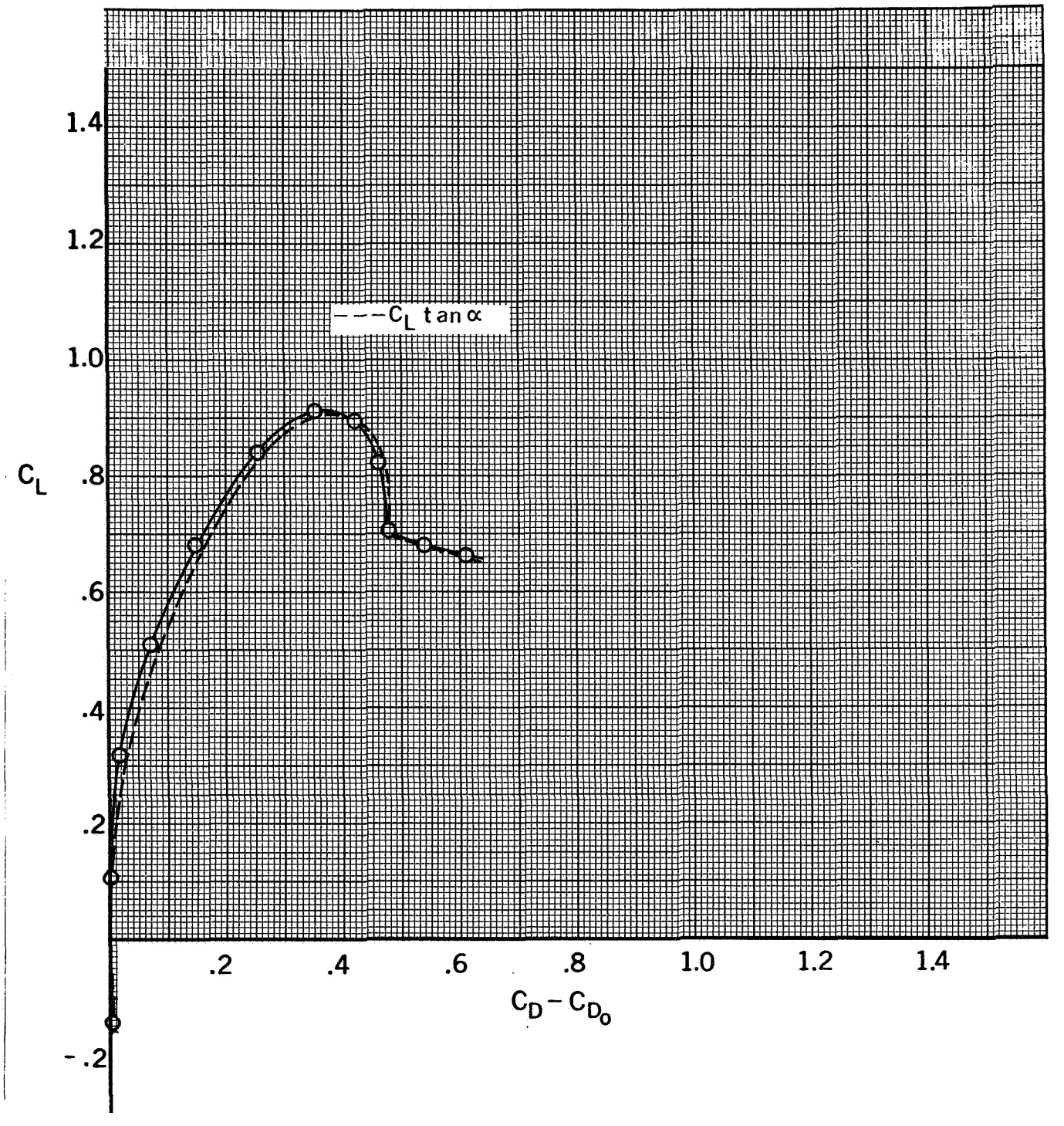

Figure 5.1.2 - Drag Due to Lift - 45° Delta Wing

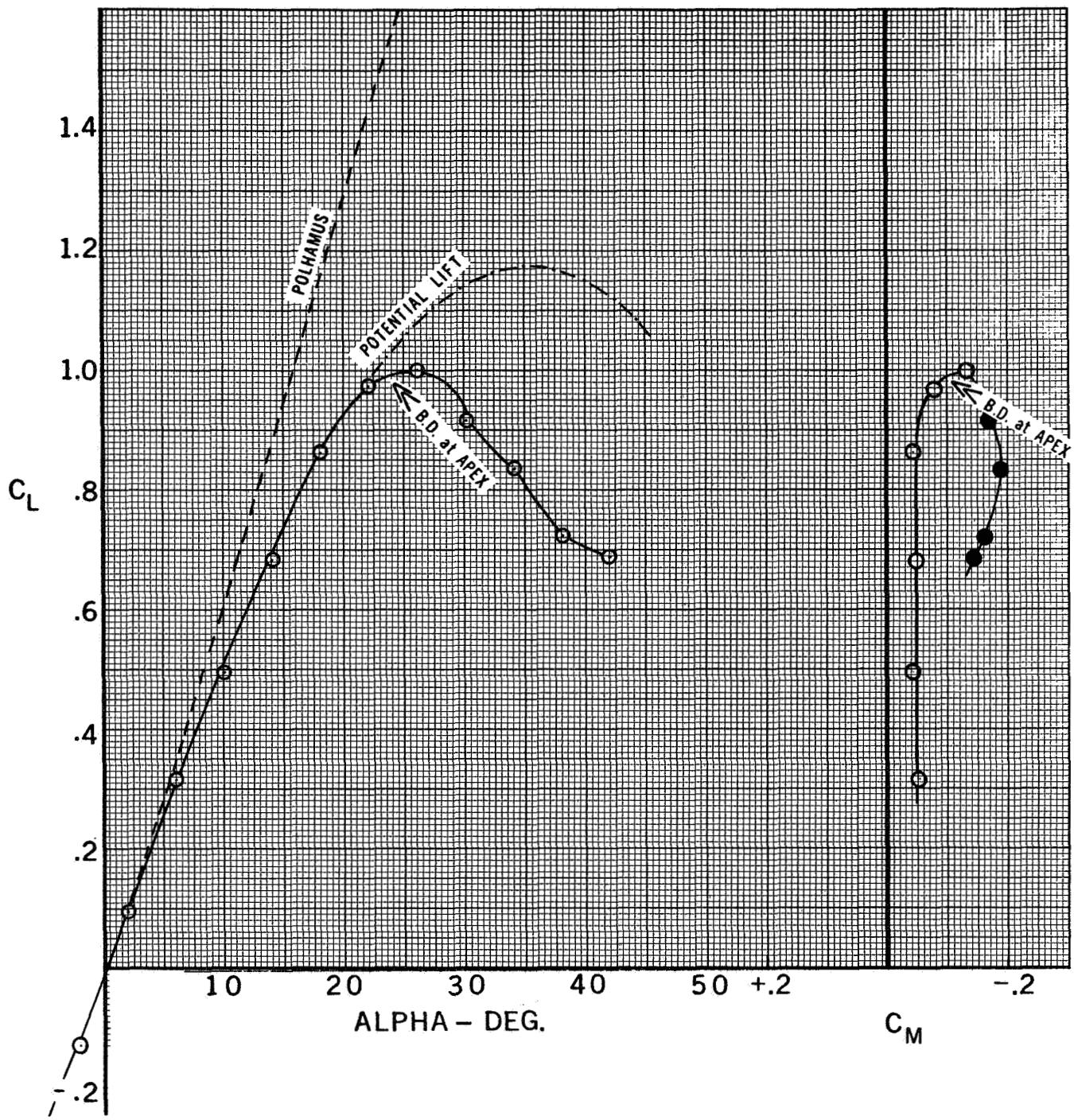

Figure 5.2.1-Lift and Pitching Characteristics - 50° Delta Wing

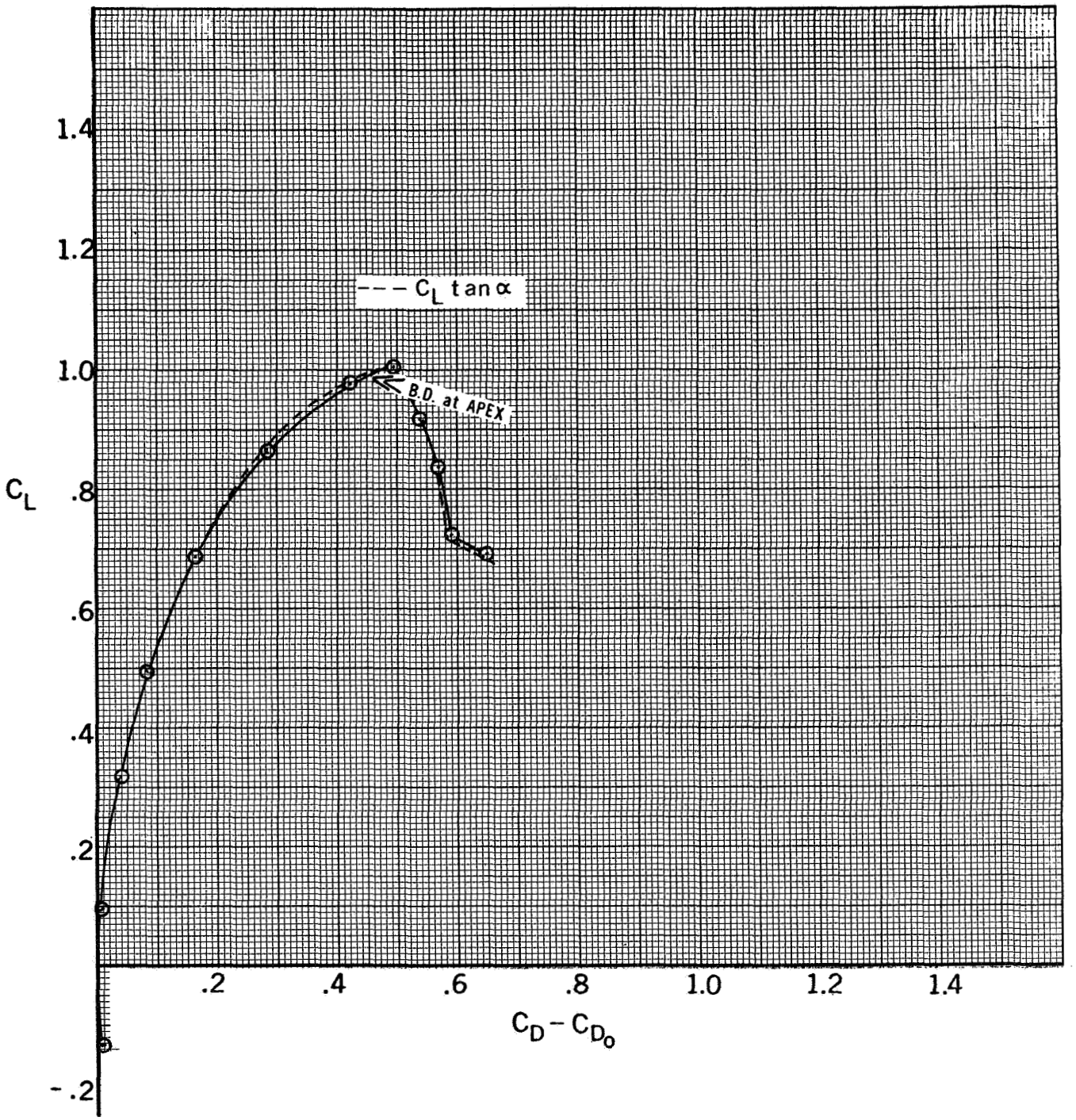

Figure 5.2.2 - Drag Due to Lift - 50° Delta Wing

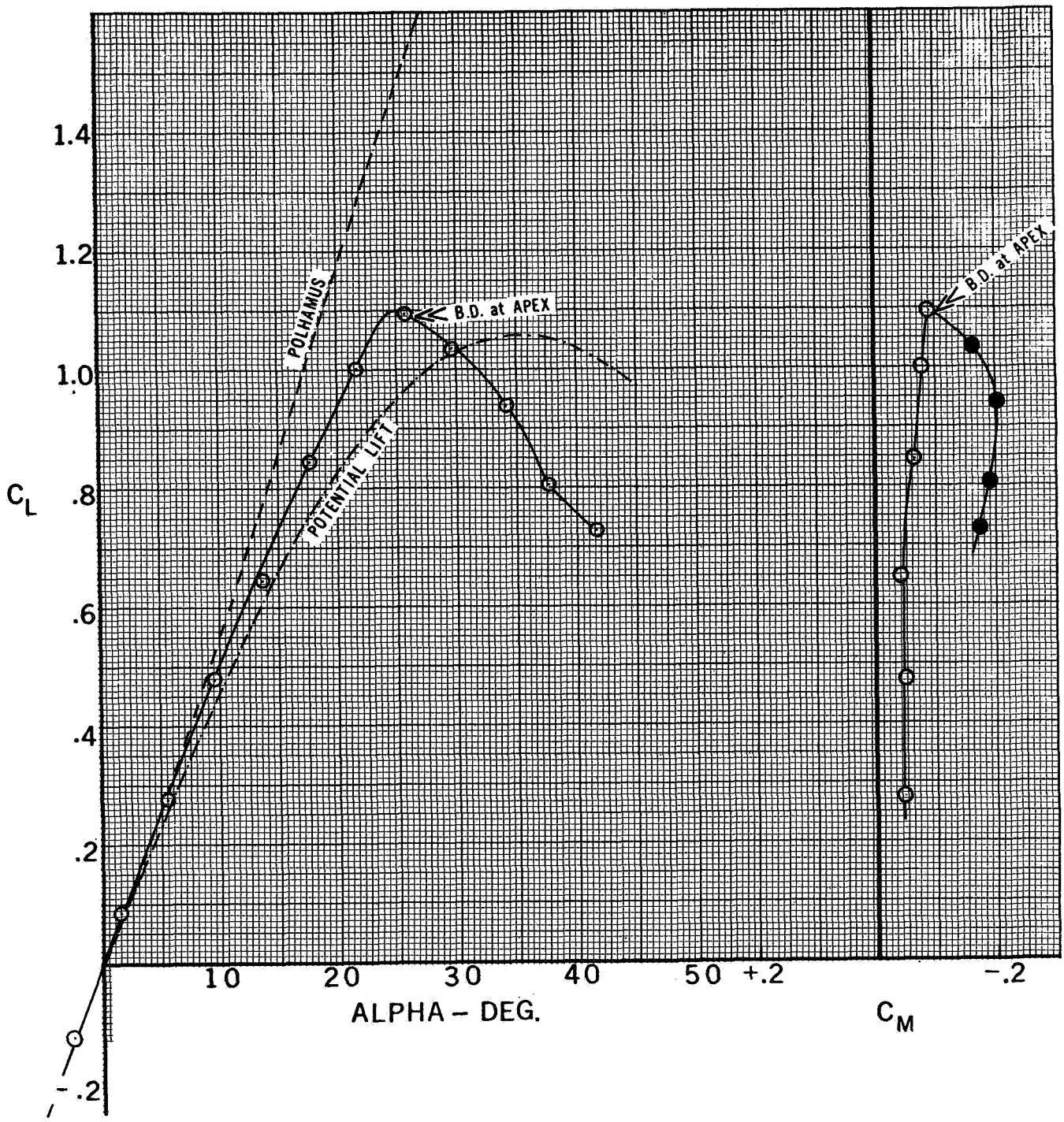

Figure 5.3.1-Lift and Pitching Characteristics - 55° Delta Wing

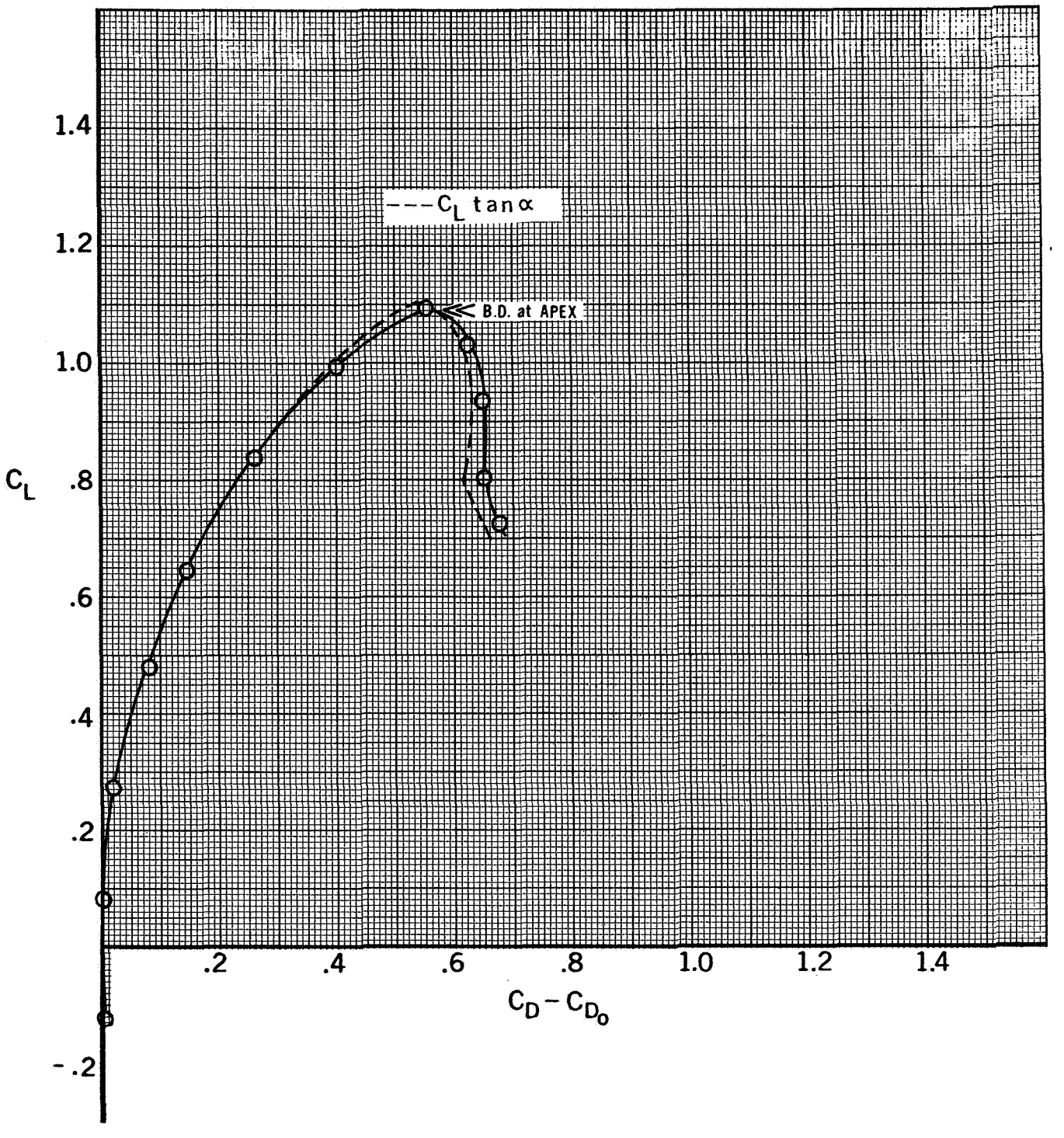

Figure 5.3.2 - Drag Due to Lift - 55° Delta Wing

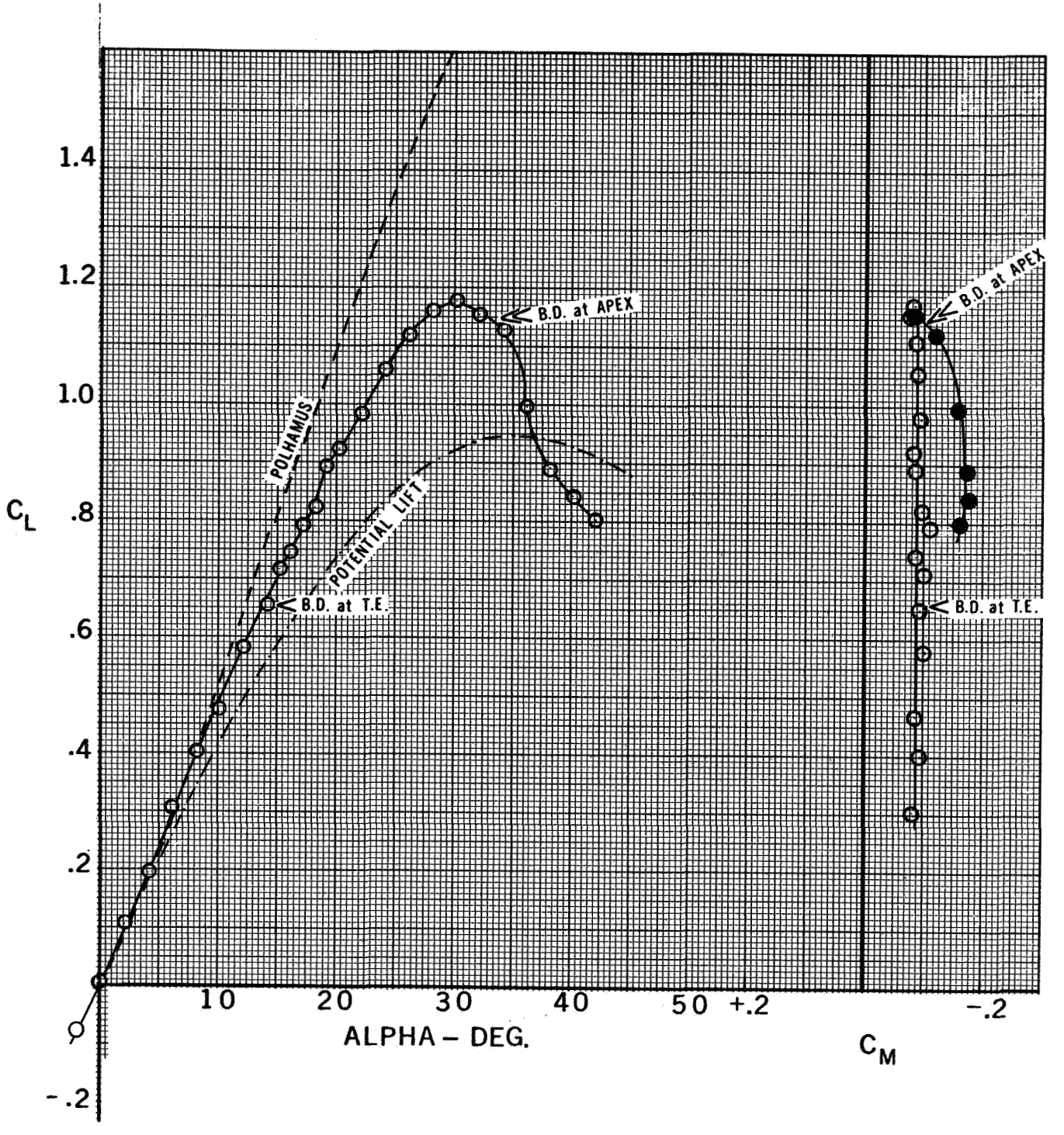

Figure 5.4.1-Lift and Pitching Characteristics - 60° Delta Wing

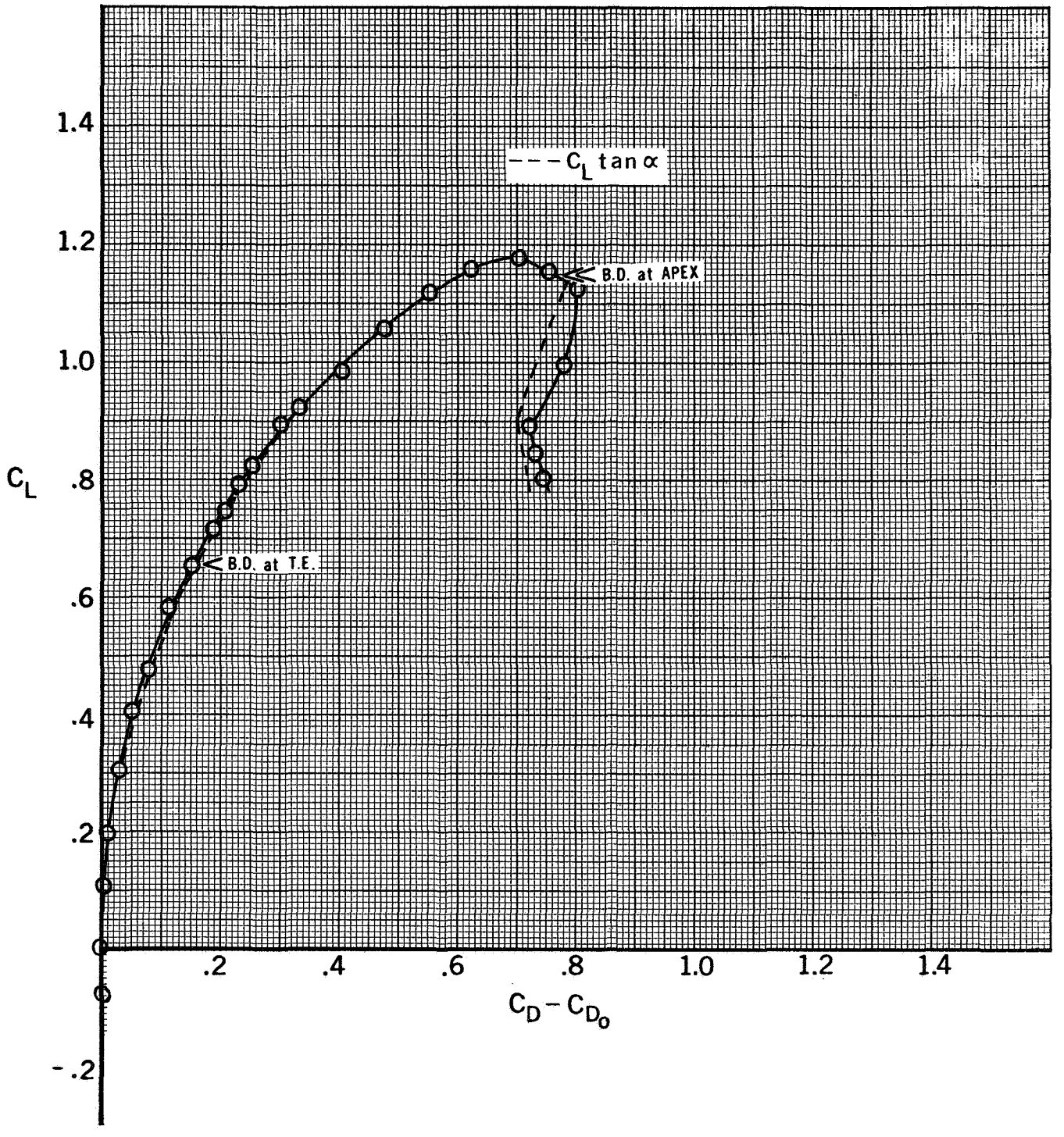

Figure 5.4.2 - Drag Due to Lift - 60° Delta Wing

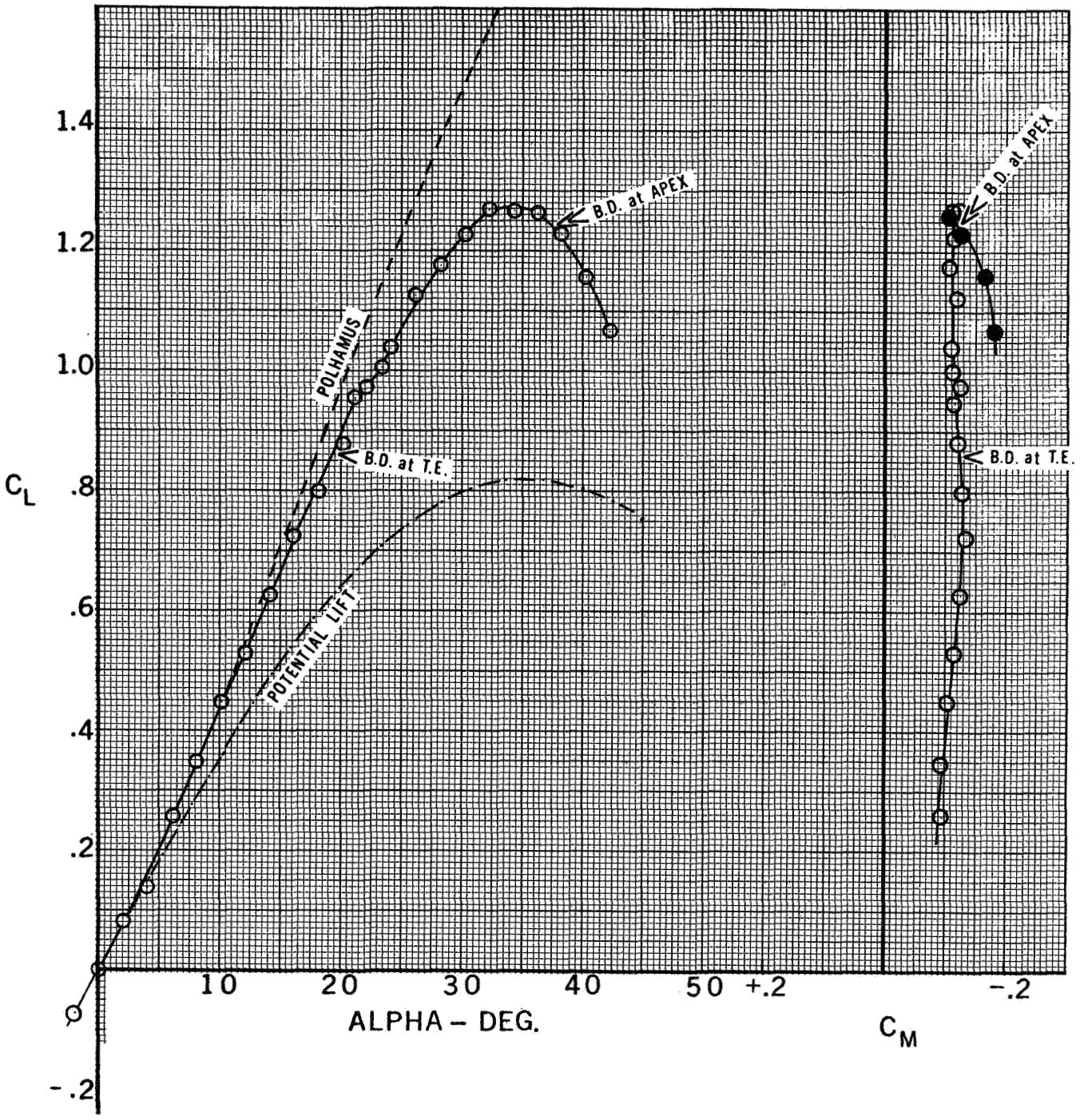

Figure 5.5.1-Lift and Pitching Characteristics - 65° Delta Wing

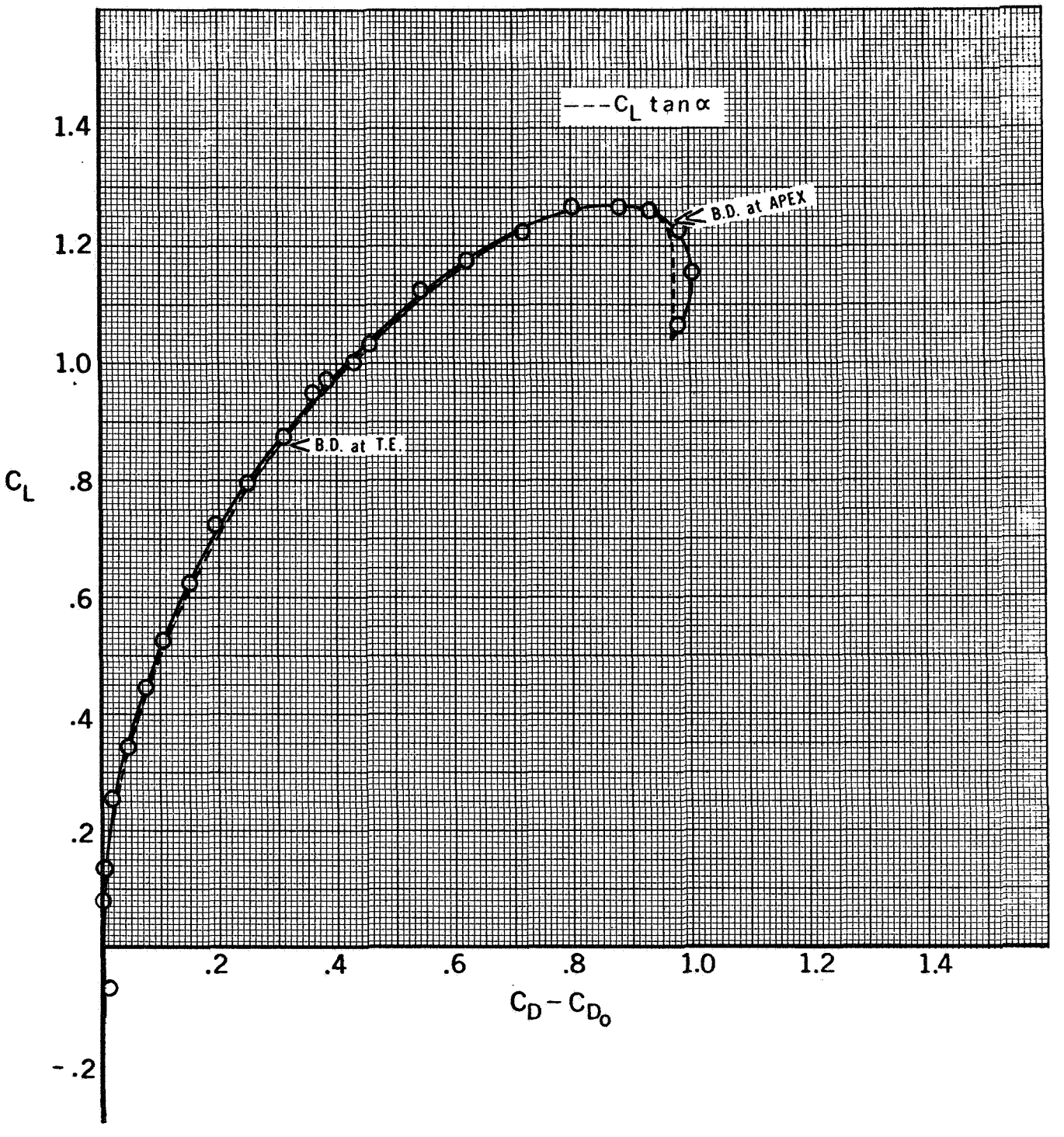

Figure 5.5.2 - Drag Due to Lift - 65° Delta Wing

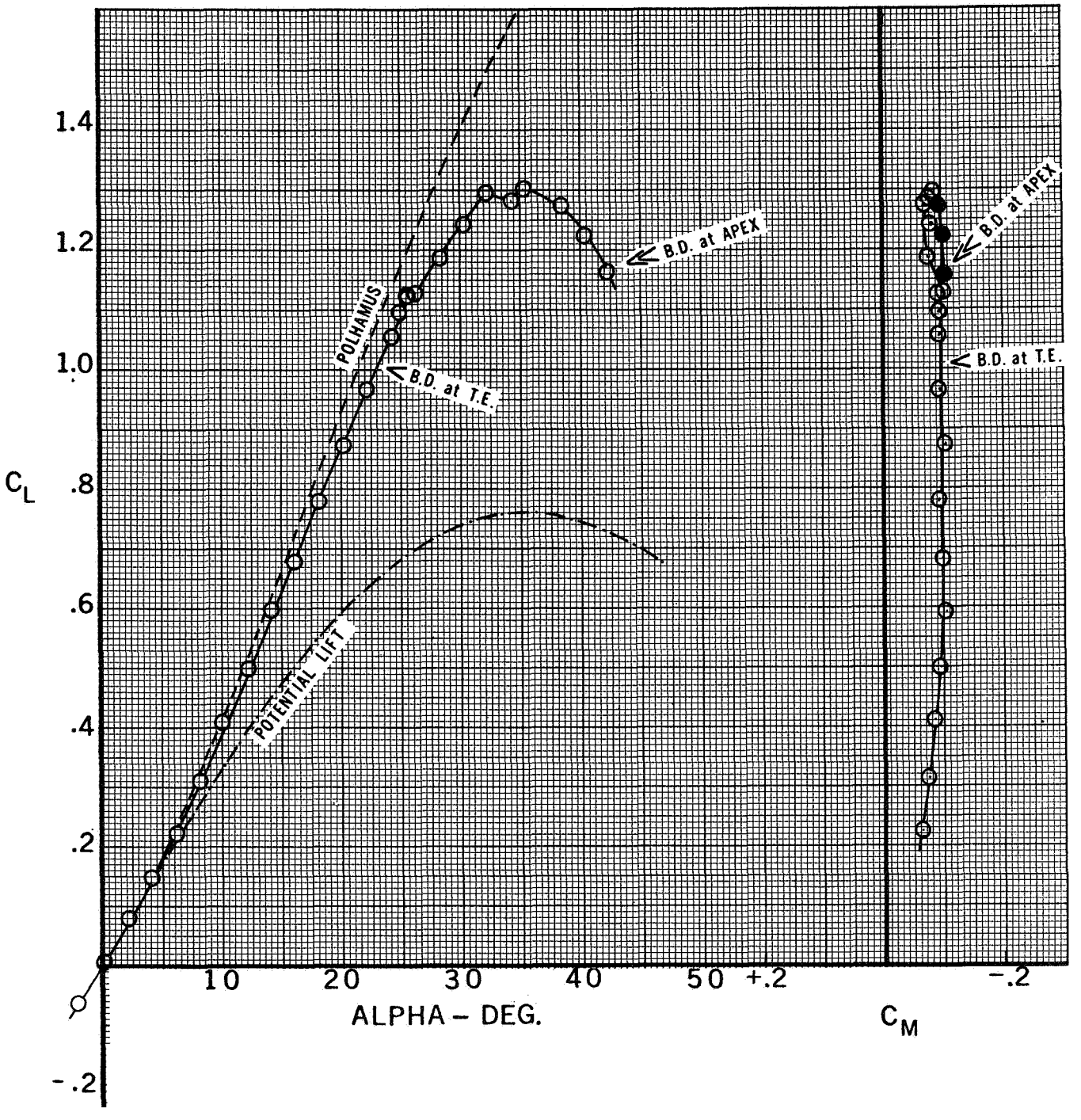

Figure 5.6.1-Lift and Pitching Characteristics - 67.5° Delta Wing

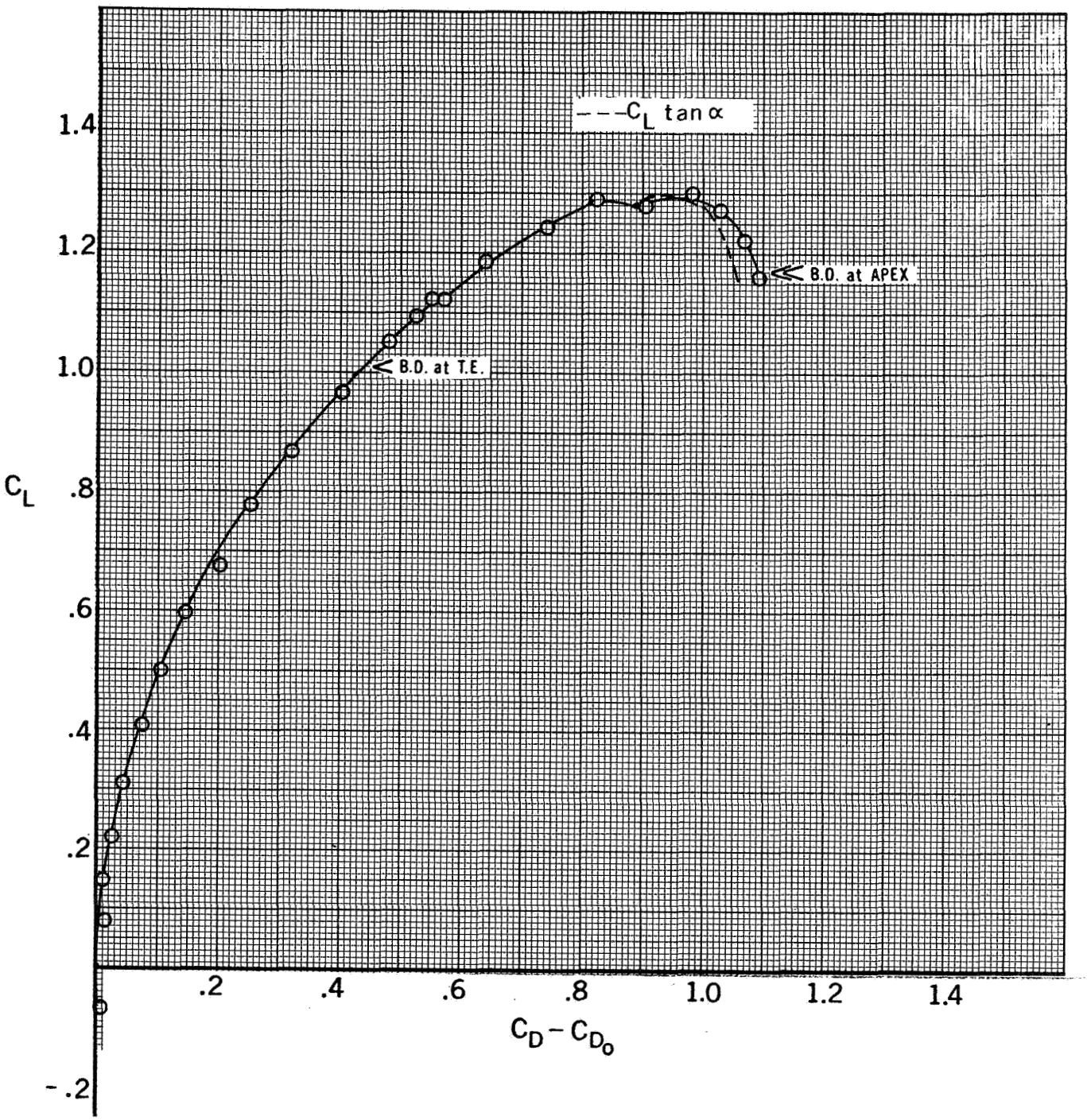

Figure 5.6.2 - Drag Due to Lift - 67.5° Delta Wing

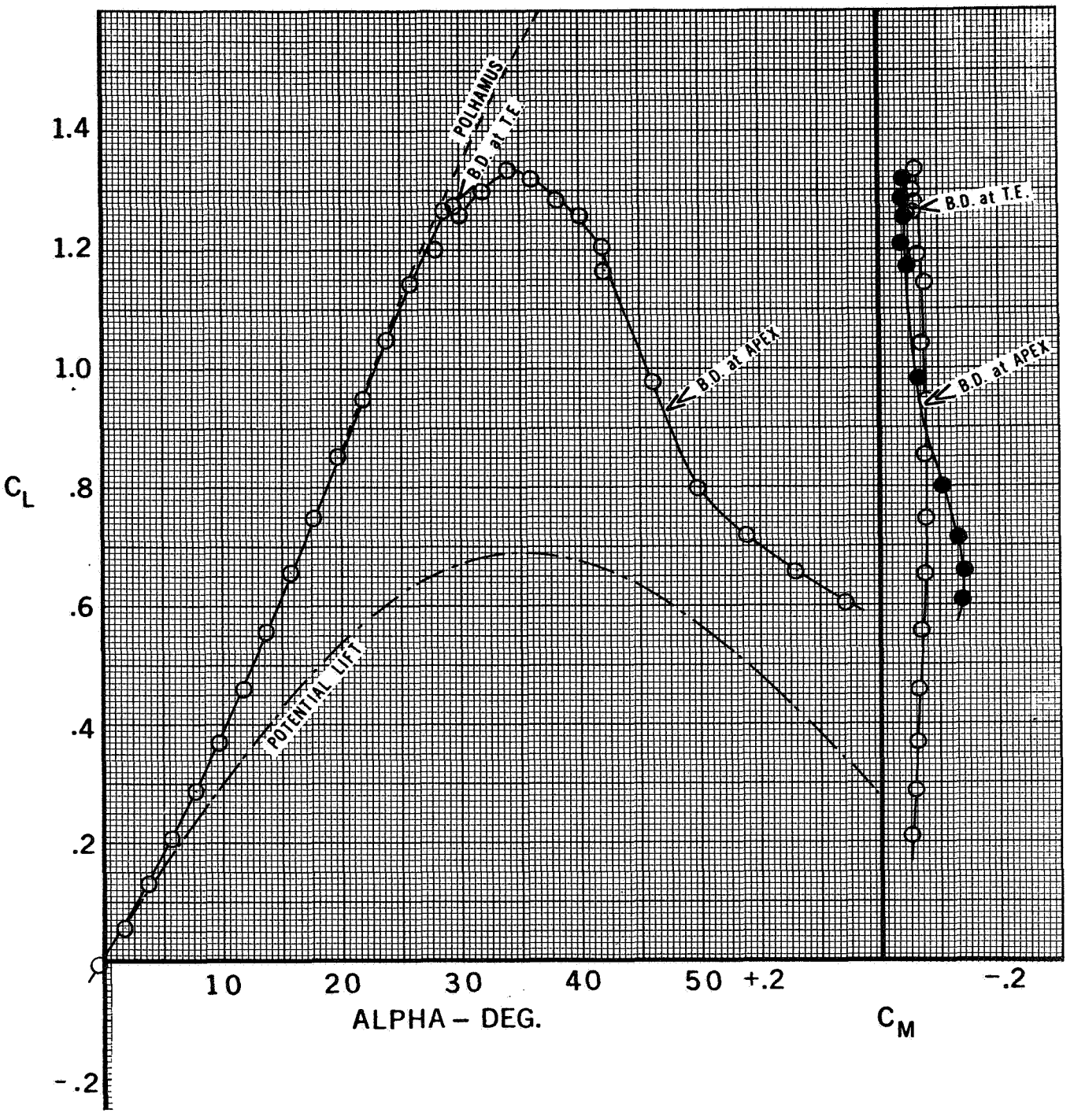

Figure 5.7.1-Lift and Pitching Characteristics - 70° Delta Wing

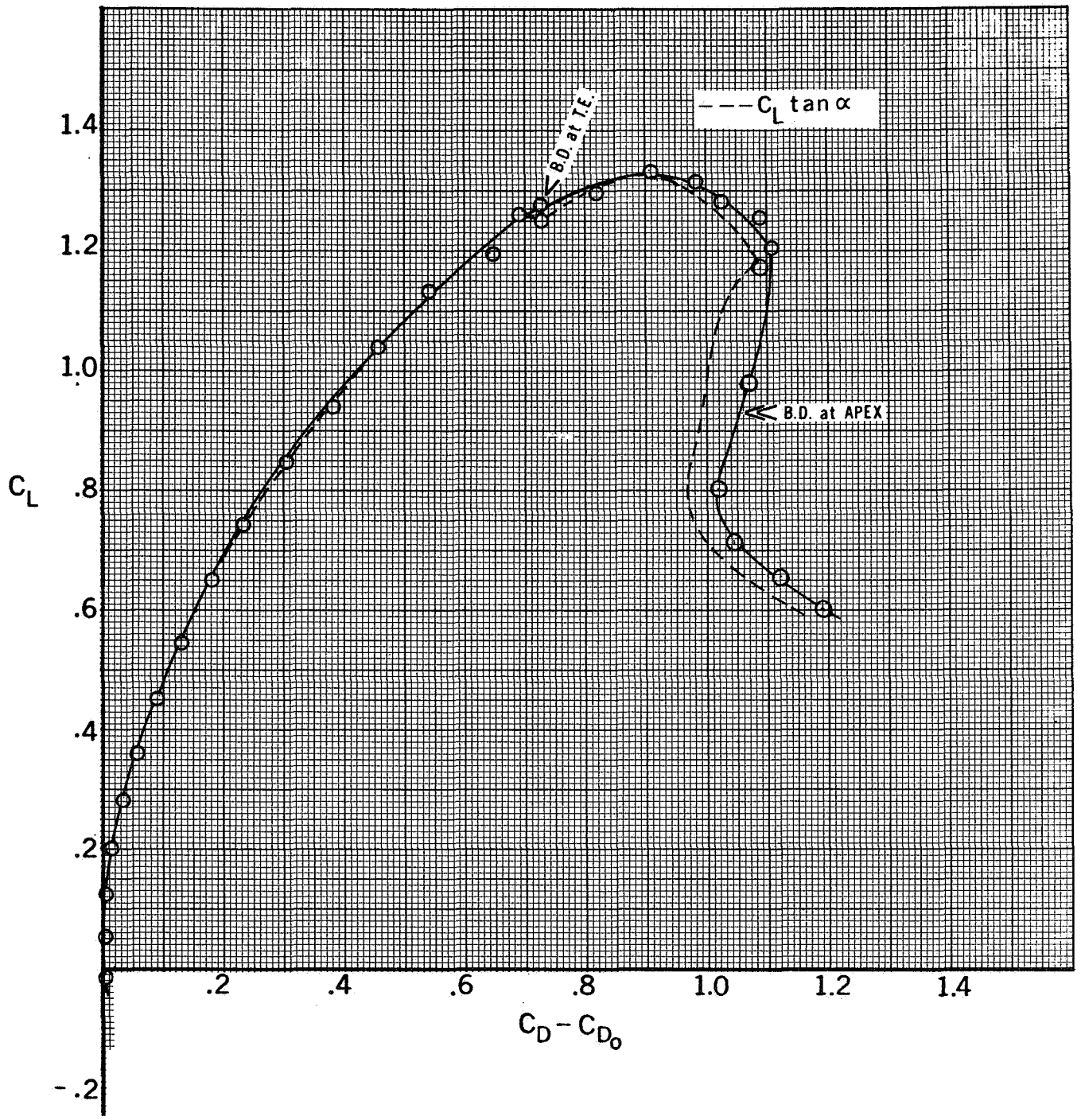

Figure 5.7.2 - Drag Due to Lift - 70° Delta Wing

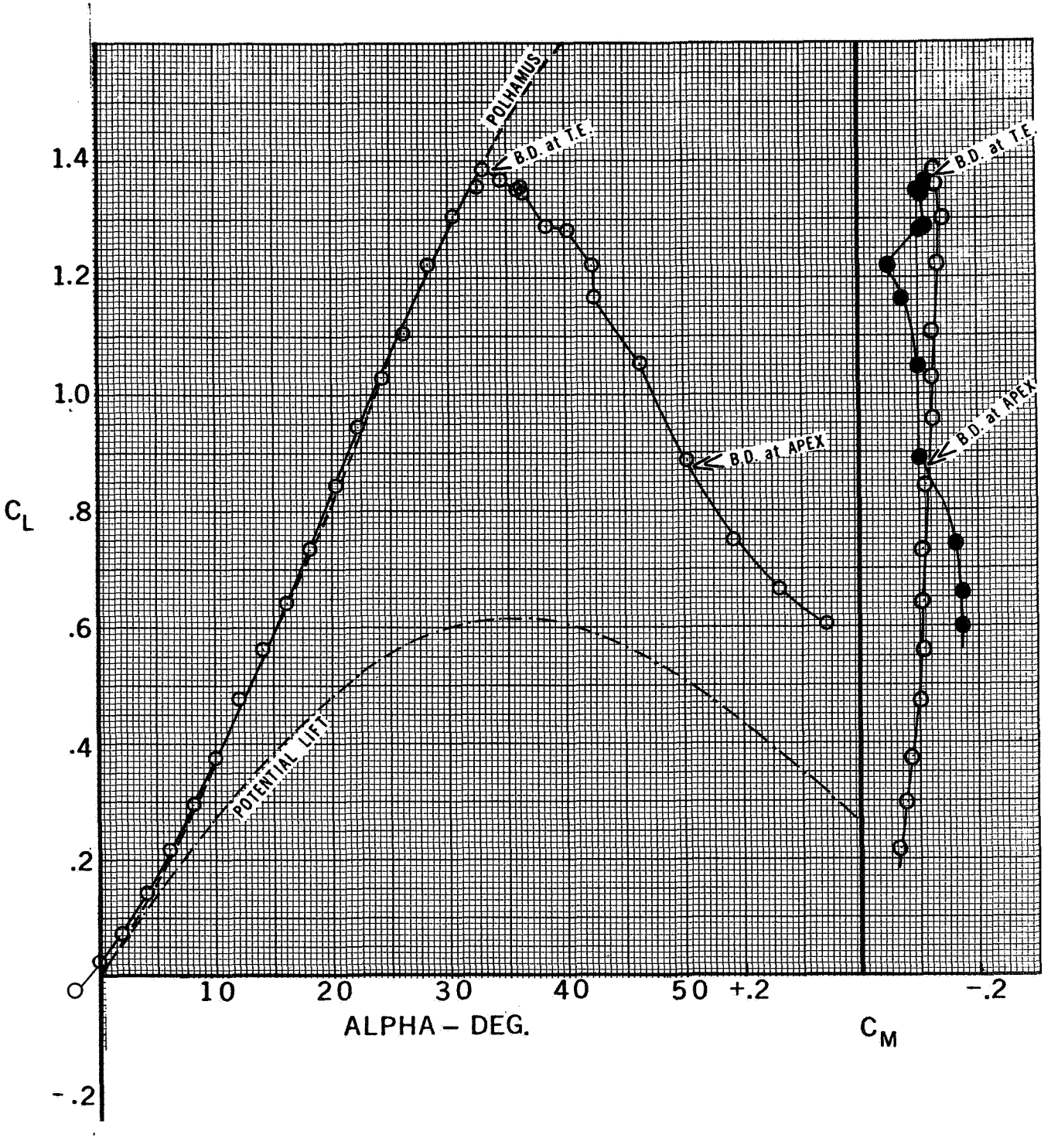

Figure 5.8.1-Lift and Pitching Characteristics - 72.5° Delta Wing

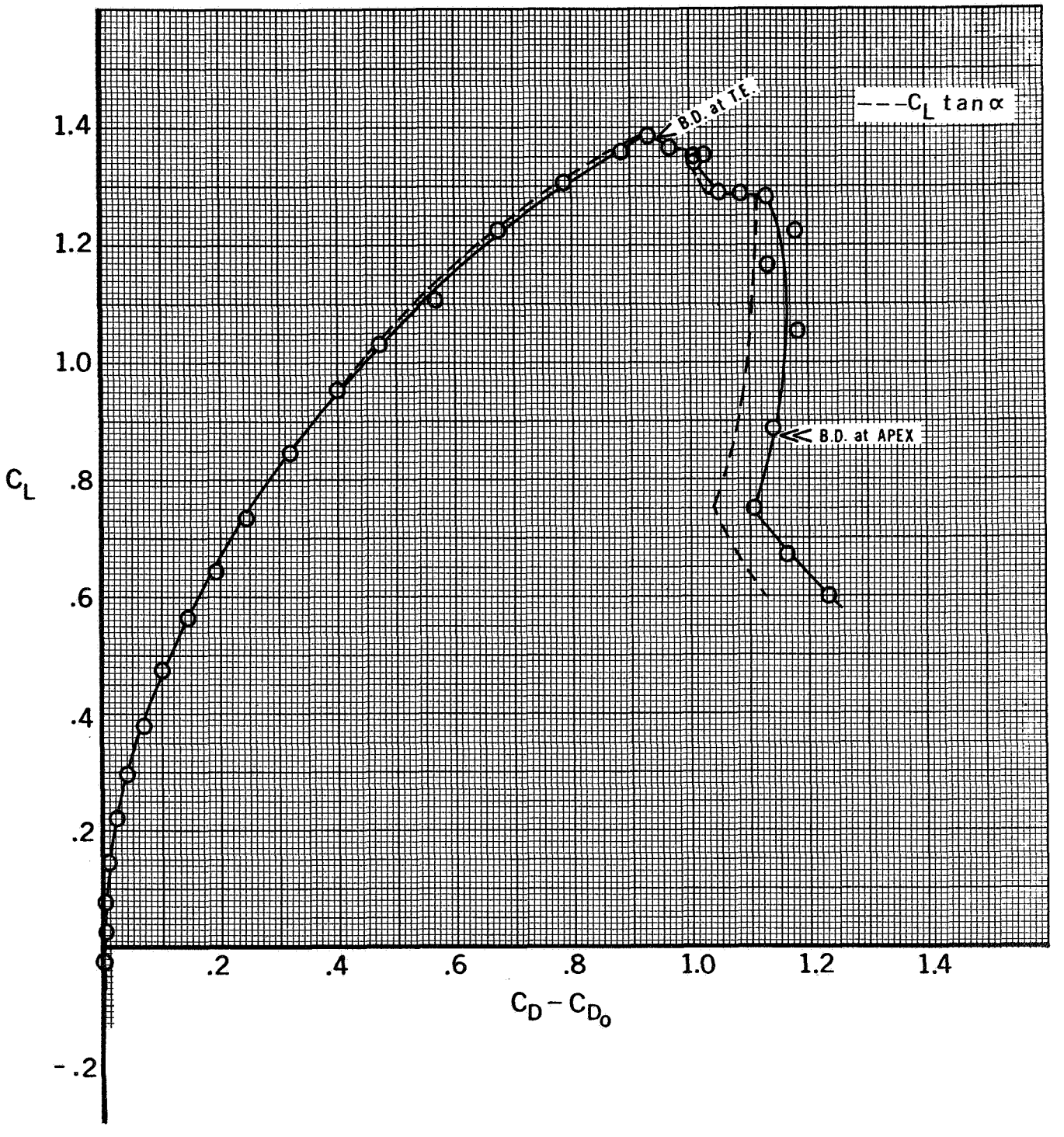

Figure 5.8.2 - Drag Due to Lift - 72.5° Delta Wing

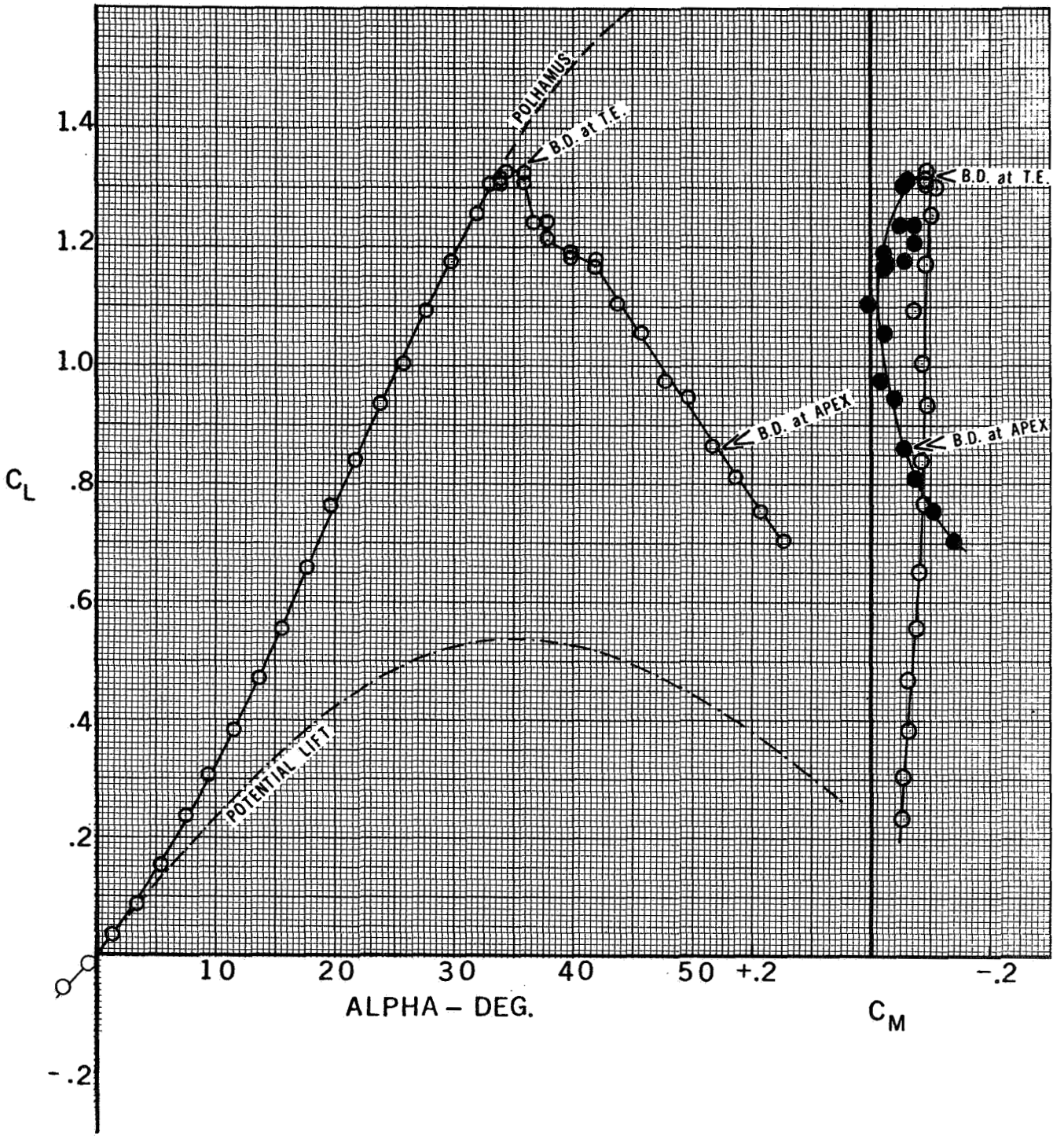

Figure 5.9.1-Lift and Pitching Characteristics - 75° Delta Wing

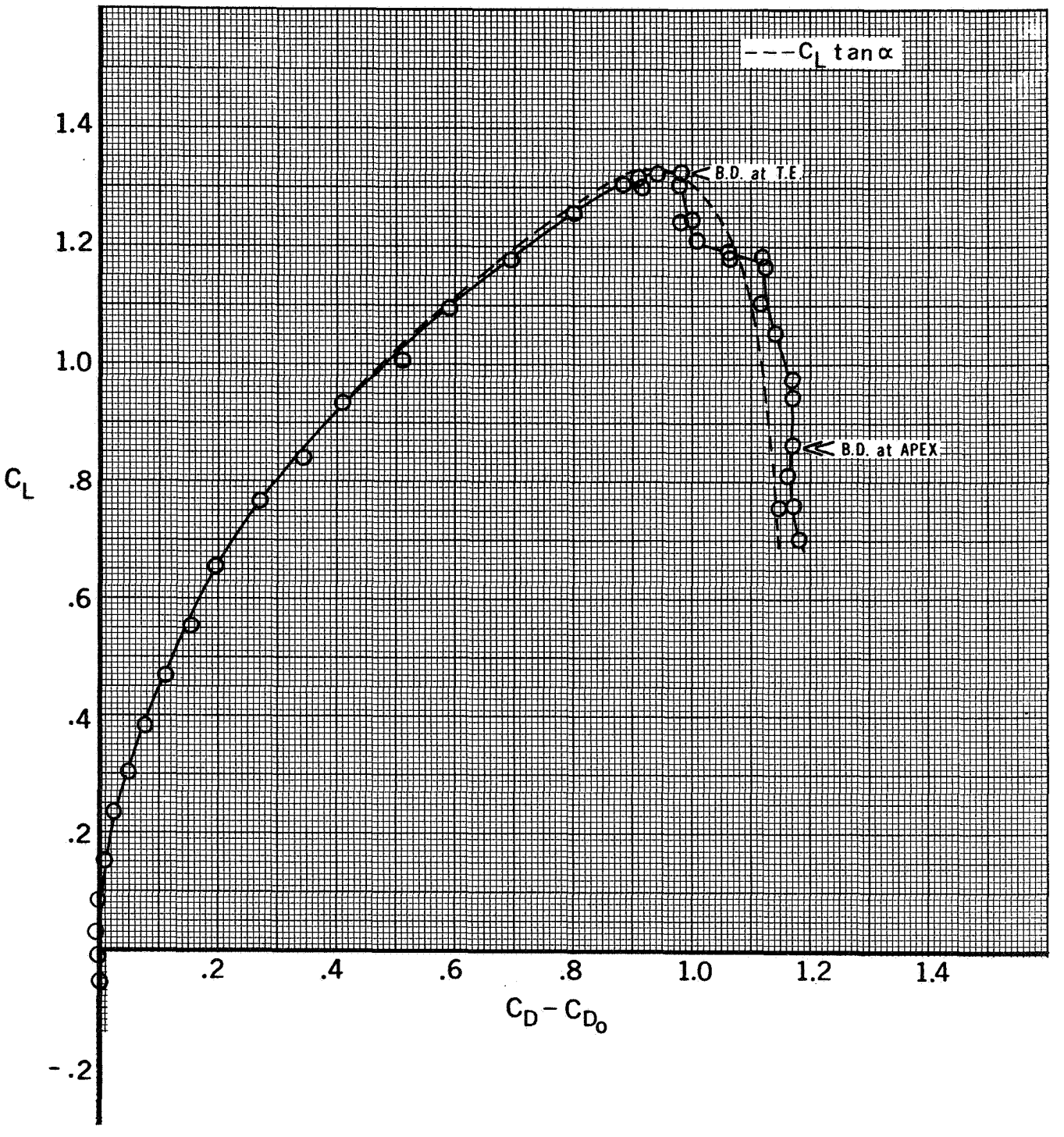

Figure 5.9.2 - Drag Due to Lift - 75° Delta Wing

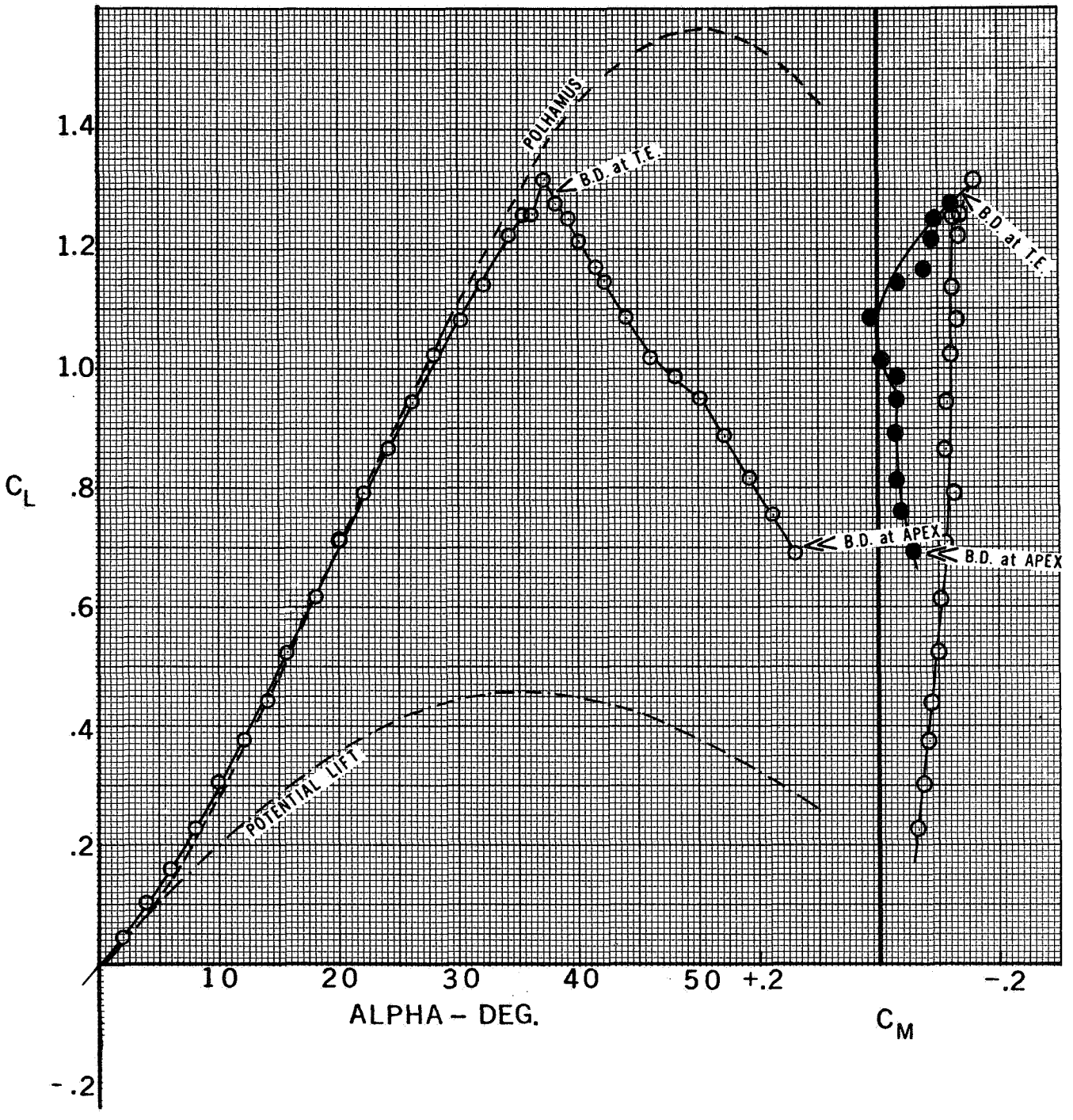

Figure 5.10.1-Lift and Pitching Characteristics - 77.5° Delta Wing

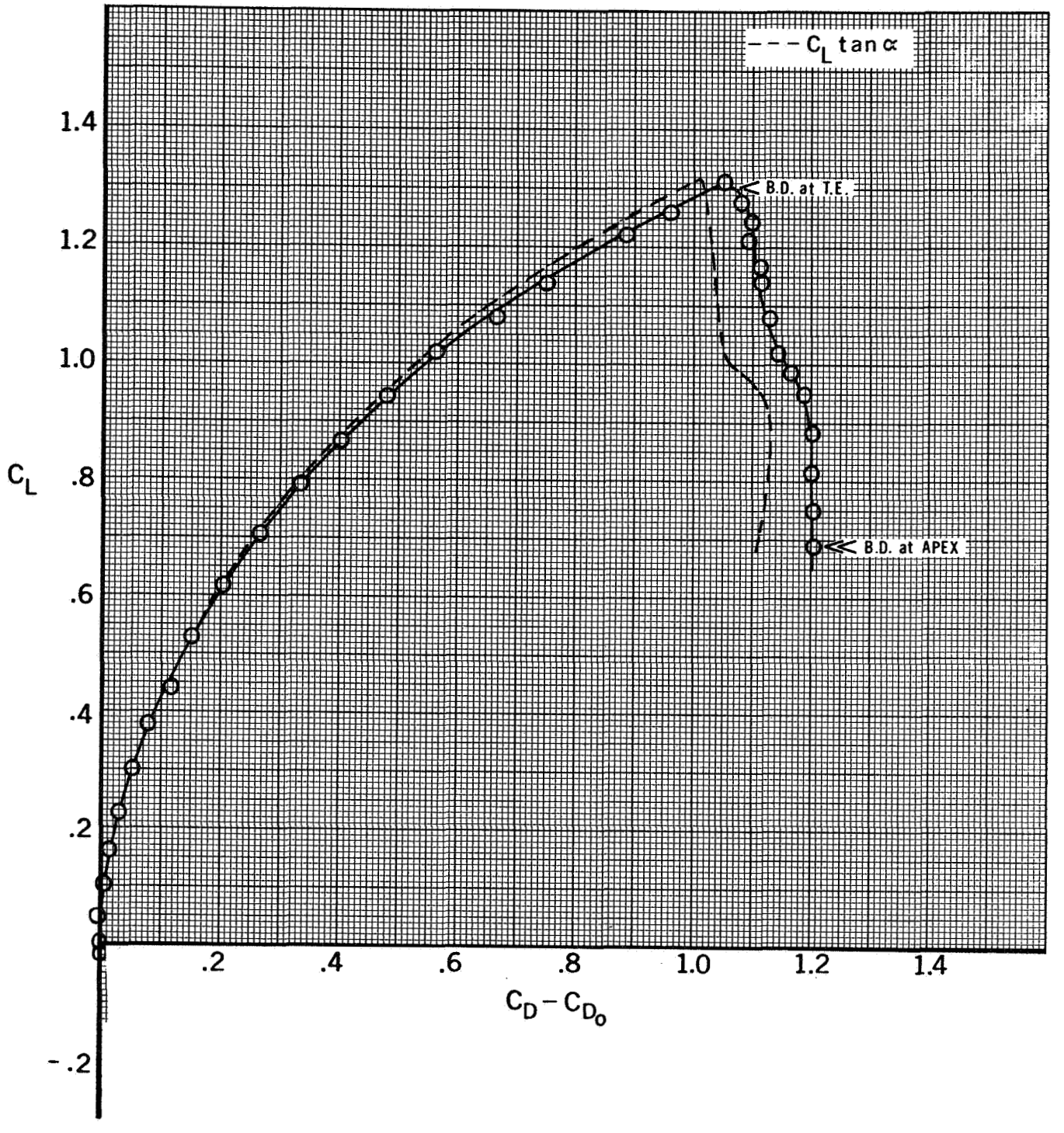

Figure 5.10.2 - Drag Due to Lift - 77.5° Delta Wing

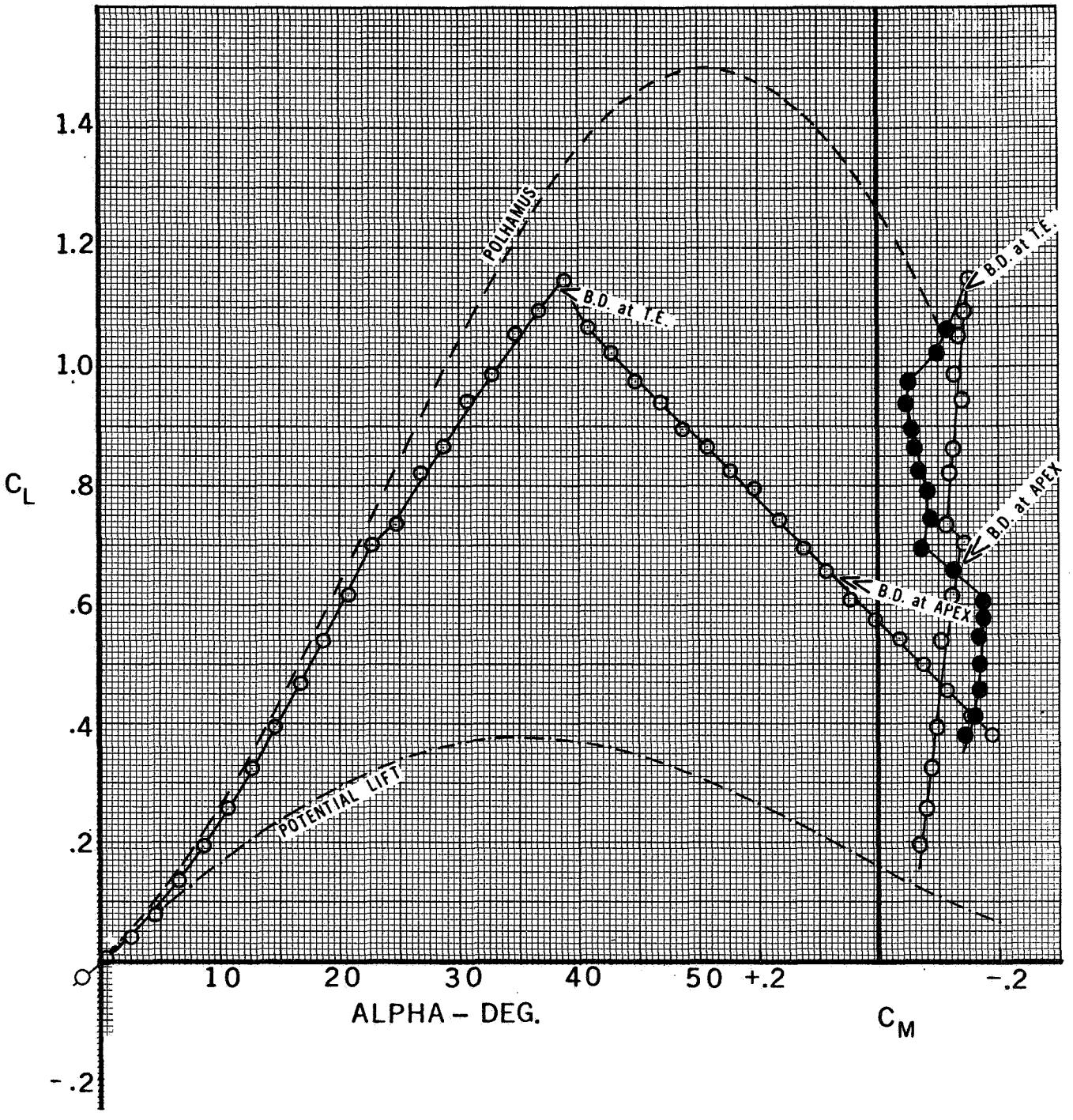

Figure 5.11.1-Lift and Pitching Characteristics - 80° Delta Wing

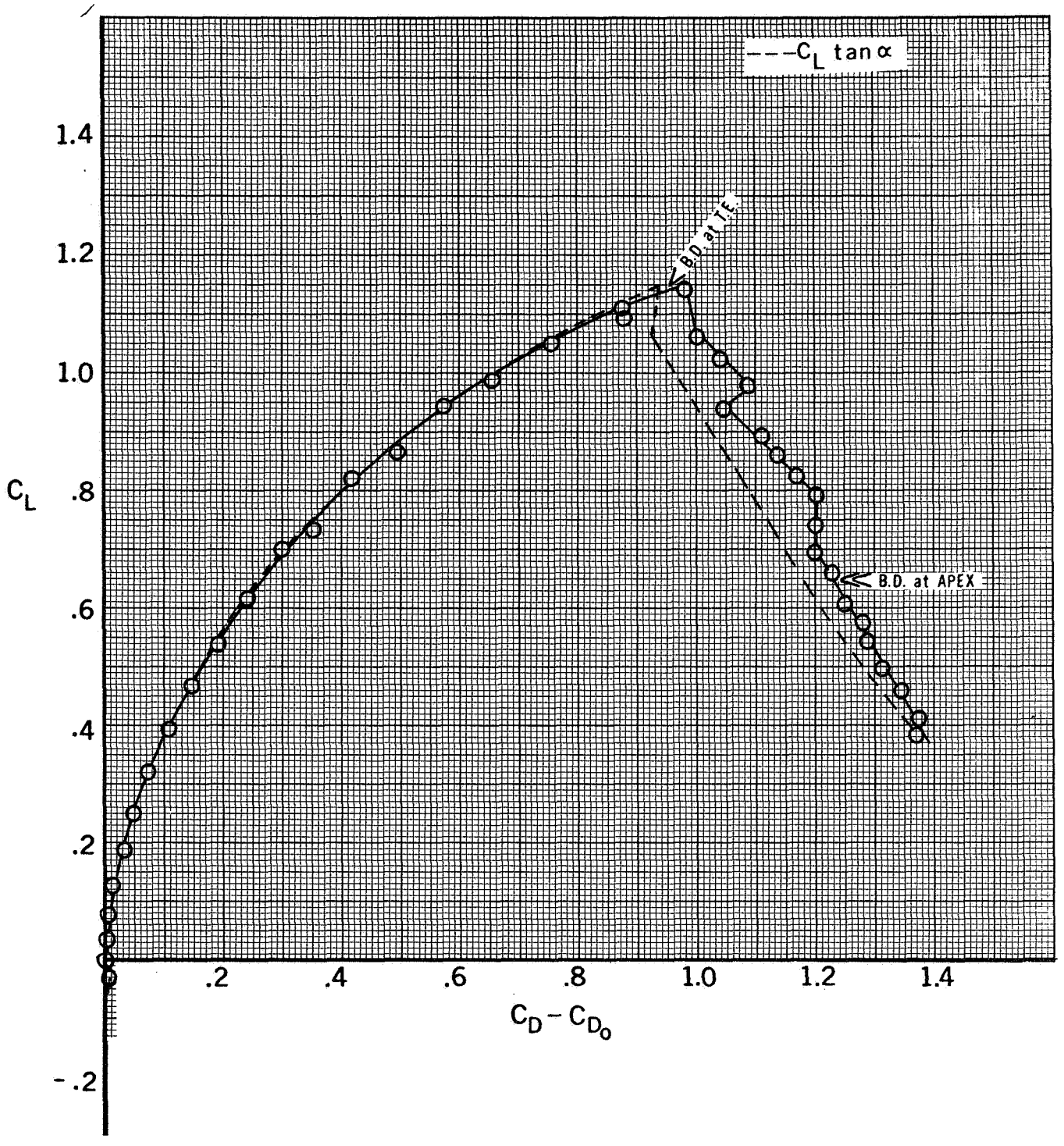

Figure 5.11.2 - Drag Due to Lift - 80° Delta Wing

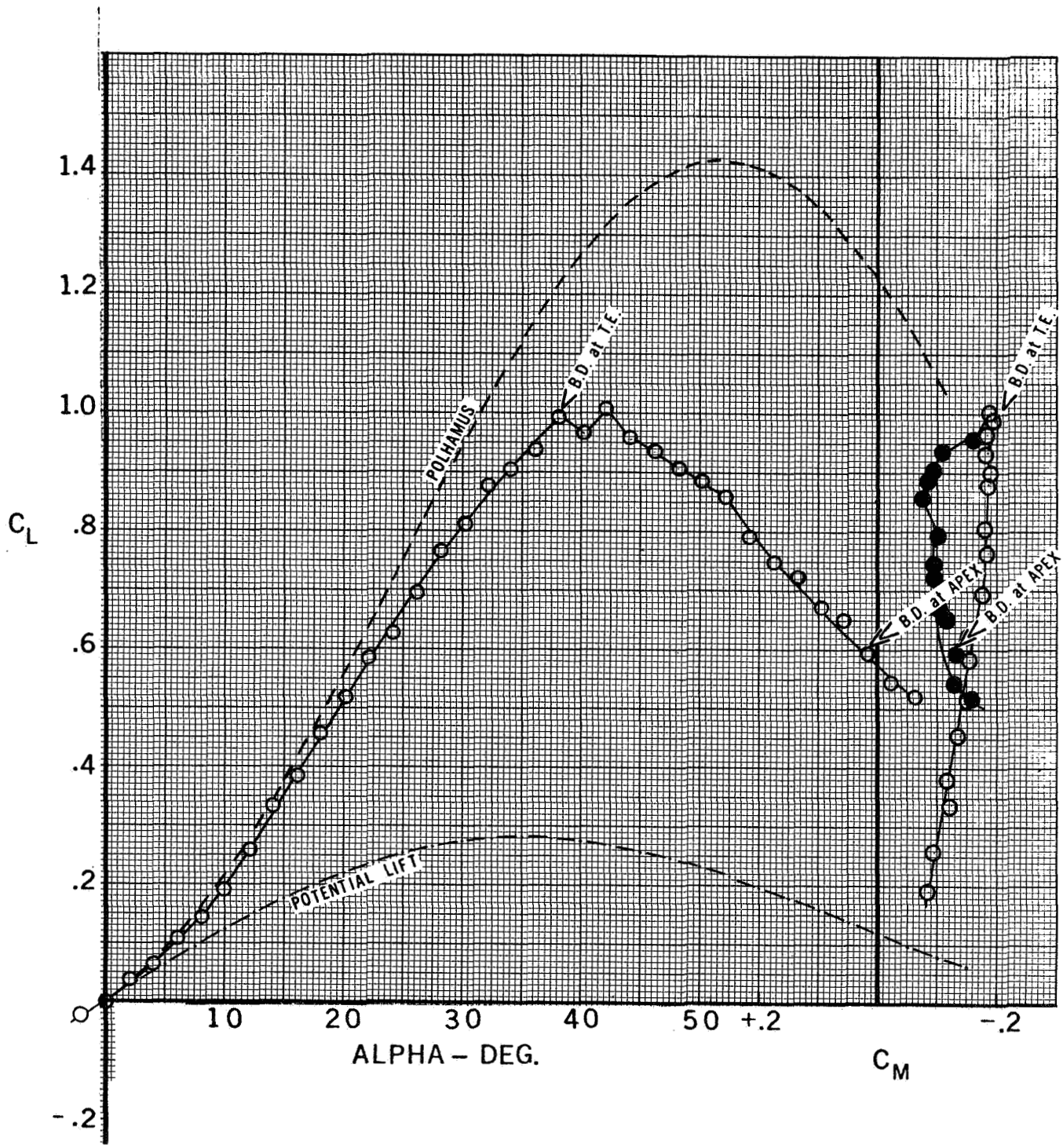

Figure 5.12.1-Lift and Pitching Characteristics - 82.5° Delta Wing

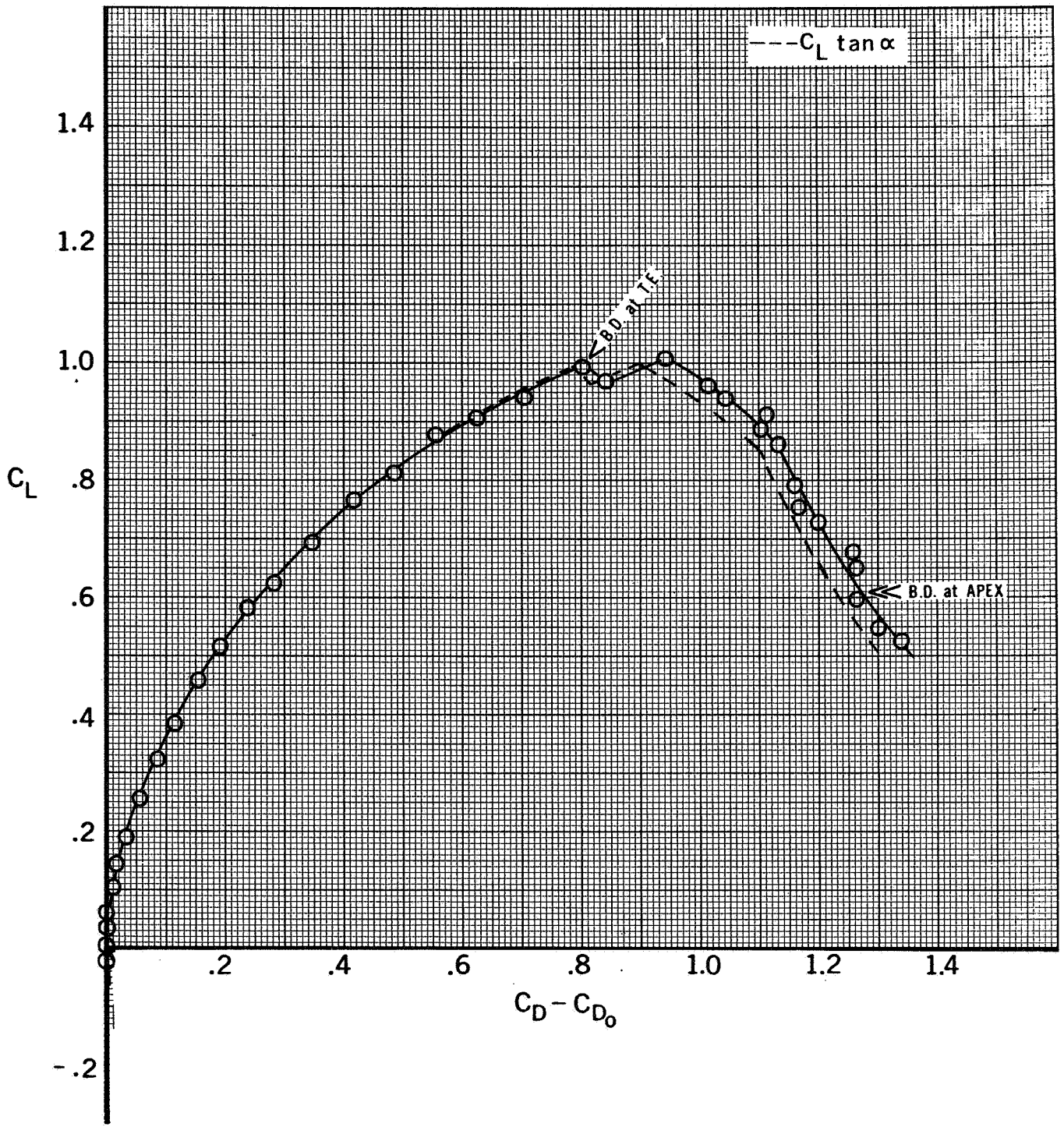

Figure 5.12.2 - Drag Due to Lift - 82.5° Delta Wing

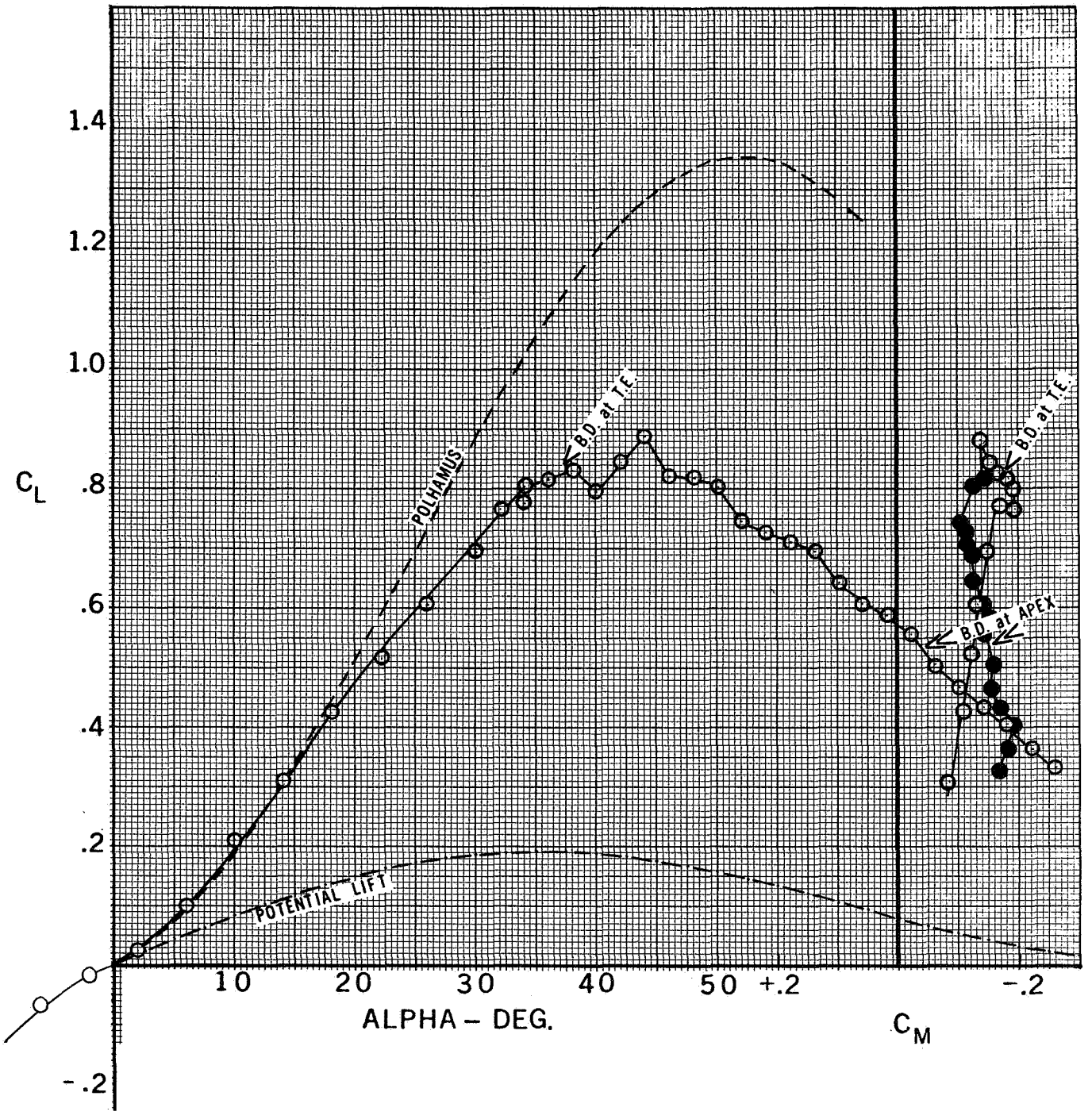

Figure 5.13.1-Lift and Pitching Characteristics - 85° Delta Wing

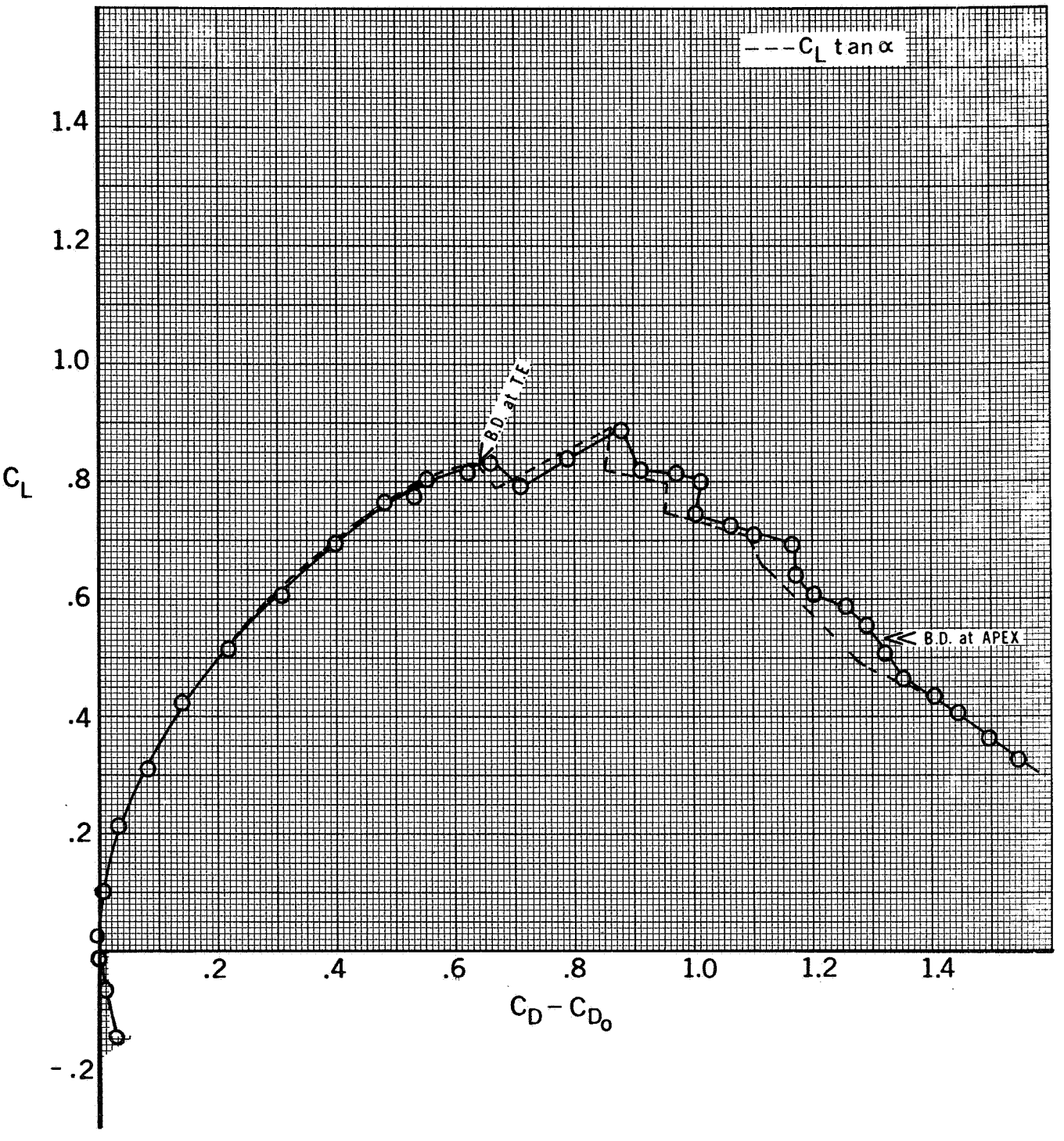

Figure 5.13.2 - Drag Due to Lift - 85° Delta Wing

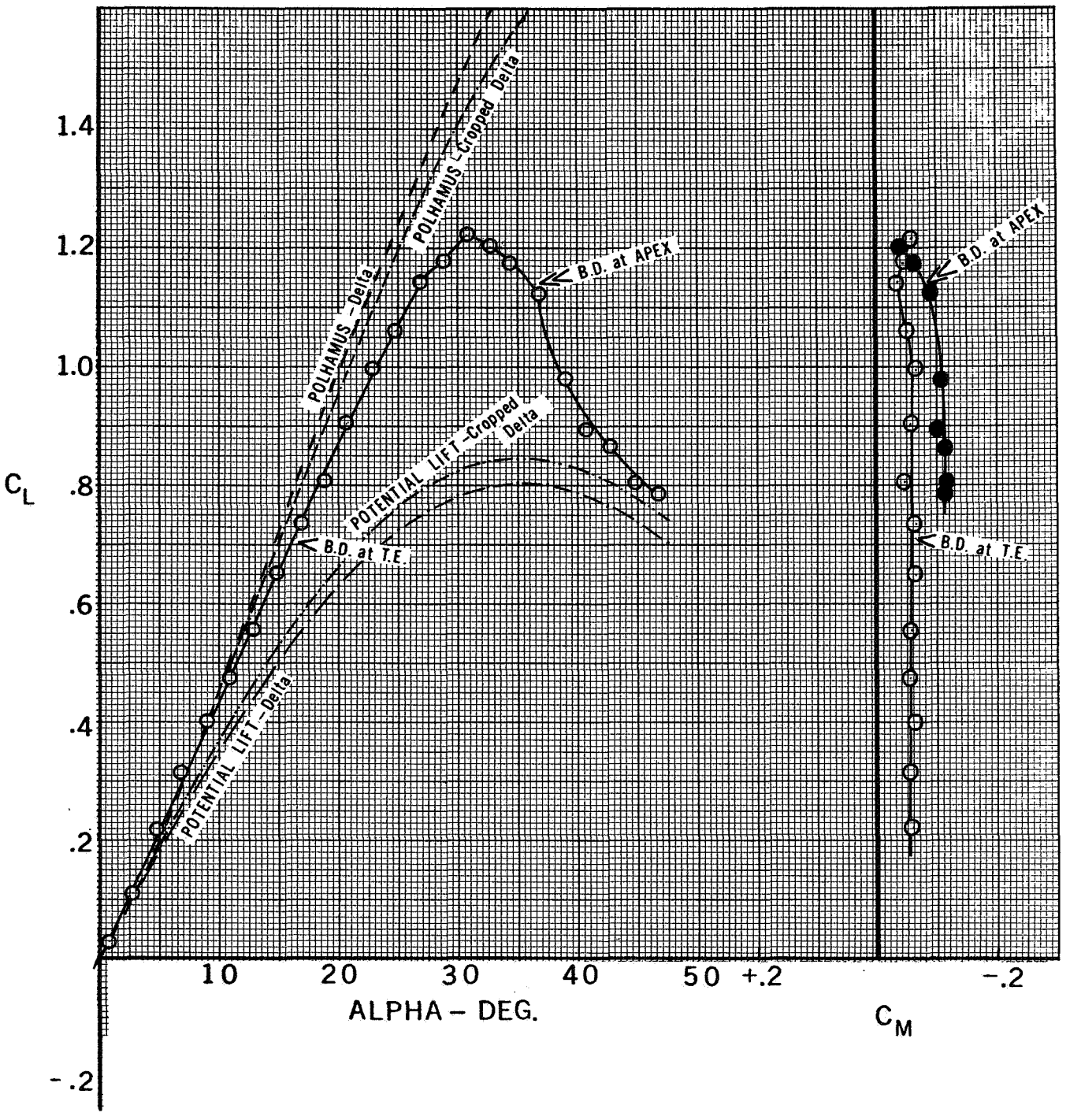

Figure 5.14.1-Lift and Pitching Characteristics

- Cropped 60° Delta Wing

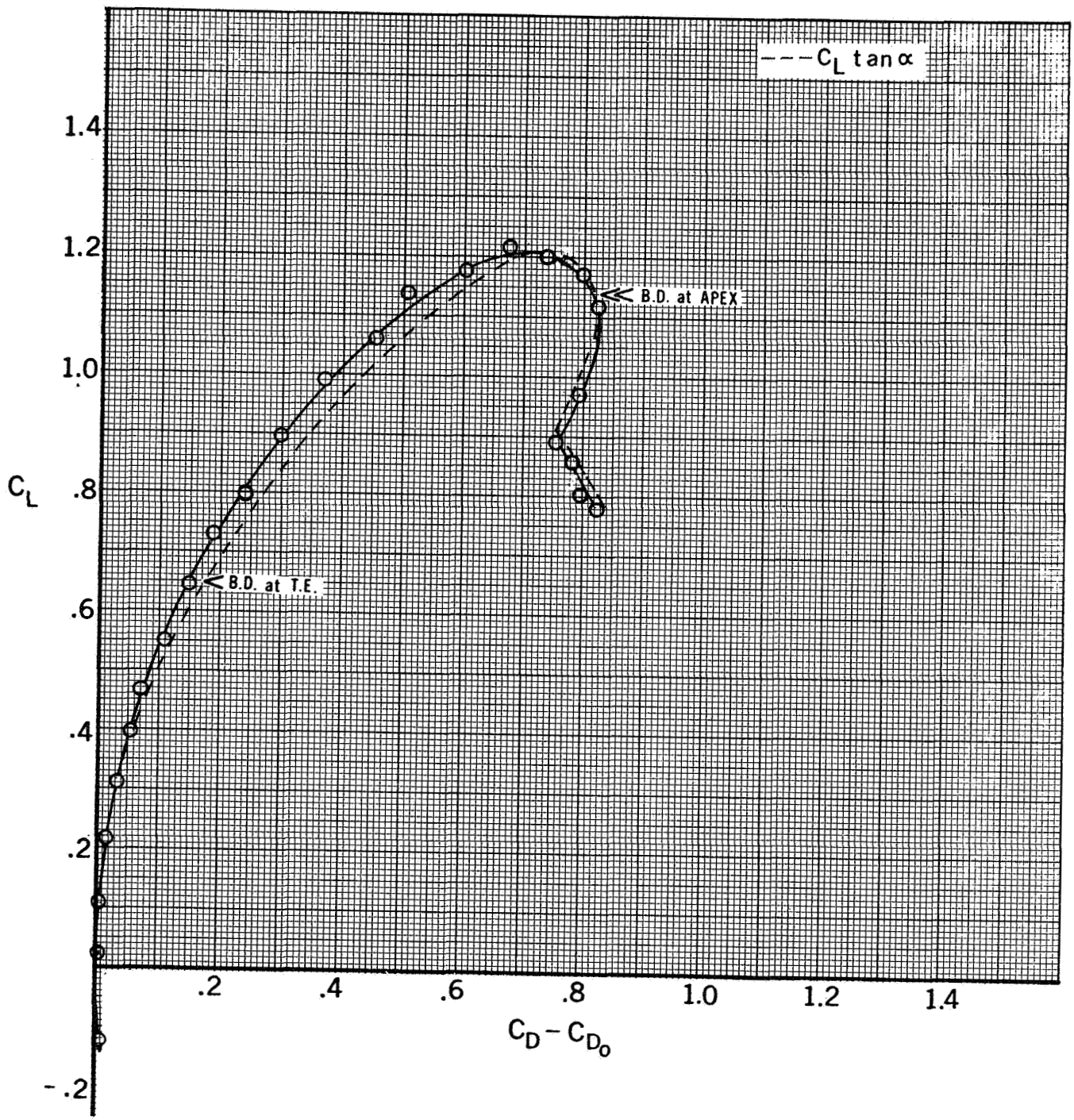

Figure 5.14.2 - Drag Due to Lift - Cropped 60° Delta Wing

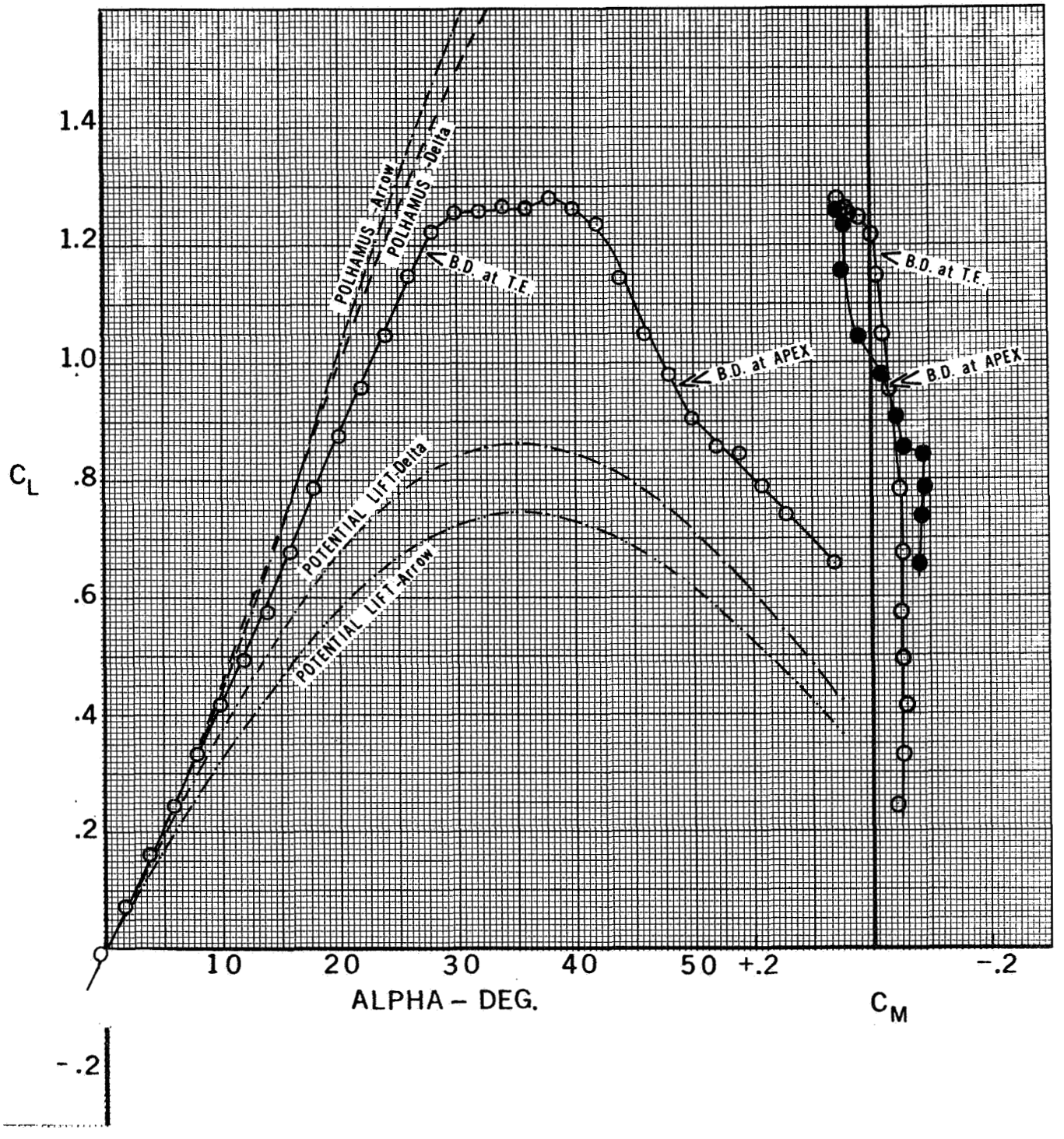

Figure 5.15.1-Lift and Pitching Characteristics - 70° Arrow Wing

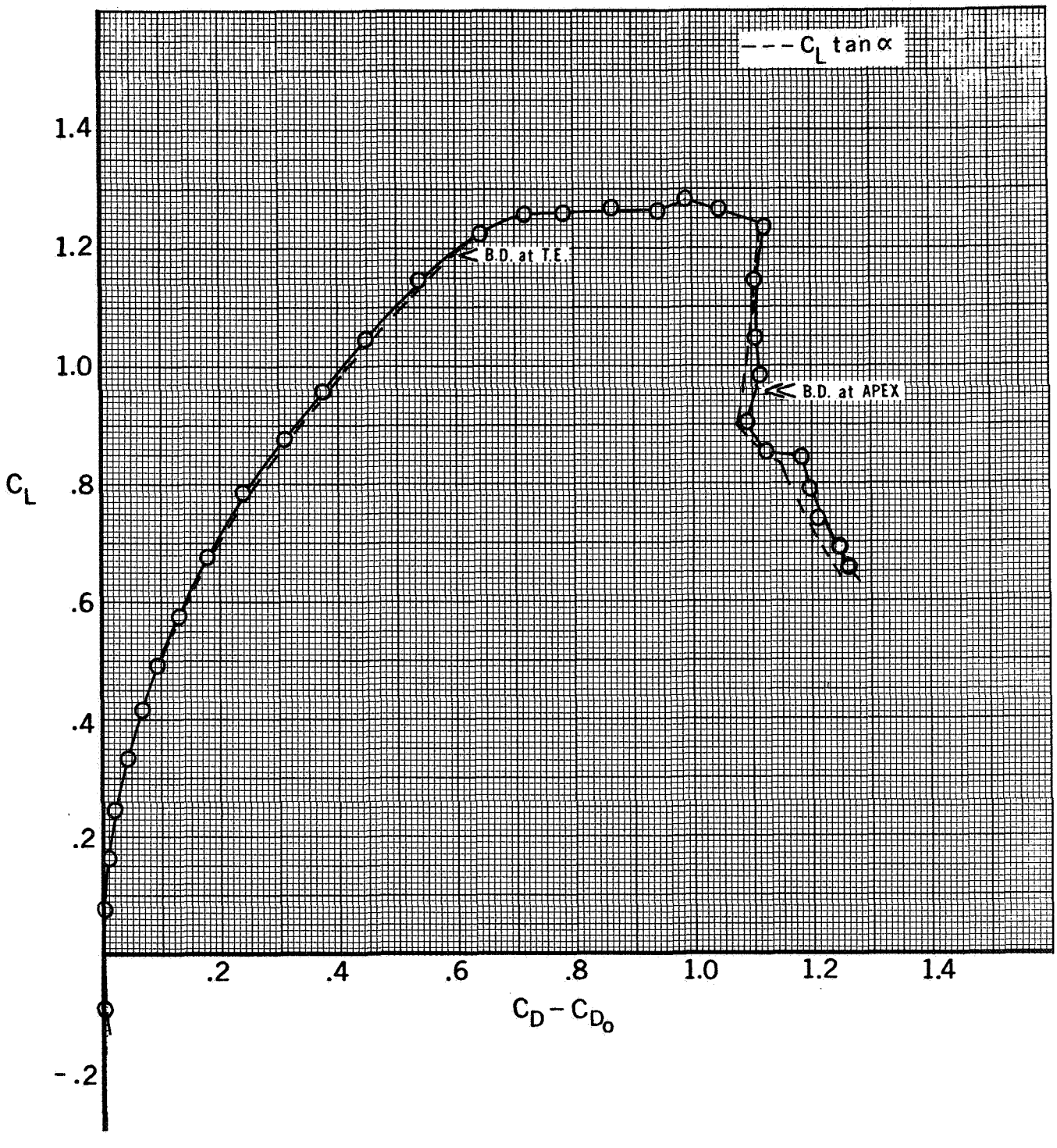

Figure 5.15.2 - Drag Due to Lift - 70° Arrow Wing

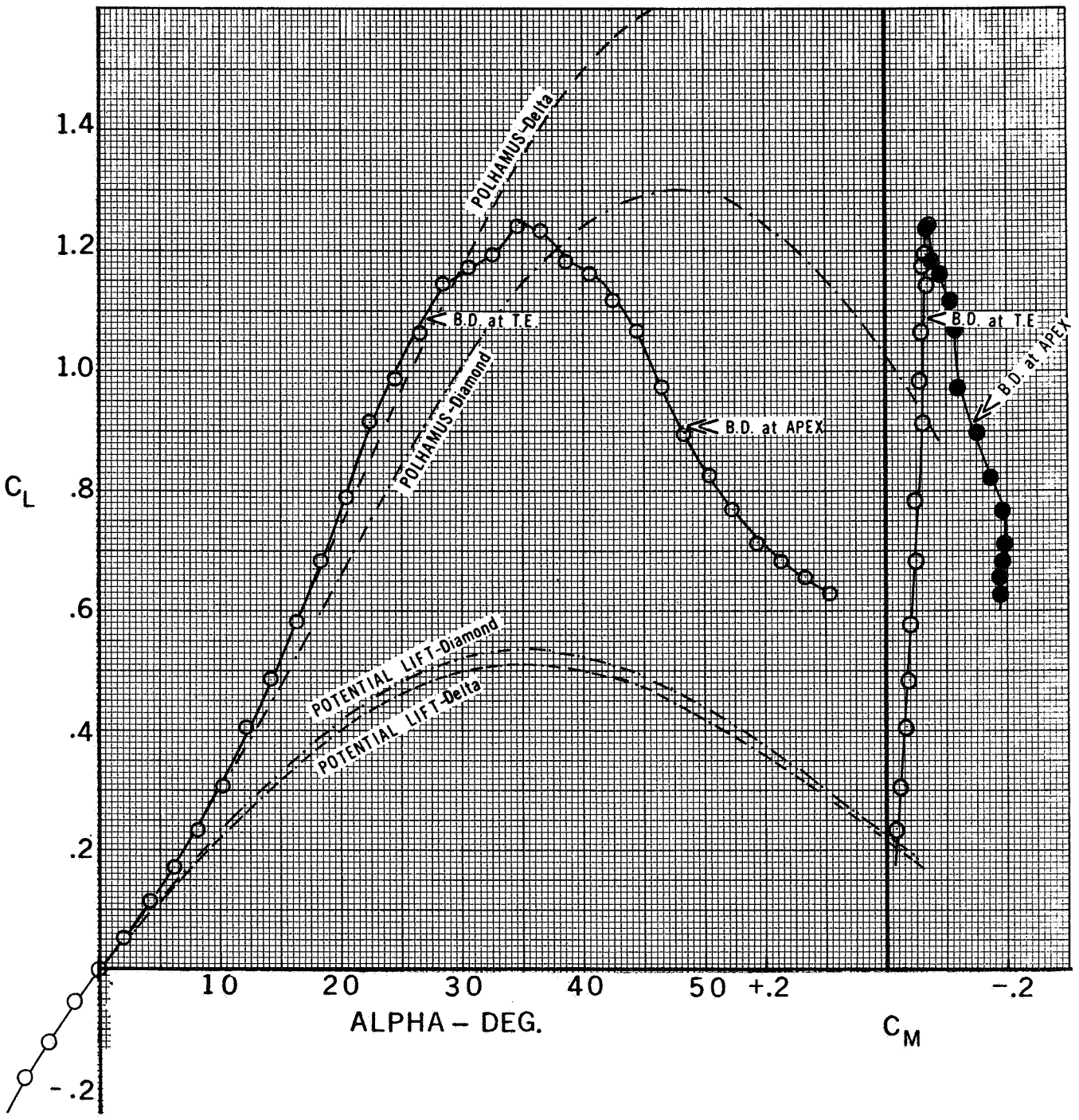

Figure 5.16.1-Lift and Pitching Characteristics - 70° Diamond Wing

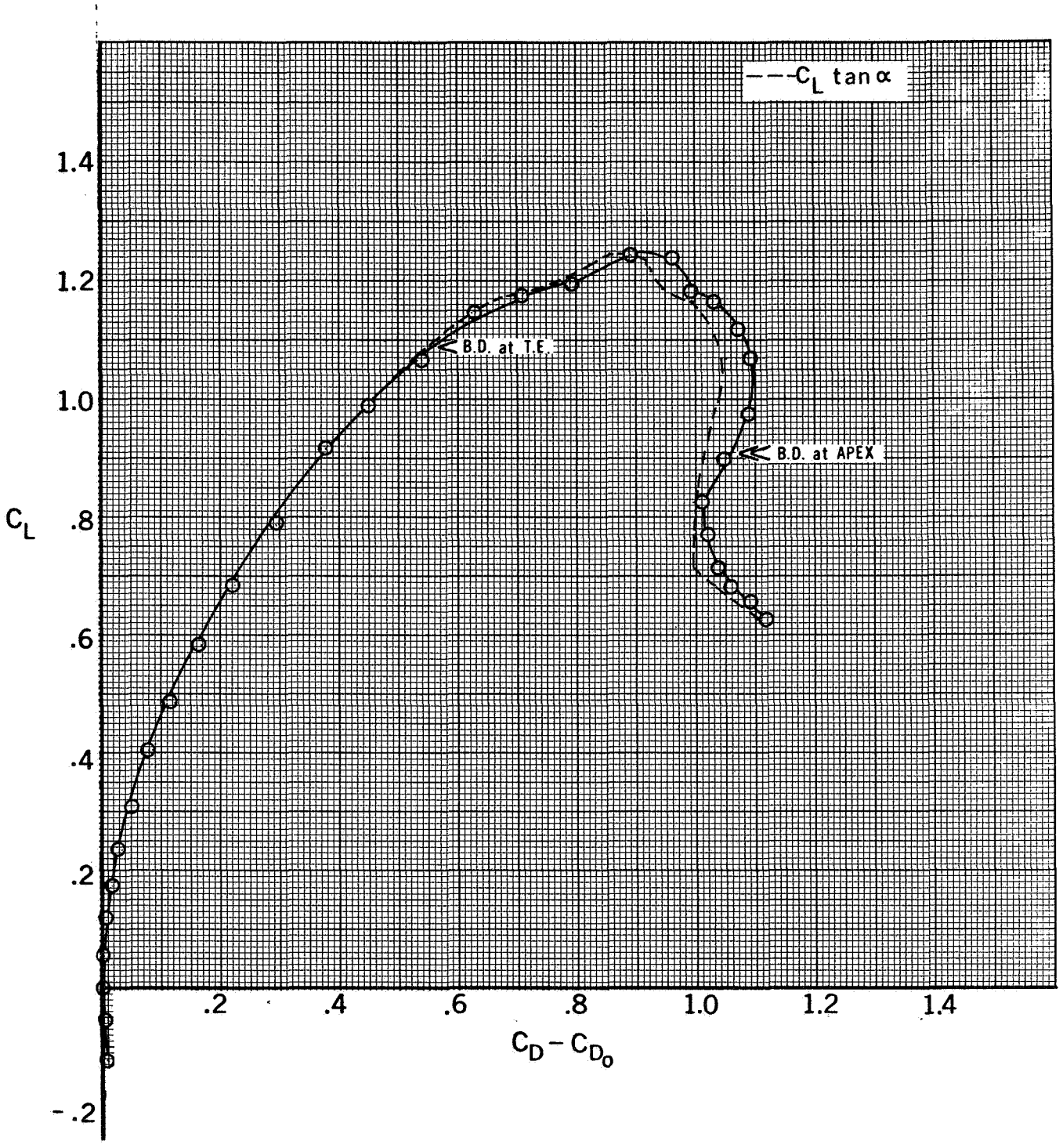

Figure 5.16.2 - Drag Due to Lift - 70° Diamond Wing

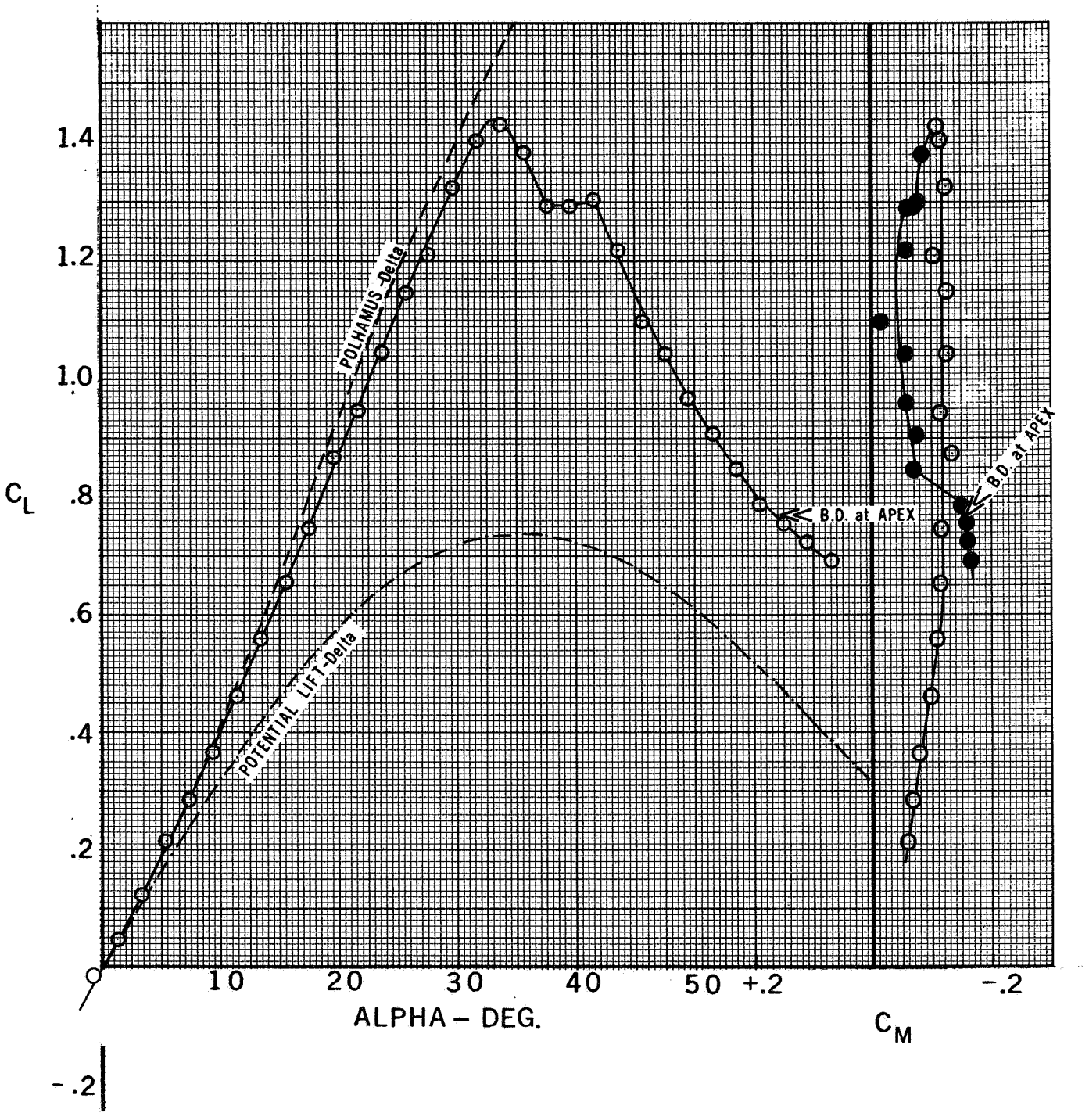

Figure 5.17.1-Lift and Pitching Characteristics - 75°/65° Double-Delta Wing

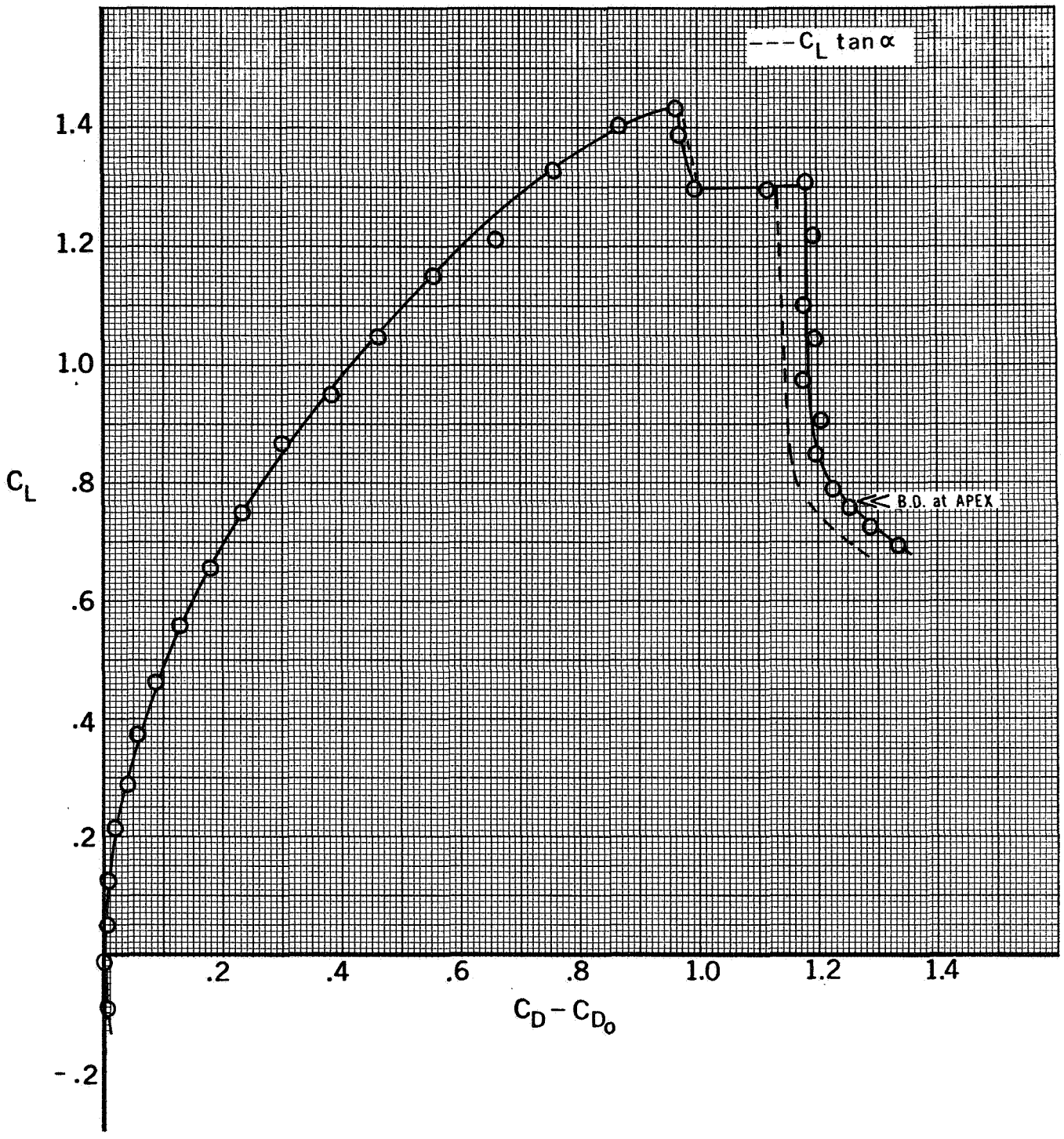

Figure 5.17.2 - Drag Due to Lift - 75°/65° Double-Delta Wing

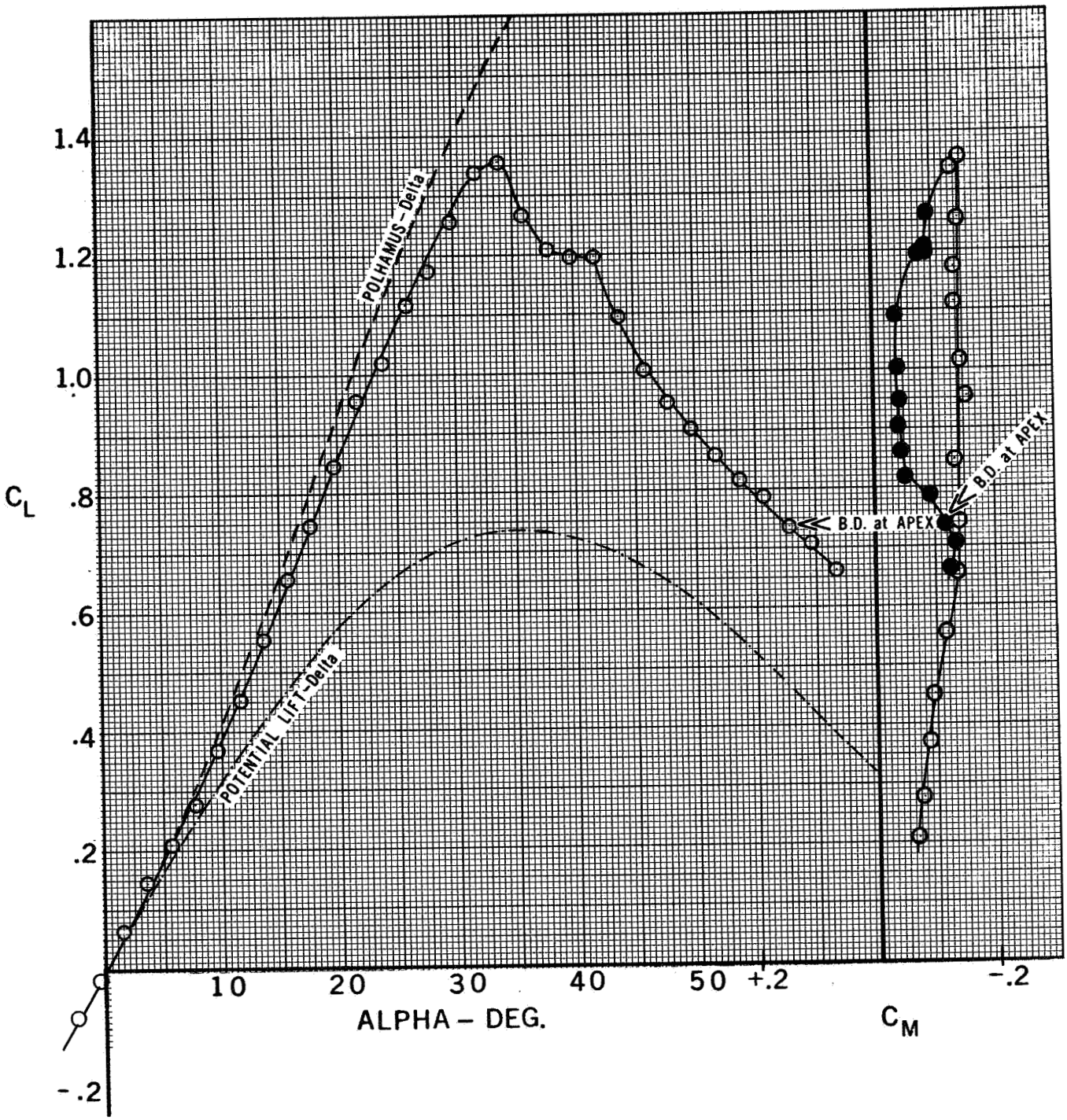

Figure 5.18.1-Lift and Pitching Characteristics
– 80°/65° Double-Delta Wing

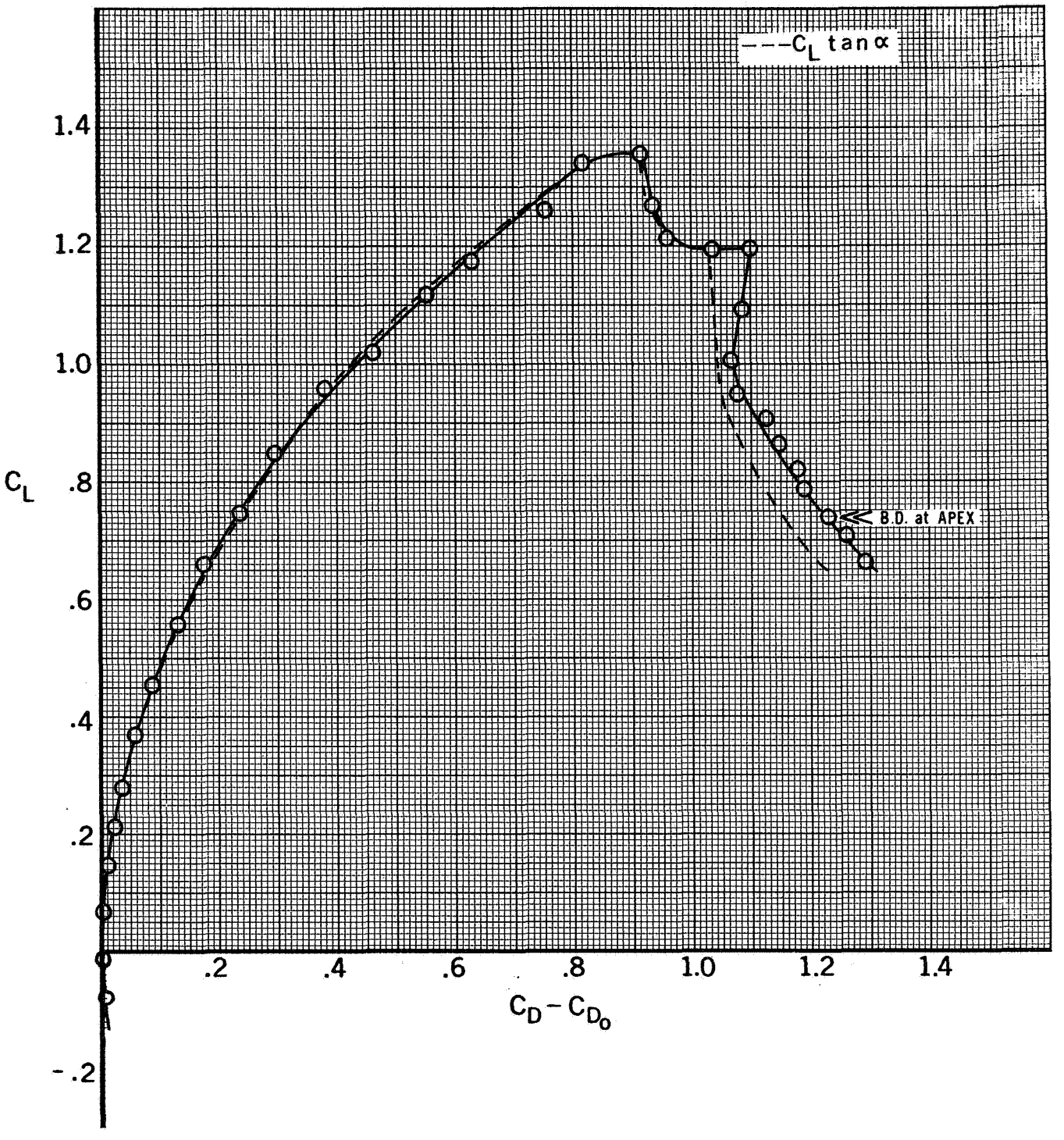

Figure 5.18.2 - Drag Due to Lift - 80°/65° Double-Delta Wing

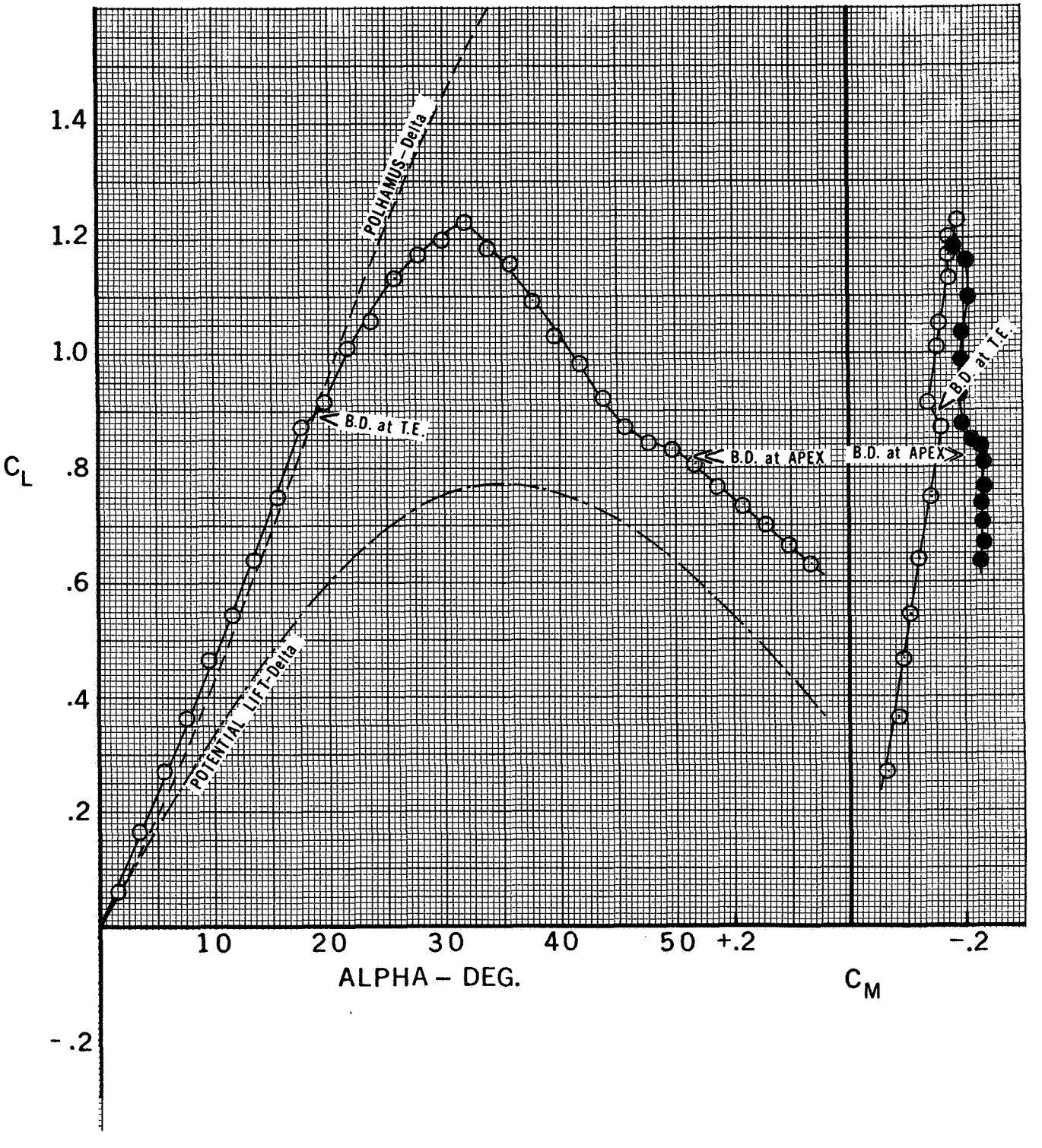

Figure 5.19.1-Lift and Pitching Characteristics - Ogee Wing

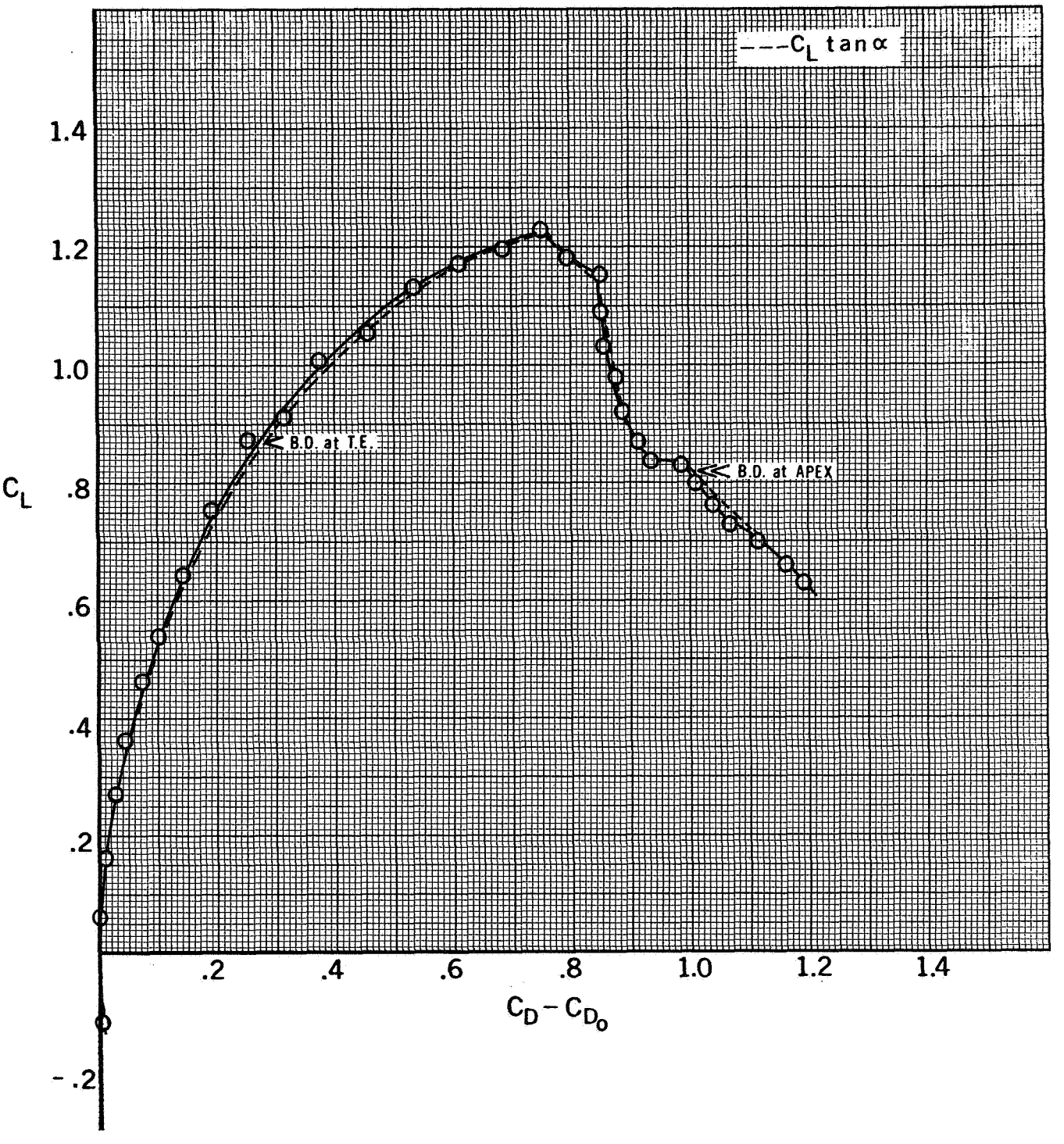

Figure 5.19.2 - Drag Due to Lift - Ogee Wing

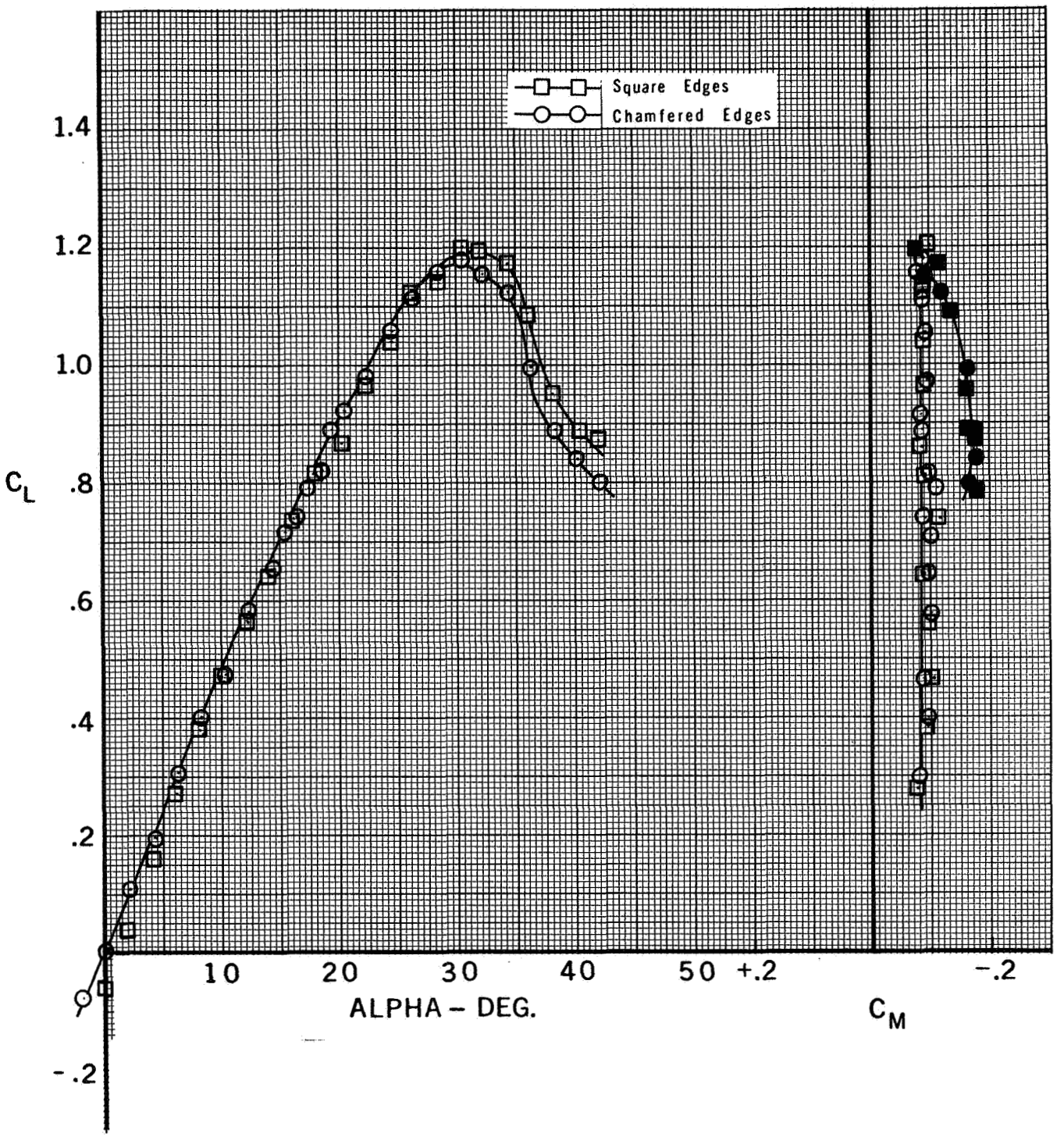

Figure 5.20.1 - Effect of Edge Shape on Lift and Pitching Characteristics – 60° Delta Wing

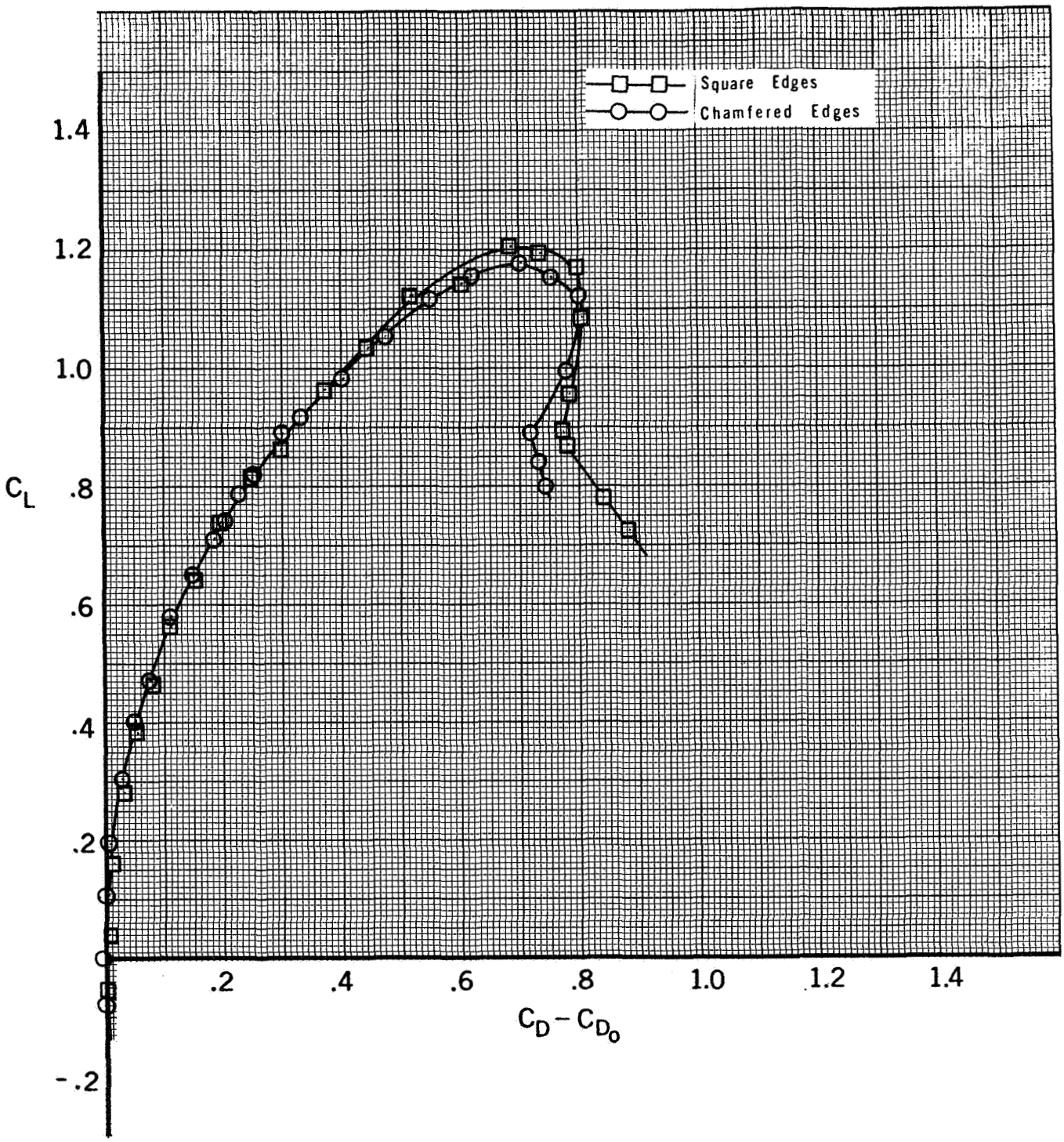

Figure 5.20.2 - Effect of Edge Shape on Drag Due to Lift

- 60° Delta Wing

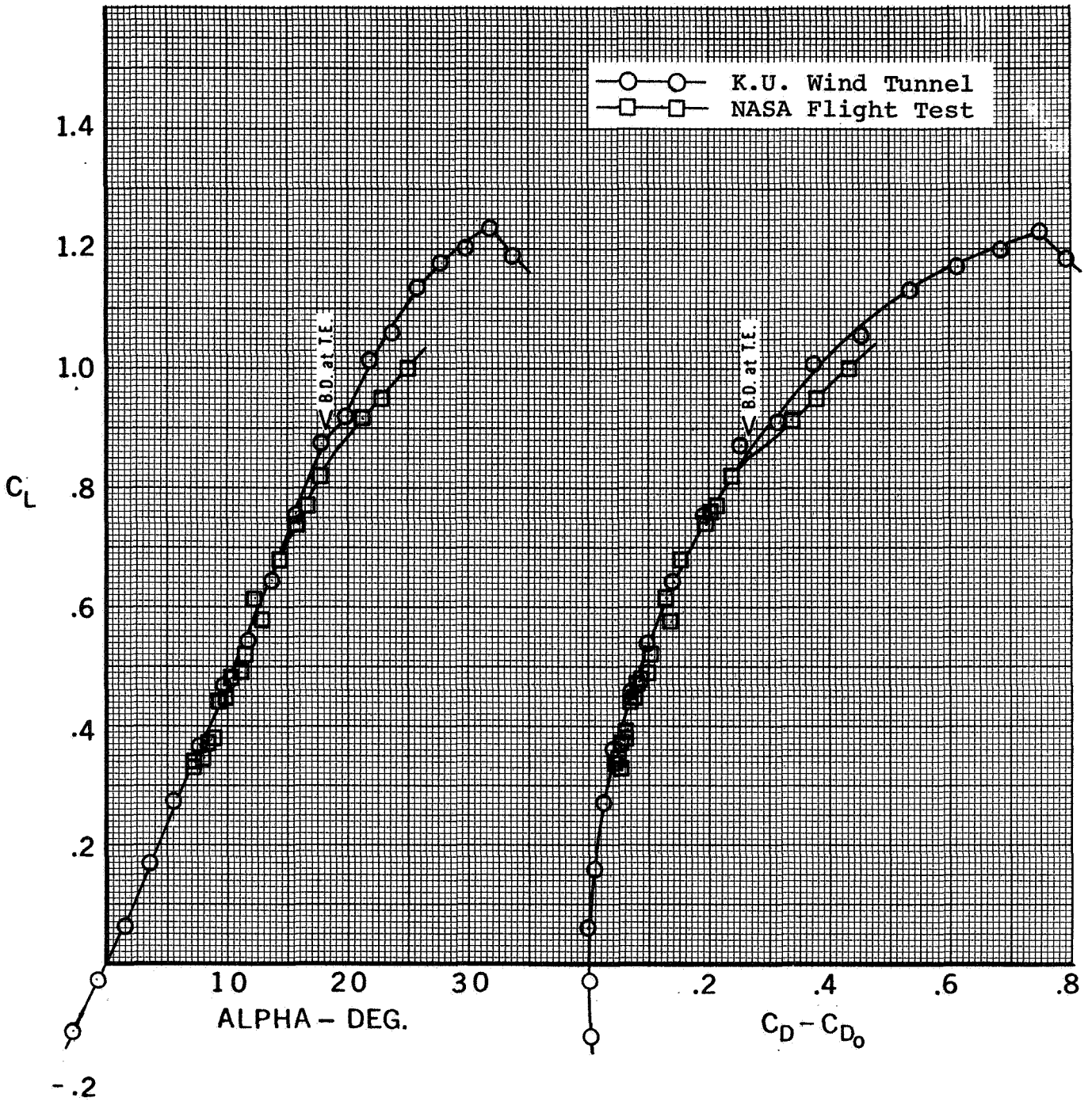

Figure 5.21 - Lift and Drag Comparisons with Flight Test Data - Ogee Wing

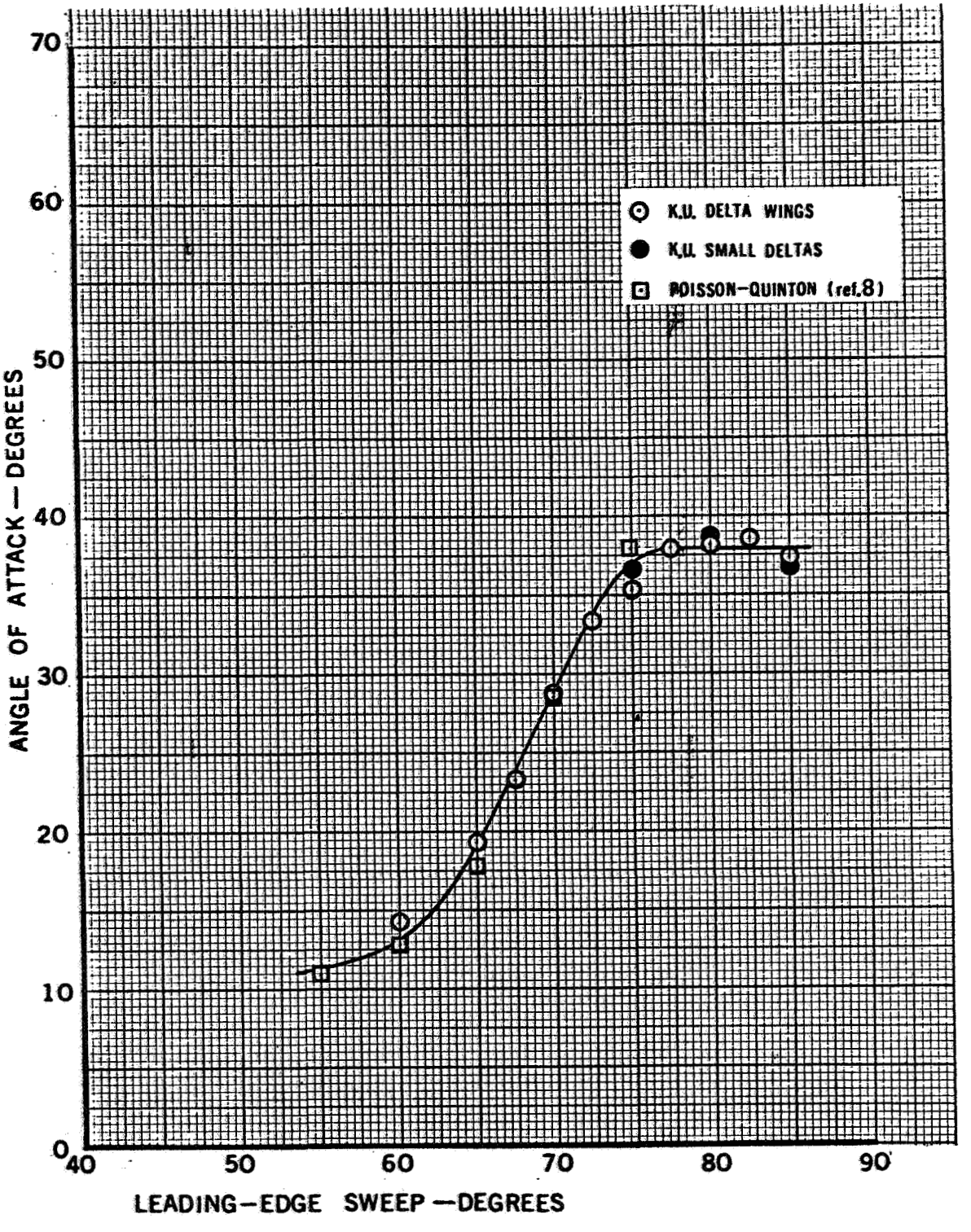

Figure 6 - Effect of Sweep on Vortex Breakdown at Trailing Edge - Delta Wings

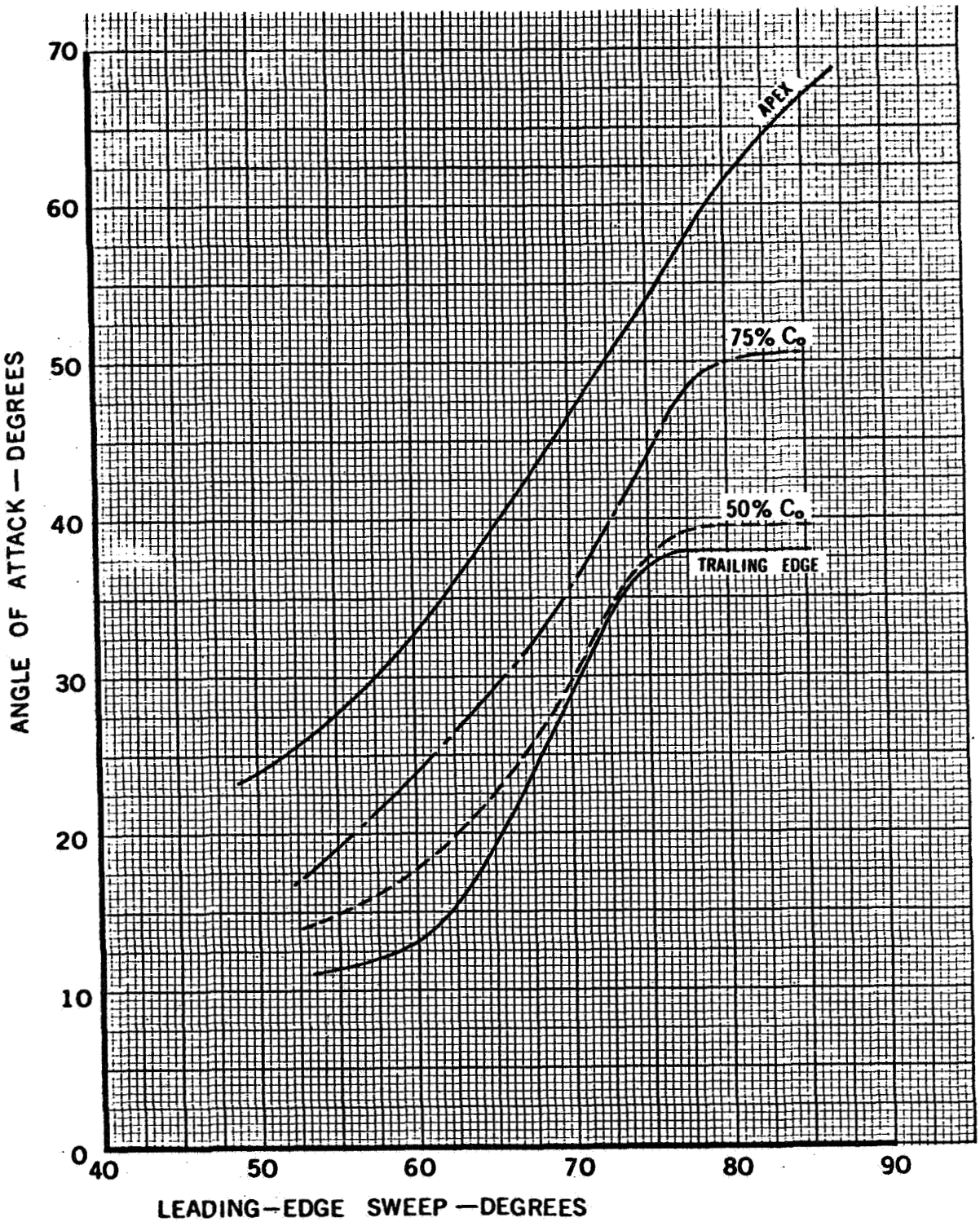

Figure 7 - Effect of Sweep on Vortex Breakdown Position - Delta Wings

CRES LABORATORIES

Chemical Engineering Low Temperature Laboratory

Remote Sensing Laboratory

Electronics Research Laboratory

Chemical Engineering Heat Transfer Laboratory

Nuclear Engineering Laboratory

Environmental Health Engineering Laboratory

Digital Computer Technology Laboratory

Water Resources Institute